THE SYNTHESIS OF AZA-DIPYRROMETHENES AS POTENTIAL PDT AGENTS AND MEASUREMENT OF SINGLET OXYGEN GENERATION

SCOTT MICHAEL CASSIDY

A thesis submitted in partial fulfilment of the
requirements of
Robert Gordon University
for the degree of Master of Research

May 2011

Declaration

This thesis in candidate for the degree of Masters by Research has been composed entirely by myself. The work which is documented was carried out by myself. All sources of information contained within which have not arisen from the results generated have been specifically acknowledged.

Contents   Page

List of Figures

List of Schemes

List of Tables

List of Appendices

Scott Michael Cassidy
Master of Research
**The synthesis of aza-dipyrromethenes as potential PDT agents and measurement
of singlet oxygen generation**

Abstract

Photodynamic therapy is a relatively new treatment for various cancers and other diseases using a photosensistiser that produces cytotoxic singlet oxygen ($^1O_2$) after light irradiation. Current approved photosensitisers have limitations, such as a low extinction coefficient in the desired therapeutic wavelength of absorption (600 – 900 nm), as in the case of Photofrin$^®$. The discovery of improved photosensitisers is essential if photodynamic therapy is to become more common and successful than other treatments. In this research a selection of aza-dipyrromethenes and their intermediates were synthesised to create photosensitisers that were able to absorb light within the therapeutic wavelength and create $^1O_2$ by energy transfer from the photosensitiser. As shown by others, receptors can be used to control $^1O_2$ generation *via* photoinduced electron transfer (PET). The synthesis of aza-dipyrromethenes using intermediates containing pyridine groups and crown ethers was unsuccessfully attempted to create photosensitisers with receptors sensitive to environmental factors, such as pH and sodium ion concentration, in the hope that such receptors would control $^1O_2$ generation *via* PET. Evaluation of the synthesised compounds for use as photosensitisers was carried out using a range of light sources. Measurement of singlet oxygen generated was carried out using diphenylbenzofuran (DPBF), a singlet oxygen scavenger, and the depletion of the absorbance of DPBF used to quantify the rate of $^1O_2$ generation. Comparison with methylene blue, a known photosensitiser, gave a singlet oxygen quantum yield of the compounds to evaluate their efficacy as potential photosensitisers. It has been shown from the photophysical data that the synthesised compounds in this research absorb within the desired range, (600 – 900 nm), but $^1O_2$ generation is insufficient and further modification of the aza-dipyrromethene scaffold is needed to create useful photosensitisers for photodynamic therapy.

Acknowledgements

Chapter 1

Introduction

1.1 Photodynamic Therapy Background

With 297,991[1] cases diagnosed in the United Kingdom in 2007, and one in four deaths as a direct result of, it is not surprising that Cancer remains one of the most feared topics of today's society. With over two hundred different types of cancer, it is therefore easy to justify the money and time invested by researchers in the medical and scientific community to this cause.

The treatments for cancer are diverse, not least due to the significant number of different types. Treatments include surgery, chemotherapy, radiotherapy, bone marrow and stem cell transplants, hormone therapy, alternative therapies and photodynamic therapy (PDT) among others. This thesis focuses on utilizing photodynamic therapy as an alternative to the more invasive treatments by developing potential new compounds capable of acting as photodynamic agents.

Photodynamic therapy is generally considered to be in its infancy as a cancer treatment with many of the most significant advances and important research made in the last three decades. However, if we are to consider the concept, of using light combined with a photosensitiser, and not the terminology then we discover that PDT has actually been around for over 3000 years. The Egyptians, Chinese and Indians have all used photodynamic therapy to treat a number of different diseases whereby they would cover the affected area with plant extract and then use the sun as the radiation source.[2]

It was only at the turn of the twentieth century when Von Tappeiner and his student Oscar Raab [2] reported the death of the single celled eukaryotes, paramecium, by acridine that they realised the significance of light in the process, the cells only became damaged in the presence of light and thus the concept was born. In 1900, Raab reported that acridine dyes killed protozoan paramecia that had been exposed to light for 1.5 hours. In contrast, when the experiments were repeated in the absence of light, acridine dyes took up to 15 hours to kill paramecia. Von Tappeiner et al. later introduced the term 'photodynamic action' to describe the process. This group studied a range of dyes and their effects on the treatment of skin disease and tumours.

2

One particular dye, eosin **1**, was used with light to treat a basal cell carcinoma starting the field that would become photodynamic therapy.[2]
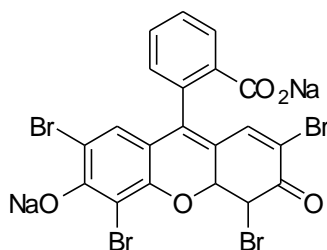
1

It was, however, to take a number of decades before the knowledge gained from Von Tappenier and Raab was applied to the clinical setting. A vast amount of research has been invested in PDT between then and now with significant advances made in the mid 1960's. An example of such research is found in the use of the photosensitiser hematoporphyrin derivative (HpD). In 1964, Lipson et al. demonstrated that HpD accumulated preferentially in tumour tissue compared to healthy tissue.[3] HpD, formed by the treatment of hematoporphyrin with 5% sulphuric acid in acetic acid, is a mixture of porphyrin monomers, dimers and ogliomers linked covalently by ether or ester bridges.[4] The hematoporphyrin monomer **2** is a poor photosensitiser and seperation of the monomer porphyrins by size-exclusion gel chromatography gives more tumour specific ogliomeric fractions.[5] Purified HpD was marketed as Photofrin by QLT Phototherapeutics (Vancouver, Canada). Photofrin first received approval in Canada in 1993 for the treatment of cervical, bladder and gastric cancers.[3,4]
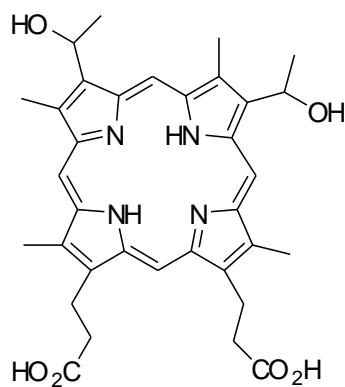
2

Since then approval has been achieved in a number of countries with the popularity of this non-invasive technique ever growing.

PDT is the use of a drug, light and endogenous molecular oxygen to produce a cytotoxic effect in the treatment of cancerous and non-cancerous diseases.[6] The principle of PDT is that once the drug, called the photosensitiser, is administered it accumulates in the malignant tissue. Light, of a wavelength specific to the photosensitiser, is then used to excite the photosensitiser which in turn undergoes an energy transfer with molecular ground state oxygen (already present in the surrounding environment) to produce singlet oxygen, the principle cytotoxic species.[6] The therapeutic wavelength of light is considered to be between 600 - 900 nm as this allows for maximum penetration of tissue while the excitation of the photosensitiser remains energetically favourable. The reason for the near-infrared requirement is that light is usually absorbed in the dermis region of the skin. In the dermis there are blood chromophores, such as hematoporphyrin, that absorb within the visible region of light between 400 - 600 nm so therefore light above this wavelength is required for greater transmittance.[7]

The pharmacodynamics of PDT is where cell necrosis occurs by the oxidation of cell organelles, nucleotides and membranes by singlet oxygen, generated directly due to the photosensitiser, the mechanism for which is further discussed in section (1.2.2.).[8] In contrast to surgery, radiation therapy or chemotherapy, PDT offers greater selectivity; malignant tissue can be targeted specifically by administering light externally or internally *via* fibre optic cable directly to that region minimising damage to healthy cells. The major side effect from PDT is skin photosensitivity, where the patient has to avoid sunlight to prevent inadvertent phototoxic reactions until the photosensitiser has cleared from the body.[6] However, when the side effects caused by PDT are compared with those from the previously mentioned treatments it is plain to see the benefits to be achieved from this course of treatment. The severity and invasive nature of surgery, radiation or chemotherapy renders PDT as a non-invasive, patient friendly alternative to the treatment of particular types of cancer.

The research invested in PDT over the last few decades has deepened the understanding and potential applications for the therapy, nevertheless there are surprisingly few examples of

photosensitisers utilised in the clinical setting. The major and leading photosensitiser was that discovered by Lipson, Photofrin®, as mentioned previously. Despite its widespread use in North America, Europe and Japan, Photofrin® has some major disadvantages. The absorption band used clinically to excite the photosensitiser, 630 nm, has a low extinction coefficient, meaning there is less energy absorbed owing to the Beer Lambert Law of $A = \varepsilon\, c\, l$ (where A = absorbance, ε = extinction coefficient, c = photosensitiser concentration and l = path length of light beam), and thus has a proportional impact on the phosphorescence emission. Also, Photofrin, has a long duration of skin photosensitivity of 2-3 months.[4] Currently there is a need for new photosensitisers which have a higher extinction coefficient for an absorption band between 600 - 900 nm with faster metabolism to allow for fewer weeks of skin photosensitivity. Alternatively, these adverse properties could be prevented with a tumour specific photosensistiser, localising within tumour cells, thereby limiting the damage done to healthy tissue while at the same time maximising that caused to the diseased cells.

A successful photosensitiser would therefore have the following six criteria: [6]

(1) Preferential pharmacokinetics, allowing for uptake of the photosensitiser within the tumour cell over non-cancerous cells allowing for minimal damage done to healthy cells and maximise efficacy of the drug.

(2) Possess negligible dark toxicity; that is, ensuring the PDT drug candidate should be active only when there is a light source of specific wavelength.

(3) High quantum yield of singlet oxygen; this is a number between one and zero that shows how efficiently singlet oxygen is produced per photon absorbed by the photosensitiser.

(4) The wavelength of light at which the photosensitiser phosphoresces is greater than 600 nm. This gives maximum penetration of the tissue (~2.5 cm) while still emitting phosphorescence energetic enough to form singlet oxygen.

(5) High extinction coefficient (ε) at the excitation wavelength, since the extinction coefficient is directly proportional to absorbance, a strong absorption equates to more photons of energy absorbed and hence a greater singlet oxygen generation.

(6) Chemically pure and stable, the pharmacodynamics and pharmacokinetics of the photosensitiser will be simplified and clarified if there is only one compound/enantiomer present, the photosensitiser must also be stable enough to allow for appropriate storage and administration.

When all the criterion are assessed, it is perhaps not so astonishing that there are few photosensitisers currently on the market. However , this is due to change shortly, as there are scores of PDT agents currently in various stages of clinical trials.[9]

1.2 Mechanism of PDT

When a photosensitiser absorbs a photon (hv) of specific energy, an electron is excited in the highest occupied molecular orbital (HOMO) from the ground singlet state (S_0) to the lowest unoccupied molecular orbital (LUMO), of the excited singlet state (S_1) (figure 1).[10,11] Within the electronic states there are vibrational energy levels that an electron falls through by vibrational relaxation until it reaches the lowest vibrational state. When the electron reaches the lowest vibrational state it can potentially fall back to the S_0 state by emitting a photon of light, however due to vibrational relaxation, this light is of a lower energy than that originally absorbed. This emitted light is recorded as fluorescence, the wavelength of fluorescent emission is always greater than that of the absorbance due to the wavelength being inversely proportional to light energy, energy of a photon $= hv = hc/\lambda$ (where h = Planck's contstant, $v = c/\lambda$, where c = speed of light and λ = wavelength). If however the electron undergoes a spin forbidden transition or a 'spin flip' and changes multiplicity to become a triplet state, a process known as intersystem crossing (ISC), the electron can continue to lose energy to the surroundings and step down the vibrational energy ladder of the excited triplet state (T_1) until it reaches the lowest vibrational energy level where return to the ground state $T_1 \rightarrow S_0$ results in a phosphorescent emission.[12]

Energy

S_1 ISC T_1

Type I → Hydrogen Abstraction or Electron Transfer → Radicals

Type II → $^3O_2$ → Energy Transfer → $^1O_2$ → Oxidised Biomolecules

$h\nu$ Fluorescence

$h\nu$ Phosphorescence

S_0
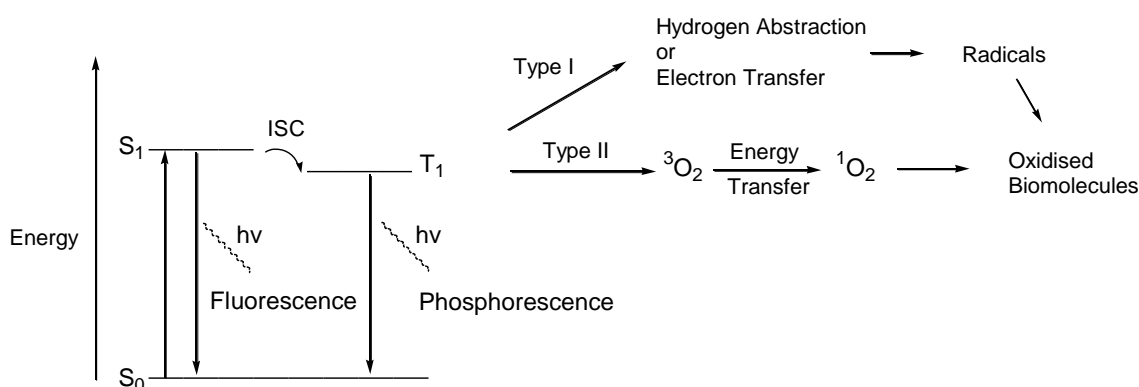
Figure 1. Jablonski diagram illustrating the mechanism of PDT when a photosensitiser absorbs a photon. For clarity the vibrational energy levels are omitted. Adapted from Konan et al.[10]

The lifetime of the T_1 state is much longer than the S_1 state (in the order of milliseconds as opposed to nanoseconds).[13] This is due to the spin-forbidden transition that must occur in order for the excited electron to fall from the T_1 state to the singlet S_0 ground state.[14] When the photosensitiser is in the triplet excited state, the photosensitiser can create cytotoxic species by two main mechanisms. In the type I mechanism, radicals are produced by hydrogen abstraction or electron transfer of biomolecules that collide with the photosensitiser.[4] In the type II mechanism an energy transfer between molecular oxygen produces singlet oxygen by collisional transfer of the photosensitiser in the T_1 state. Both the radicals and singlet oxygen then oxidize surrounding biomolecules causing cell death. The photosensitiser can then absorb another photon and continue to participate in type I and type II mechanisms as long as it is not destroyed by photobleaching.

1.2.1 Multiplicity of Molecular Oxygen

Multiplicity is determined by the following equation, multiplicity = 2S + 1 (where S = spin angular momentum a value of $\pm$ 1/2 for each unpaired electron). If two electrons occupied the same orbital their spins would cancel each other out, S = 2 [½ + (-½)] +1 = 1, so the multiplicity is a singlet state. In molecular oxygen, there are two unpaired electrons in the ground state electron configuration. Using the equation above S = 2(1) + 1 so S = 3, hence molecular oxygen ground state is triplet (Figure 2).
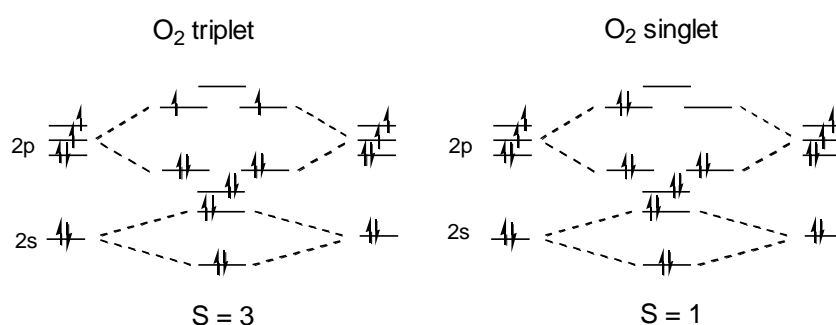
Figure 2. Multiplicities of ground triplet state and excited singlet state oxygen

The ground triplet state (T_0) oxygen and the excited singlet state (S_1) oxygen are energetically and magnetically different. The T_0 state oxygen is paramagnetic due to two unpaired electrons in degenerate orbitals with the same spin, whereas the S_1 state oxygen is diamagnetic due to paired electrons in the same orbital. The energy difference between the two states is 94 kJ/mol since the S_1 state is more energetically unfavourable due to the pairing energy that is required to have two electrons in the same orbital.[15] In PDT the S_1 state oxygen is created by the spin flip of an electron in the T_0 state oxygen by energy transfer of photosensitiser in the T_1 state.

1.2.2 Methods for Determining Photocytotoxicity

In PDT, photocytotoxicity can be caused by two quite distinct mechanisms, namely Type I and Type II. The generation of singlet oxygen ($^1O_2$) is known as Type II whereas in the Type I mechanism; hydroxyl radicals ($OH^.$) and super oxide anions (O_2^-) are the reactive species produced. It may be that in PDT the cytotoxicity is caused by either one of the mechanisms or a combination of both. Dougherty et. al. have shown that by using a singlet oxygen quencher, 1,3-diphenylisobenzofuran **3**, the cytotoxic effect could be attributed to singlet oxygen when haematoporphyrin derivative was used as a photosensitiser.[16] Diphenylisobenzofuran has an absorbance at 410 nm that decreases upon reaction with singlet oxygen. The rate of the disappearance of this band also gives a method for determining how efficiently the photosensitiser can generate singlet oxygen.

3
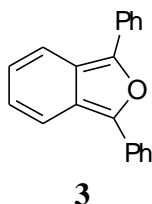
Sodium azide (NaN_3), a $^1O_2$ quencher, and D-mannitol, a $OH^.$ scavenger, has been used to determine the dominant mechanism of photocytotoxicity when using HeLa cells incubated with a photosensitiser.[17] HeLa cells in the presence of either NaN_3 or D-mannitol were photoirradiated and the % cell survival taken after 24 h incubation. HeLa cells incubated with NaN_3 showed the highest % cell survival, indicating photocytoxicity was no longer inhibited and $^1O_2$ generation was the dominant mechanism of photocytotoxicity.

9

1.3 Light Sources for Photodynamic Therapy

There are a number of various light sources available clinically for PDT, of which there are two main groups- lasers and lamps. In general, laser light sources are beneficial for endoscopic treatment as they can be coupled to fibre optic cables. Conversely the lamp light source does not have sufficient power for irradiation when coupled to fibre optic cables so the use of lamps are limited to superficial lesions.[18] Laser light sources produce monochromatic light so that in some cases a different laser light source is needed to compensate the different absorption maxima between various photosensitisers. It may be the case that there is no advantage to be gained from monochromatic light sources since lamps, which have a broad spectrum of light wavelength, can be tuned to emit within the required wavelength with the use of filters. This means that some lamp light sources can provide excitation for 5-aminolevulinic acid (ALA), Foscan and hematoporphyrin.[18] Future light sources may be the use of light emitting diodes (LED) and femtosecond solid state lasers. The LED would give a choice of wavelengths from 350 - 1100 nm, covering the absorption maxima of all currently approved photosensitisers. The use of femtosecond solid state lasers would exploit two-photon excitation, where two photons of the same energy are able to excite an electron in the photosensitiser to an energy level that is the sum of the two photons' energy. This means that light in the near infra-red region, for example 800 nm, could be used to excite a photosensitiser the has an absorption maxima at around 400 nm, allowing for increased penetration of tissue.[8]

1.4 Second Generation Photosensitisers

Due to the low absorption bands of HpD and Photofrin at therapeutic wavelengths (600 - 800 nm), high photosensitivity and other disadvantages associated with these photosensitiers, research has focused on the development of new 'second generation' photosensitisers.

10

Foscan (meso-tetrahydroxyphenylchlorin, m-THPC, temoporfin) **4** has shown greater PDT results in treatment of rats with mammary carcinoma than its corresponding porphyrin (m-THPP) or Photofrin.[19] At a 4 times lower concentration, m-THPC has a higher absorbance than m-THPP at 652 nm. There is a preferential uptake of m-THPC in the skin over tumour cells but this does not hinder the efficacy of the treatment and damage of the tumour occurs around the vasculature and neoplastic cells where the photosensitiser is uptaken. When tumour regrowth was measured the tumour doubled in size after 2 days when treated with m-THPP or Photofrin but exponential growth did not occur until 12 days after treatment with m-THPC at a 10 times lower concentration than Photofrin.[20]

Skin cancers such as basal cell carcinoma (BCC), squamous cell carcinoma (SCC) and actinic keratosis (thought to be pre-malignant form of squamous cell carcinoma) are optimal for treatment with PDT. Since cancers of this type are superficial, light can be focused on the region where the lesions are, minimising damage to healthy cells. Alternatively, the problem of selective uptake of a photosensitiser in a tumour could be avoided since the photosensitiser can be topically applied to the lesion rather than injected into the blood stream. Foscan was used in a clinical study in 1999 for the treatment of BCC and SCC lesions in the head and neck region.[21] The irradiation is within the therapeutic window at 652 nm and effective at a light source of energy 5 - 20 J/cm^2 with skin photosensitivity of 2 weeks. Tumour necrosis was visible after 48 h in all the lesions treated, 88 BCC lesions in 14 patients and 9 SCC lesions in 4 patients, with a complete response rate of 92 % for BCC patients and 100 % for SCC patients. Foscan was approved in October 2001 for use in the European Union, Iceland & Norway for treatment of head and neck cancer.
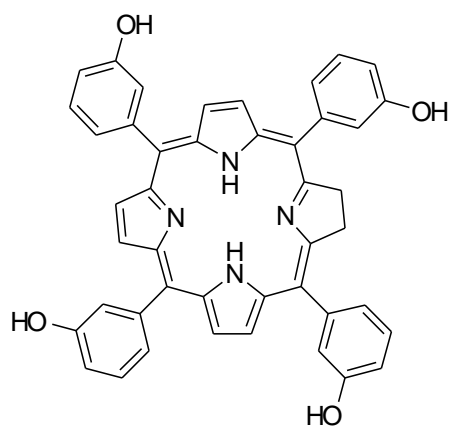
4

ALA **5** induces the production of protoporphyrin IX (PpIX) **6** in the haeme pathway of the mitochondria (Figure 3).[22] Haeme is a precursor to haemeproteins such as haemoglobin, myoglobin and cytochromes. The conversion of PpIX to haeme through a series of pathways has a rate-determining step, the addition of iron by the enzyme ferrochelatase.[22] In tumour cells where there is faster proliferation, and ferrochelatase is inhibited, the addition of ALA causes PpIX to build up rapidly. Since ALA is hydrophobic, alkyl-esters were created to improve lipophilicity and increase uptake of the drug across the membrane to give a higher endogenous PpIX concentration at lower concentrations than ALA.[23] In contrast to structural changes of ALA, the importance of the mode of drug delivery has been shown when a higher concentration of ALA over ester derivatives methyl-ALA and hexyl-ALA was observed by using a bioadhesive-patch based system in porcine skin.[24] Currently in Europe and Australia the methyl-ester of ALA, Metvix developed by Photocure, is approved for treatment of actinic keratosis and basal cell carcinoma.[22]
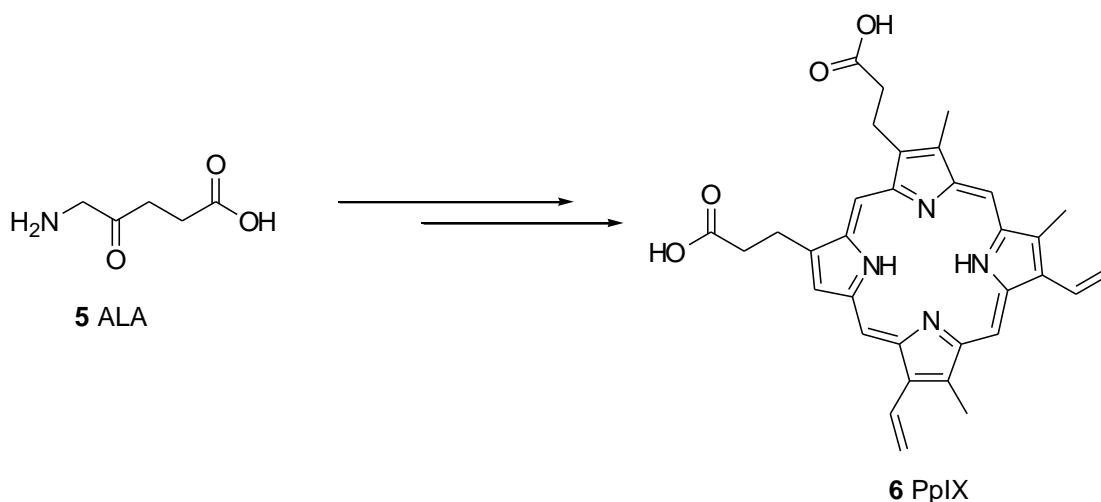
Figure 3. Simplified Scheme showing PpIX 6 is produced from ALA 5

Light intensity, length of time of irradiation, number of treatments and wavelength of light are some of the variables that alter the results of treatment in PDT by ALA. One study showed that it was possible to use light of a lower intensity to achieve a complete response of 84 % for patients with basal cell carcinoma.[25] When lesions were illuminated with light of intensity 45 J / cm^2 twice, with a period of 2 h between first and second illumination, efficacy was greater than if a single illumination had been used at a much higher intensity. Protoporphyrin IX (PpIX) has an absorption maximum at 410 nm. Blue light has a closer wavelength than red light to this absorption maximum and light administered at 417 nm successfully treated actinic keratosis. [22, 26] This is due to blue light being a more efficient activator for PpIX and actinic keratosis occurs in the epidermis so light does not have to penetrate deep to excite PpIX.[27]

1.4.1 Addition of Receptors and Photoinduced Electron Transfer (PET)

As previously mentioned, phosphorescence or fluorescence is emitted when an electron in an excited state of the photosensitiser falls back down to the ground state via a radiational pathway. Photoinduced electron transfer (PET) can quench these emissions by the donation of an electron from a covalently attached donor atom. This redox process must be energetically favourable allowing for the reduction of the photosensitiser entity and therefore quenching the emission by replacing the excited electron while the donor moiety can accept the electron in the excited state of the photosensitiser by back donation.[28] This process is illustrated in Figure 4.
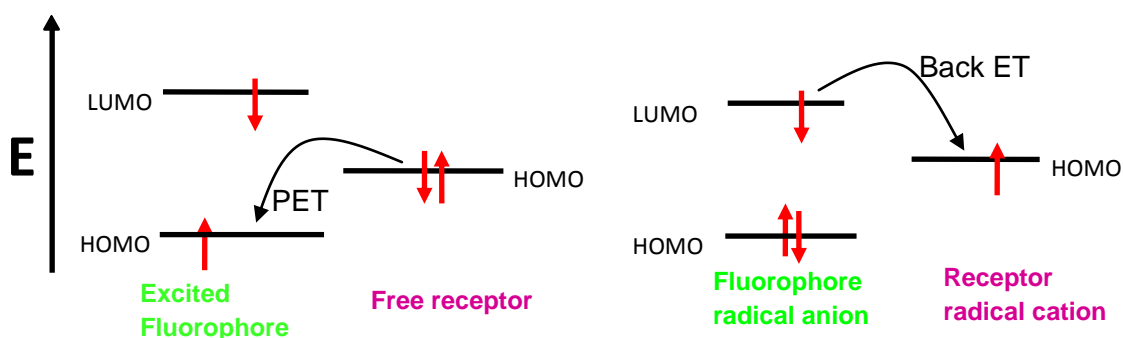
Figure 4. Frontier orbital diagram displaying a two component system illustrating the potential electron transfer occurring in a PET system designed to quench emission.

The use of PET provides a potential mechanism for control over when a molecule will or will not emit phosphorescence or fluorescence. In PDT this control would be beneficial if phosphorescence could be switched "on" only when the photosensitiser was in a tumour cell but "off" in healthy tissue. The diagram below (Figure 5) shows two photophysical pathways. The first pathway has a receptor which is unbound and the lone pair of electrons are energetically favourable to quench the emission of the photosensitiser by PET. When the receptor is bound by the relevant substrate the oxidation potential of the electrons in the highest occupied molecular orbital (HOMO) has risen substantially no longer allowing an electron to participate in PET,

phosphorescence is no longer blocked and singlet oxygen may be produced from the resulting phosphorescence emission.

Unbound receptor

Bound receptor
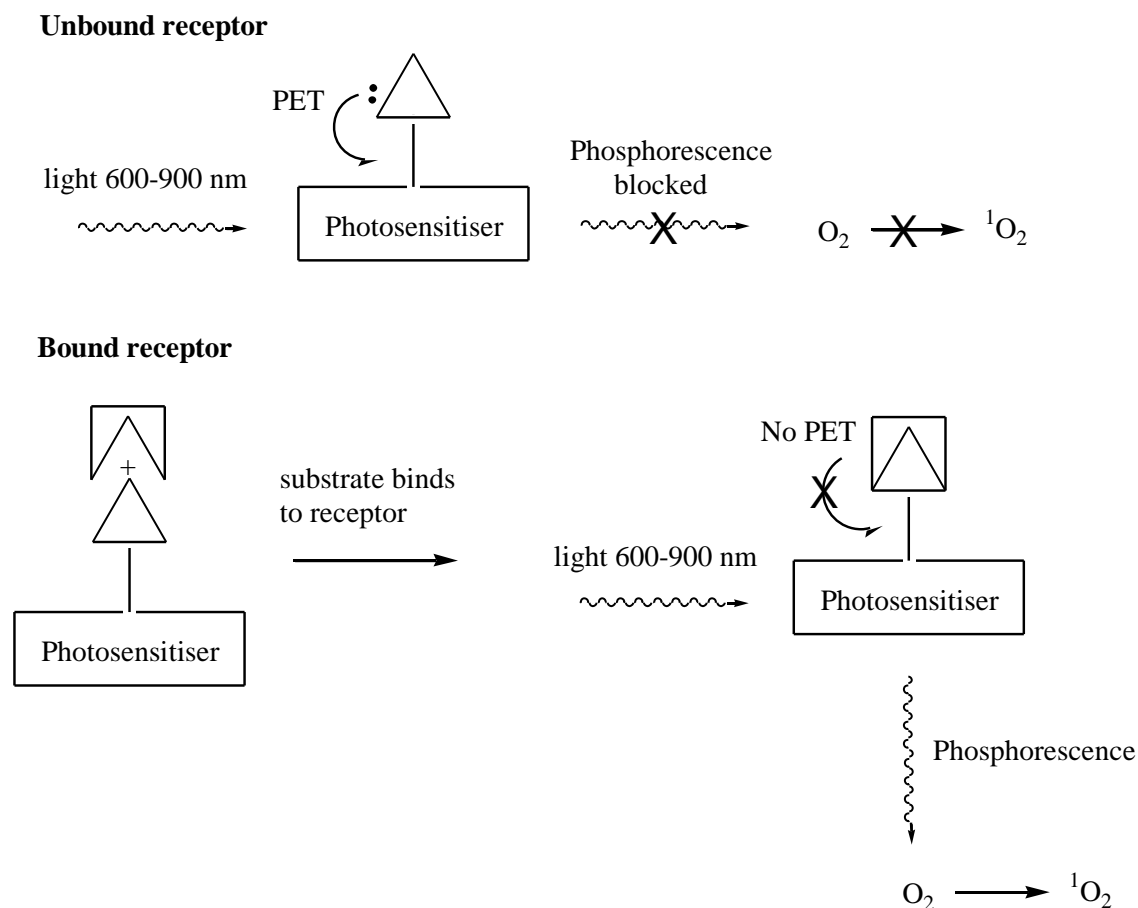
Figure 5. PET from receptors influencing photosensitiser phosphorescence generation

Tertiary amines covalently attached to bromonaphthalene derivatives were shown to act as phosphorescent pH sensors, where phosphorescence was emitted in acidic conditions.[29] In addition to proton receptors, crown ethers are able to act as phosphorescent metal cation sensors (Na^+,Ca^{2+},K^+,Mg^{2+}).[30] Since tumour sites have a higher concentration of protons and metal cations the development of photosensitisers that are only cytotoxic under identical environments to cancer sites should help the efficacy of PDT treatment.

1.5 Potential Candidates for PDT Drug Structures

Dipyrromethene (DIPY) compounds (**7-9**) and their analogues are being explored as potential photosensitisers for PDT. The core structure of the DIPY compound can incorporate aryl substituents with the tetra-aryl moieties being the most common. This extended conjugation increases the maximum wavelength of absorption from around λ_{max}= 500 nm for compound **8** to greater than λ_{max} = 600 nm as is the case in compound **9**. The C-8 carbon of the DIPY **7** can be substituted for a nitrogen atom to give aza derivatives, and chelation with boron etherate gives aza-borondipyrromethenes (BODIPY) **9**.[31]

7   **8**   **9**
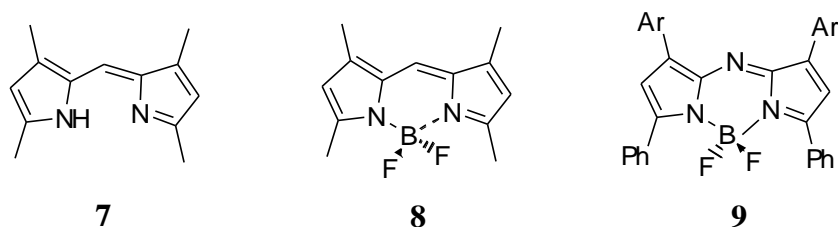
The use of a boron atom adds rigidity to the structure in **9** minimising a return to the ground state of an excited photosensitiser by non-radiative processes such as contact with other molecules, allowing for the desired phosphorescence emission.[32]

10   **11**
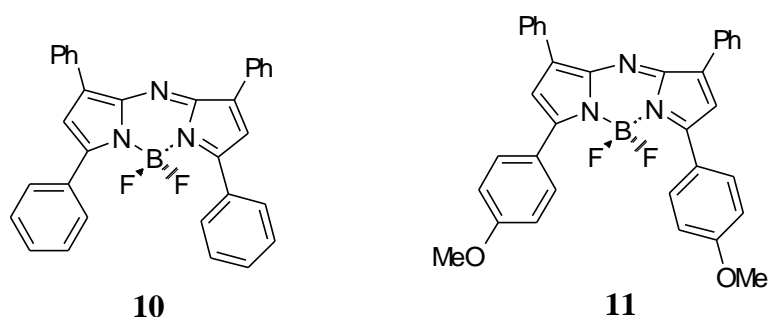
Addition of electron donating groups on aryl substituents of BODIPY compounds modifies their absorbance maximum. Attachment of a methoxy group at the para-position of a 3-aryl substituent caused a red-shift in absorbance from λ_{max}= 650 nm to λ_{max}= 688 nm in aza-BODIPYs **10** (79, 000 $M^{-1}cm^{-1}$) and **11** (85,000 M^{-1} cm^{-1}).[31] This effect was observed on other

BODIPYs, and in contrast an ortho-substituted methoxy group produced a blue shift in absorbance. The position of electron donating and withdrawing group may provide a tool for "fine tuning" the absorbance wavelength in novel photosensitisers.

Another important parameter for consideration of photosensitiser design is the quantum yield of phosphorescence. Halogens and other 'heavy atoms' are able to facilitate inter-system crossing, the covalent attachment of iodine to **12** examines the impact of the 'heavy atom effect'.[32] The quantum efficiency of fluorescence changed from $\Phi_{fl} = 0.70$ in MeOH for **12** (120,000 $M^{-1}cm^{-1}$) to $\Phi_{fl} = 0.02$ for **13** (110,000 $M^{-1}cm^{-1}$), this decrease being assigned to an increased quantum yield of phosphorescence.

12   **13**
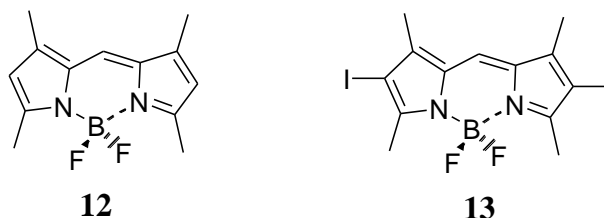
The heavy atom effect has been responsible for the higher quantum yield of phosphorescence emission seen for the brominated BODIPY compound at a 100 fold lower concentration when compared to that of the unbrominated BODIPY analogue compound.[33] In general, the halogen needs to be attached to the core structure of the photosensitiser in order to influence internal spin-orbit coupling, showing no significant change when attached to an aryl substituent. The attachment of either iodine or bromine to the BODIPY derivatives has not significantly altered the wavelength of absorbance.[33,34]

The use of receptors that quench phosphorescence by donation of an electron provides an additional parameter, allowing for enhanced selectivity in the modification of photosensitisers, specifically enabling control over the conditions that singlet oxygen may be produced. The aza-BODIPY **14** has been synthesised that uses the above mentioned strategies for design of effective photosensitisers.[35] In addition to the benefits seen from compound **9**, compound 14 has a methoxy group in the aryl region. This methoxy group causes an increase in the maximum

17

absorbance wavelength, as discussed in compound **11**. As well as containing bromine covalently attached to the core enhancing the quantum yield of phosphorescence by the heavy atom effect, compound **14** also contains a tertiary amine receptor that quenches phosphorescence via PET unless the amine is protonated when in an acidic environment. The production of singlet oxygen is dependent on the nanoevironment of the photosensitiser [36].

$$(Et)_2N— —N(Et)_2$$

Br — ... — Br

R = 4-MeOC$_6$H$_4$

14
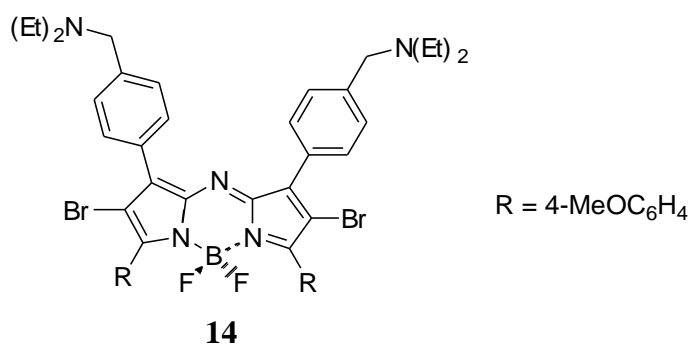
Receptors such as crown ethers and amines are able to show photoinduced electron transfer until this process is blocked by a cation such as Ca^{2+} or Na^+, or a proton. In PDT this is useful since the microenvironment of a tumour cell contains higher concentrations of cations at a lower pH. This would enable photosensitisers containing such receptors to only become cytotoxic when in an environment similar to that of a tumour cell. Following on from this work a BODIPY compound has been synthesised that contains two receptors, one for protons and the other for sodium ions.[37] This means that both conditions have to be met for phosphorescence to be emitted or PET by one or both receptors will quench the photosensitiser. Two receptors greatly enhance the selectivity of a photosensitiser and minimise cytotoxic effects towards healthy cells.

1.6 Localisation of Photosensitiser in Tumours

1.6.1 Liposomes

Another benefit of PDT is that regardless of the location of the photosensitiser in tissues light can be administered locally at the tumour site and only induce a cytotoxic effect at the area where light has penetrated tissue. The previous section looked at the development of photosensitisers that switch on and off the production of singlet oxygen depending on their micro environment, however photosensitiser modification has also been investigated and shown preferential uptake in tumour cells over normal cells thus increasing the efficacy of the treatment while minimising side effects by indiscriminate damage to healthy cells.

Photosensitisers can form conjugates with serum proteins such as albumin and lipoproteins.[38] Hydrophilic photosensitisers such as tetrasulfonated porphyrins and phthalocyanines were discovered to bind to albumin and globulins upon intravenous administration whereas hydrophobic photosensitisers show a preference for binding to low density lipoproteins.[39] Lipoproteins are responsible for transporting hydrophobic molecules such as cholesterol and consist of proteins and lipids.[40] Low-density lipoprotein (LDL) contains a higher ratio of lipid to protein than high density lipoprotein (HDL) and LDLs are considered to have the biggest effect in transport of hydrophobic photosensitisers. Tumour cells have a higher number of LDL receptors compared to healthy cells enabling more LDL to be absorbed by endocytosis.[38] In addition to the efficacy of treatment with PDT being improved by increased uptake of LDL-bound photosensitisers in tumours, the highly oxidised liposomes post PDT may contribute to an enhanced cytotoxic effect.[38]

Liposomes can be used to encapsulate photosensitisers prior to intravenous infusion. This prevents aggregation that would inhibit the ability for the photosensitiser to act as a singlet oxygen generator.[41] A study carried out using human U87 glioma implanted in rats, compared the treatment of Photofrin in a liposomal formulation with Photofrin administered in a dextrose vehicle.[42] The uptake within the U87 glioma was increased with the liposome formulation,

palmitoyldiphosphatidyl-choline (DPPC), destruction of the tumour was enhanced illustrating the ability of liposomes to act as carriers. Conventional liposomes such as those made from phosphatidylcholines have a poor plasma half-life. Disintegration occurs by interaction between lipoproteins or taken up by macrophages and releasing the photosensitiser they were carrying into the blood stream before reaching the tumour site.[41] Modification of the conventional liposomes with polyethylene glycol (PEG) can increase the plasma half-life to 12 h and improve the uptake of the non-aggregated form.[43]

There is little variation between the intracellular pH of various tumour cells compared to normal tissue cells, around 7.0-7.2 pH.[44] However the interstitial space surrounding the tumor is more acidic, creating a pH gradient between the interstitial space and intracellular compartment. If a drug is weakly basic or acidic then fewer molecules would be ionized in an environment of low pH. Since the molecule would be more lipophilic it would be able to diffuse across the membrane and once within the tumour cell dissociation would occur again and the drug would become 'trapped'.[44] It has been suggested that such a mechanism may influence the uptake of dicarboxylic porphyrins, where the ionic species will be in equilibrium with the neutral species within the cell, thereby, providing a path for the photosensitiser to eventually leave the cell.[42]

1.6.2 Nanoparticles

Another method for photosensitiser delivery is the decoration or encapsulation with nanoparticles. Nanoparticles are less than 1 µm in size which is less than the smallest blood capillaries (5 - 6 µm), and generally are made from synthetic polymers or ceramic material.[46] Loading nanoparticles with photosensitisers avoids embolism in blood capillaries that may be caused by the aggregation of a free photosensitiser. Nanoparticles that have external receptors specific to tumor cells cancels the need to incorporate this on the photosensitiser, speeding up the synthesis of potential drugs.

Two types of nanoparticles can be made: one which is biodegradable and releases the photosensitiser or a non-biodegradable nanoparticle where the singlet oxygen is able to diffuse through the pores of the nanoparticles and the photosensitiser is not released.[47]

Biodegradable nanoparticles are made from synthetic polymers such as poly (lactic acid) (PLA), poly(glycolic acid) (PGA) and their co-polymers poly (lactide-co-glycolide) (PLGA). Varying the ratios of the polymers influences the biodegradation rate, affecting how quickly the drug will be released. Hydrophobicity is controlled by a higher PLA ratio and hydrophilicity by a higher PGA ratio.[46] Controlling the biodegradation rate is important if nanoparticles are to be used in PDT since there would need to be sufficient time for accumulation within the tumour.

Non-biodegradable silica can allow singlet oxygen to diffuse through the pores of the mesh but still contain the drug. This is beneficial as a cytotoxic effect can be achieved if the nanoparticle is localized at the tumour site, removing the risk of aggregation and deactivation of the photosensitiser if it had been released.[47]

A common method to enhance biocompatibility of drugs is to use poly(ethylene glycol) PEG, a hydrophilic polymer. PEG is used to coat nanoparticles that are otherwise hydrophobic and would be rapidly cleared by phagocytes. This ensures that the nanoparticle can circulate the body for a longer amount of time and improve drug delivery.[43]

1.7 Other Treatments: Boron Neutron Capture therapy (BNCT)

Photosensitisers can be modified to be used in other cancer therapies such as boron neutron capture therapy. This form of treatment uses irradiation of a non-radioactive ^{10}B atom and particles formed from the decay cause the destruction of the tumour.[48] The boron (^{10}B) isotope can disintegrate into an alpha particle ^{4}He nucleus and ^{7}Li nucleus post irradiation when it absorbs a low energy neutron by the following equation: $^{10}\text{B} + \text{n}_{\text{th}} \rightarrow [^{10}\text{B}]^* \rightarrow {}^4\text{He} + {}^7\text{Li}$ where the enthalpy of the reaction is equal to $+ 2.31$ MeV. The ^{4}He alpha particle can deliver the cytotoxic effect within 10 μm, around the size of a red blood cell, so the treatment is localised in

a small area. The synthesis of carborane-substituted photosensitisers, such as metallophthalocyanines and porphyrins has been reported.[49,50]

 A porphyrin which was shown to localise preferentially at a tumour can act as a carrier for boron neutron capture therapy (BNCT). A metallophthalocyanine was covalently attached to a closo-carborane cage as a potential candidate for BNCT.[50]

1.8 Aims & Objectives

The following objectives were investigated to assess whether the synthesised aza-dipyrromethene compounds would be viable photosensitisers for PDT:

- Synthesise of aza-dipyrromethenes from commercially available reagents.

- Alteration of the aza-dipyrromethenes solubility, degree of conjugation and addition of functional groups to potentially enhance the compounds for use as photosensitisers.

- Characterisation of the final products and intermediates to assess exact structure and purity of the synthesised compounds.

- Obtain the wavelength of absorbtion of the final products so that the appropriate wavelength of excitation can be selected for photophysical experiments.

- Perform photophysical experiments on final products to assess the quantum yield of singlet oxygen generation by using a singlet oxygen scavenger, diphenylbenzofuran.

- Compare the results using a known photosensitiser, methylene blue, to assess the efficacy of the aza-dipyrromethene compounds as potential photosensitisers.

Chapter 2

Results & Discussion

2.1 Photosensitiser Selection

The aim of this thesis was to advance on photosensitiser compounds already available and to synthesise highly conjugated compounds which had an absorption maxima above 600 nm to allow for deeper tissue penetration of light. By varying the substituent groups on these compounds they could then be manipulated to contain functional groups that could decrease their hydrophobicity or allow for enhanced selectivity as well as introducing heavy atoms to enhance their singlet oxygen generation capabilities. These added parameters would allow for enhanced phototsensitiser compounds capable of acting as PDT agents. The chosen targets were aza-dipyrromethene (aza-DIPY) moieties which have previously been shown by O'Shea and others [33] to absorb UV in the red region of visible light. Below are five target compounds, compounds **15** - **19** (Figure 6), designed to enhance and advance on the photophyiscal properties of the aza-DIPY skeleton to allow for increased potency photosensitiser compounds. Compound **15**, a conjugated aza-DIPY compound has an increased π-conjugated area, ensuring that the $\pi - \pi^{*}$ electronic transitions are occurring at much longer absorbance wavelengths, nearing the infrared region of the electromagnetic spectrum. Compound **15** is the template compound to which methoxy substituents were added to attempt to create a more soluble compound **16**. Target **17**, again an analogue of **15** is desired since chelation with boron gives the compound extra stability. Targets **18** and **19** have pyridine and crown ether substituents respectively to act as receptors that would participate in PET, as previously mentioned, to add control over phosphorescence and allow for an extra parameter in the selectivity of photosensitisers to tumour cells. Pyridine has been chosen as the receptor in **18** as it can be protonated in weakly acidic solutions. Due to the sp^2 hybridisation of the nitrogen atom – it is considered to be only weakly basic. The pKa of the conjugate acid of pyridine is 5.21 and therefore at this pH 50 % of the pyridine compound will be ionised – if we move to increase the pH by one log unit to pH 6, only approx. 10 % of the compound will be ionised. This change in pH is similar to that found in the microenvironment surrounding tumour cells, as discussed previously. Compound **18**

therefore has the potential to act as a tumour selective photosenstiser. Following the PET mechanism, when the compound is protonated no electron transfer will occur between the donor and acceptor moiety allowing phosphorescence to occur, whereas when the compound is unprotonated, as in the case at higher pH, electron transfer occurs between the receptor and fluorophore ensuring no radiative emission occurs. In a similar fashion, compound **19** also has the potential to act as a PET selective photosensitiser, benzo 15-crown 5, as seen in compound **19**, is a known sodium sensor and only when the concentration of sodium ions is at a specific level will the emission switch on, indirectly generating singlet oxygen. These two compounds have the potential to add another dimension to photosensitisers for use in PDT.

15

16

17

18

19
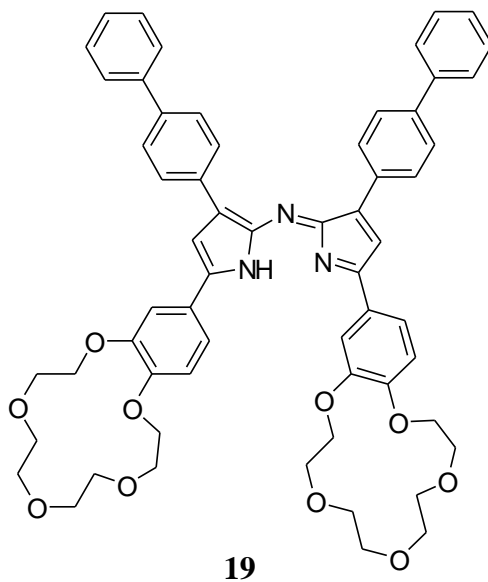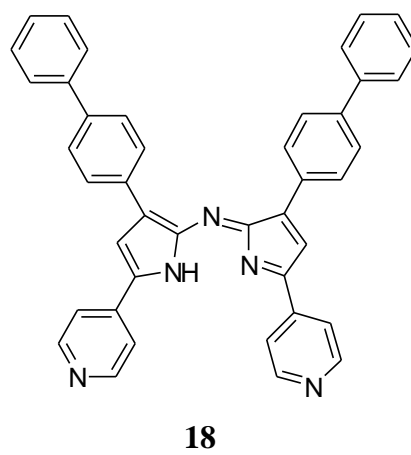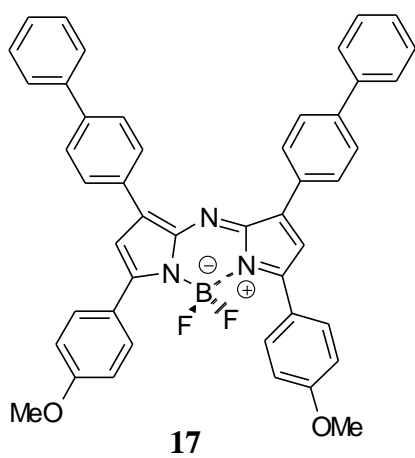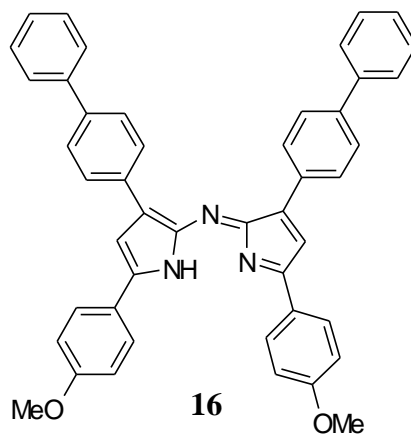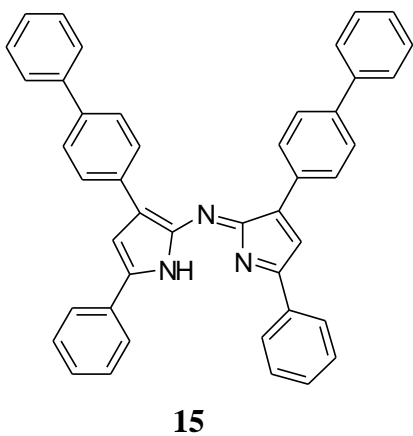
Figure 6. Target Compounds

2.2 Method of Synthesis

Adopting a method similar to that used by O'Shea et al.[33] compounds **15** -**19** were synthesised following the general synthetic scheme shown below (Scheme 1). Three steps were involved in the synthesis of the target aza-DIPY compounds.
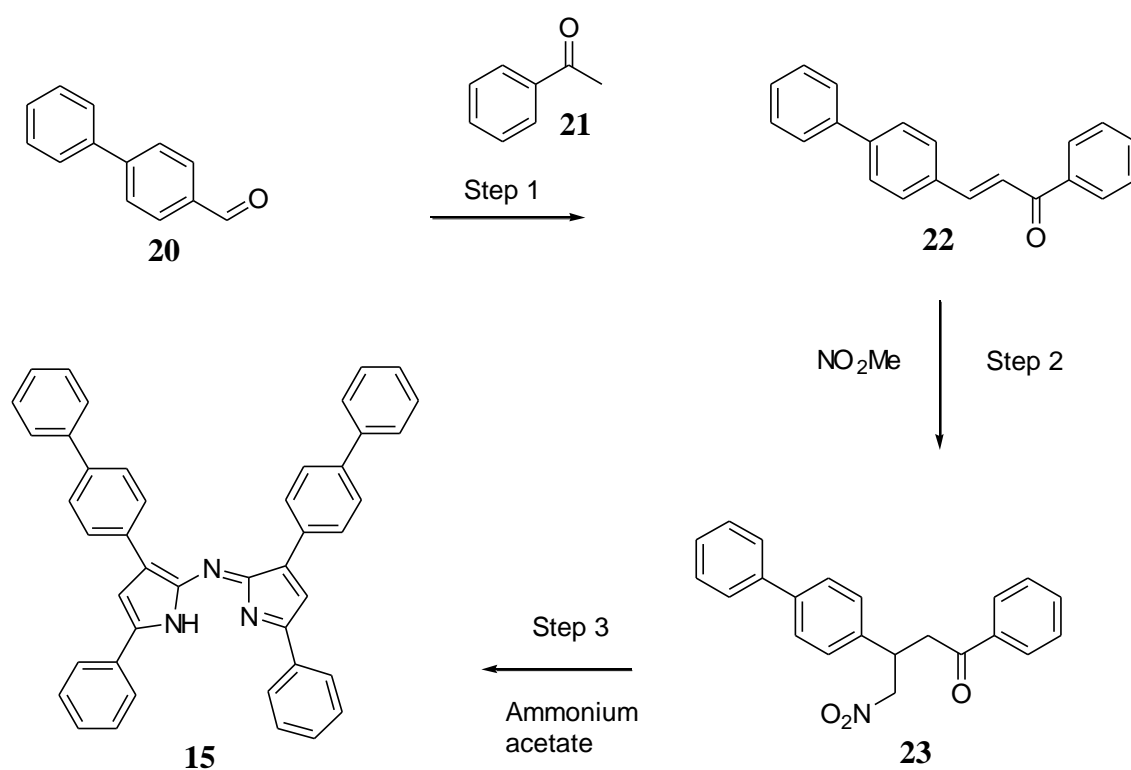
Scheme 1. Generic synthesis of aza-DIPY compounds

The initial step in the synthesis, Step 1, is an aldol condensation between an aldehyde, biphenylcarboxaldehyde **20,** and a ketone, acetophenone **21**, which leads to the chalcone **22**. The name 'aldol' comes from the product formed by reacting an aldehyde and base together, which has an **ald**ehyde and hydr**oxyl** component. Scheme 2 illustrates the general reaction mechanism occurring in an aldol condensation. A base such as sodium hydroxide can be used to create an enolate **25** from the ketone **24** which has only one acidic α-proton. This enolate **25**

then attacks the carbonyl of an aldehyde molecule **26**, giving the intermediate **27a** which can be

protonated by the previously released water molecule to give an aldol product **27b**.
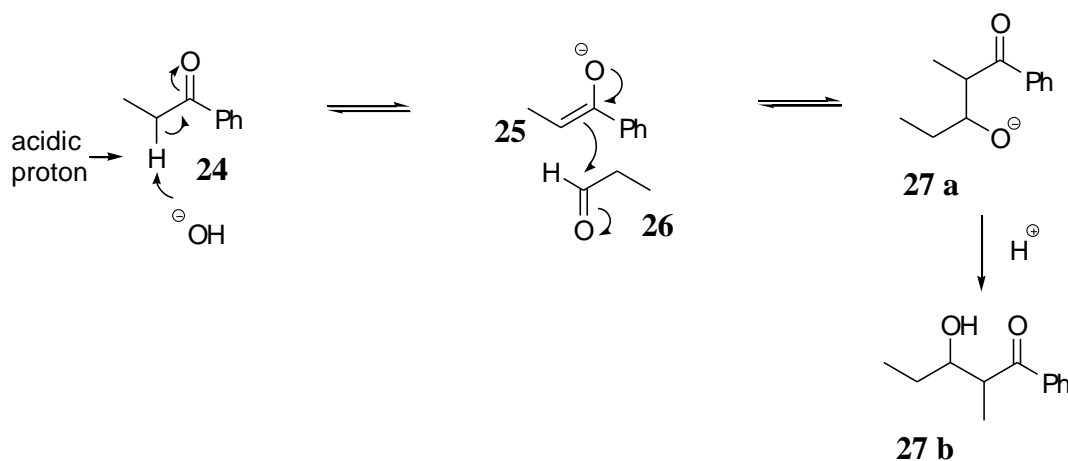
Scheme 2. *Aldol reaction mechanism*

The aldol condensation used in Step 1 of the synthesis, is a common reaction used in organic

chemistry to form new carbon-carbon bonds, usually between aldehydes and ketones. Post-aldol

reaction condensation can then occur when an acid or base causes the elimination of water to

yield an enone product.
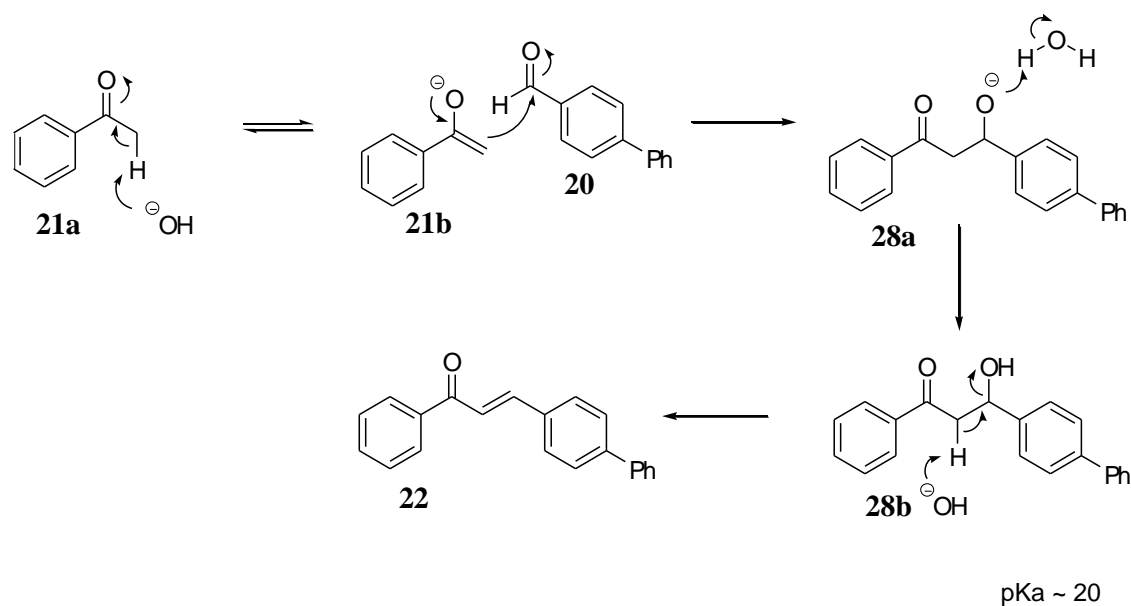
Scheme 3. *Aldol condensation reaction*

The aldol condensation follows the above reaction mechanism (Scheme 3). Deprotonation can only occur on the ketone **21a,** to form an enolate **21b**, as the aldehyde **20** does not have an available acidic α-proton next to the carbonyl group. Also the ketone **21a** has only one α-proton so the above aldol condensation is regioselective. This enolate then attacks the electrophilic carbonyl group of the more reactive aldehyde **20** to give a 1,3-carbonyl alcohol derivative **28a**. The hydrogen atom between these two functional groups is highly acidic (pKa ~20) and easily deprotonated (by the hydroxyl created by **28a** removing a proton from water). Elimination of the hydroxyl group from **28b**, which ordinarily is unfavourable as a leaving group, gives the enone **22**. The driving force for this E1cB elimination is the extra stability provided by the formation of the alkene.

The next step in the overall synthesis, Step 2, is a conjugate addition using nitromethane **29a** as a nucleophile, occurring via a Michael addition reaction (Scheme 4). Nitro groups are more electron withdrawing than carbonyl groups and therefore create a greater degree of polarisation about the adjacent C atom. This means deprotonation to create the enolate **29b** occurs more readily and therefore can be achieved using a weaker base, such as diethylamine (DEA).
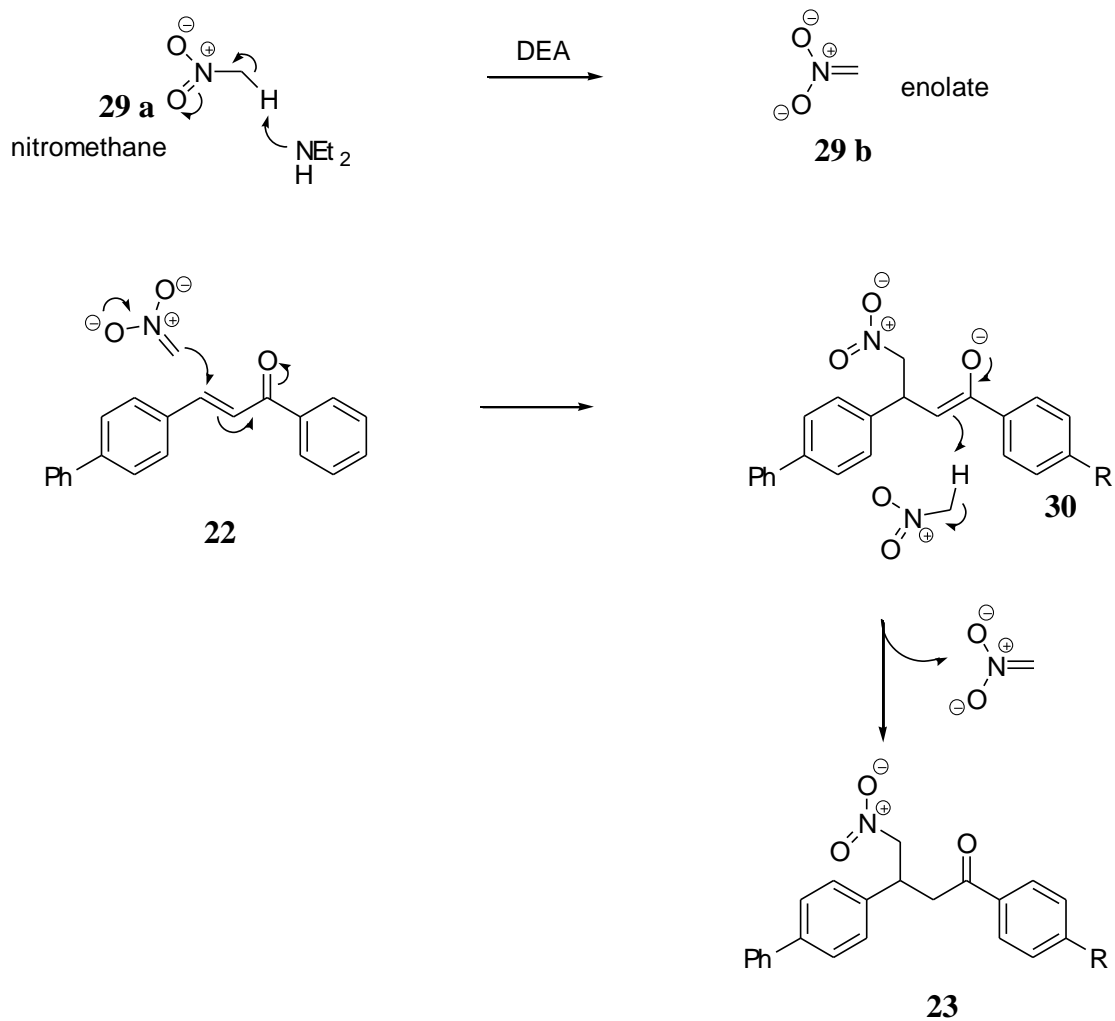
Scheme 4. *Nitration mechanism*

In the mechanism above, Scheme 4, the enolate **29b** is first formed from DEA which can attack the Michael acceptor, in this case the enone **22**, at the electrophilic β-carbon. Another enolate **29b** can be formed when the intermediate **30** takes a proton from another molecule of nitromethane, driving the reaction to give the nitro-ketone **23**.

2.3 Synthesis of Compounds

2.3.1 Synthesis of Compound 15

As previously discussed in the method of synthesis (Section 2.2), an aldol condensation reaction was carried out using NaOH as base at room temperature for 24 h (Scheme 5).
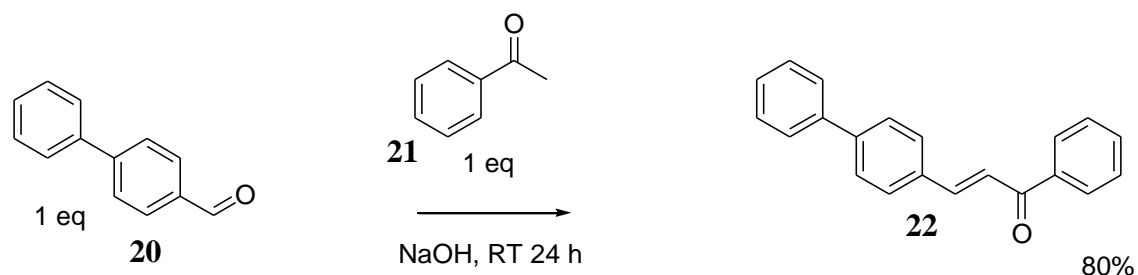
Scheme 5. Step 1, synthesis of 22

The long reaction time and low temperature were chosen in order to favour the production of the desired thermodynamic product rather than the alternative kinetic product (see section 2.4.1). A yellow precipitate formed and was dried to give the crude product before being purified by crystallisation to remove minor impurities of starting material. The structure was determined (see section 2.4.1) to reveal the desired product **22**.
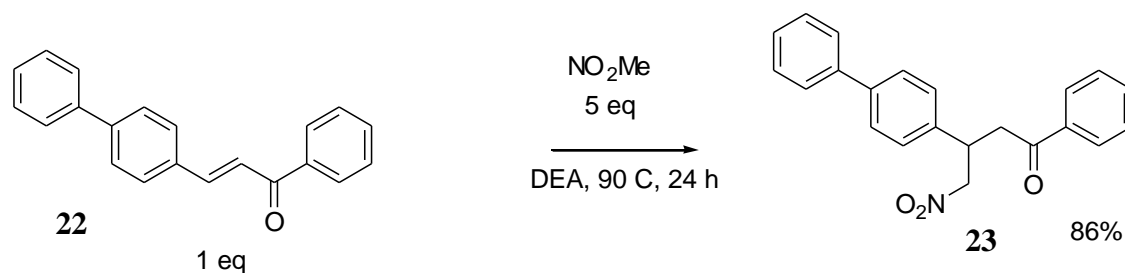
Scheme 6. Step 2, synthesis of 23

The synthesis of the second intermediate **23** was carried out using nitromethane as described in Scheme 6. This gave a brown sticky product **23** which was dried to give a yield of 86% and was fully characterised (see section 2.4.1).
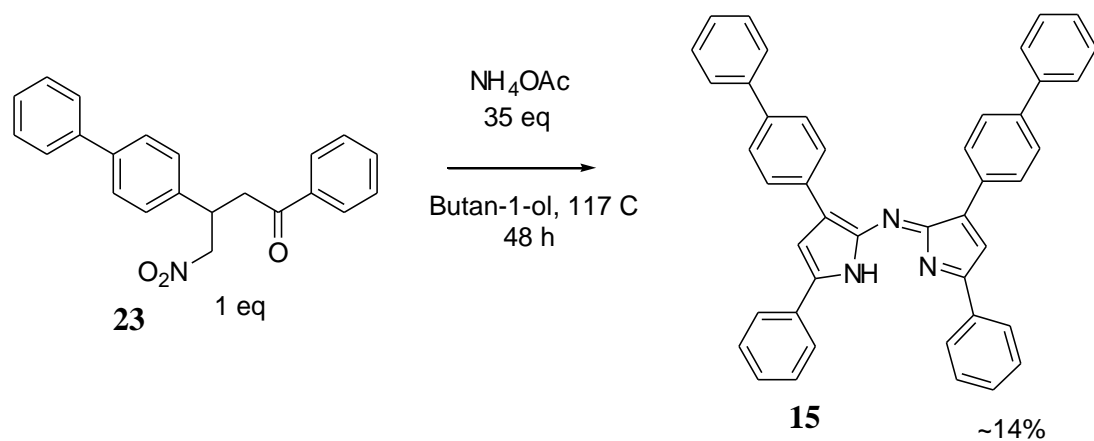
Scheme 7. *Step 3, synthesis of* **15**

The final step to achieve the aza-DIPY compound **15** (Scheme 7) was very low yielding (~14%). This was reported as the best yielding method for the synthesis of aza-DIPY by O'Shea and no further attempts were made to purify following washing with ethanol. Characterisation is difficult due to how insoluble the compound is in various solvents because of the high degree of conjugation. Chloroform was found to be the best solvent and the nmr is discussed (2.4.1) the mass spectra was obtained and confirms the molecular weight of the desired product.

2.3.2 Synthesis of Compound 16

To improve on the issues of insolubility and to attempt to create a photosensitiser with a different absorbance maximum an aza-DIPY compound with electron donating groups was selected, compound **16**. The synthesis was carried out using the same methods as described in the reactions in (2.2). Step 1 was the creation of a chalcone **32** similar to compound **22** but with an additional ether substituent in the para position of the acetophenone **31**.
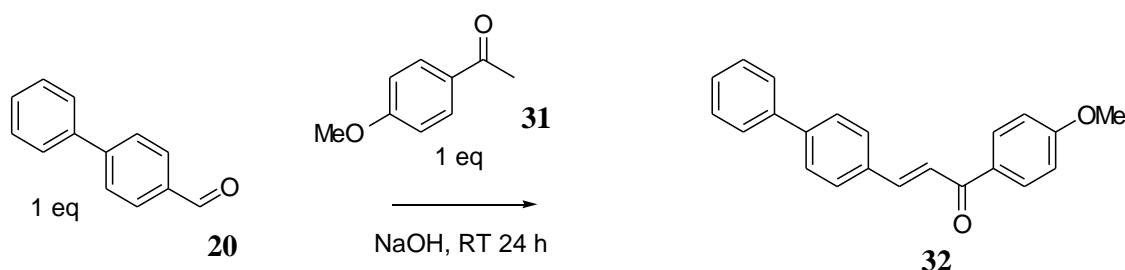
Scheme 8. *Step 1, synthesis of* **32**

There was a similar yield of 74% for a yellow precipitate in the first step (Scheme 8), with full characterisation carried out as before (2.4.2).
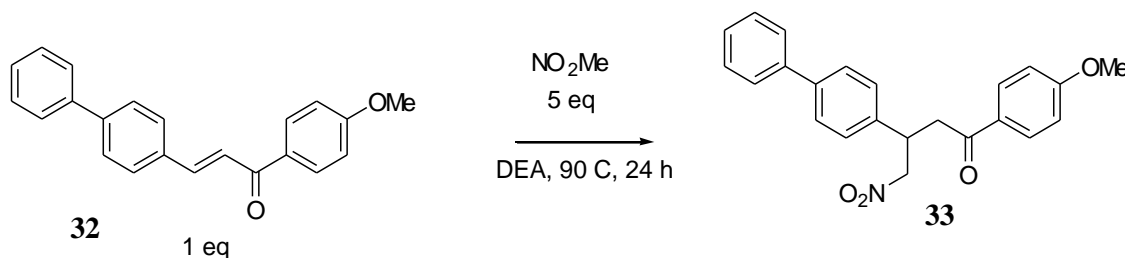
Scheme 9. *Step 2, synthesis of* **33**

The nitration afforded a brown solid **33**, compound (yield 75%), (scheme 9) and characterisation is discussed in (2.4.2).
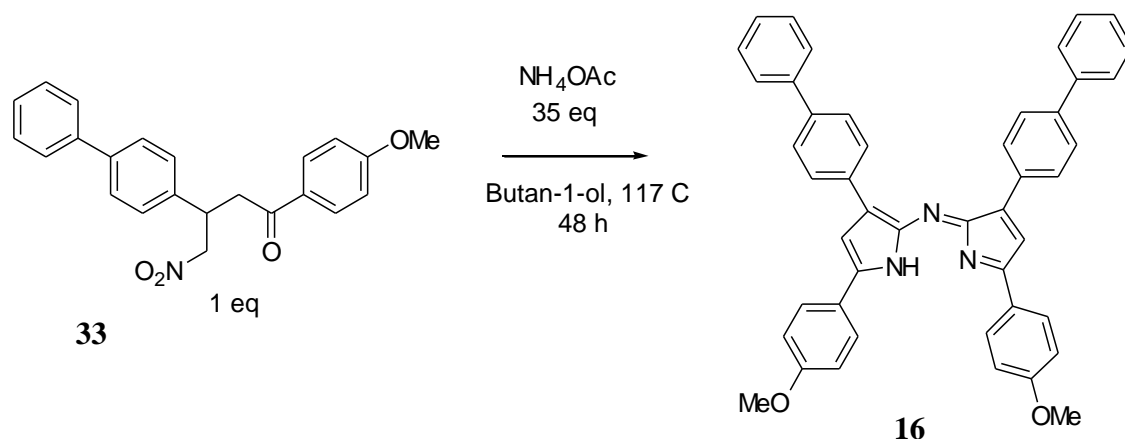
Scheme 10. *Step 3, synthesis of* **16**

The final step was carried out using the product of step 2 (Scheme 9) unpurified and the blue/violet solid formed **16** (yield 10%) was washed in ethanol without further purification, using the reaction conditions described above (scheme 10). Characterisation is discussed in (2.4.2).

2.3.3 Synthesis of Compound 17

Treatment of the aza-DIPY with the lewis acid BF_3OEt_3 was attempted to try to generate the structurally more stable chelate with boron.
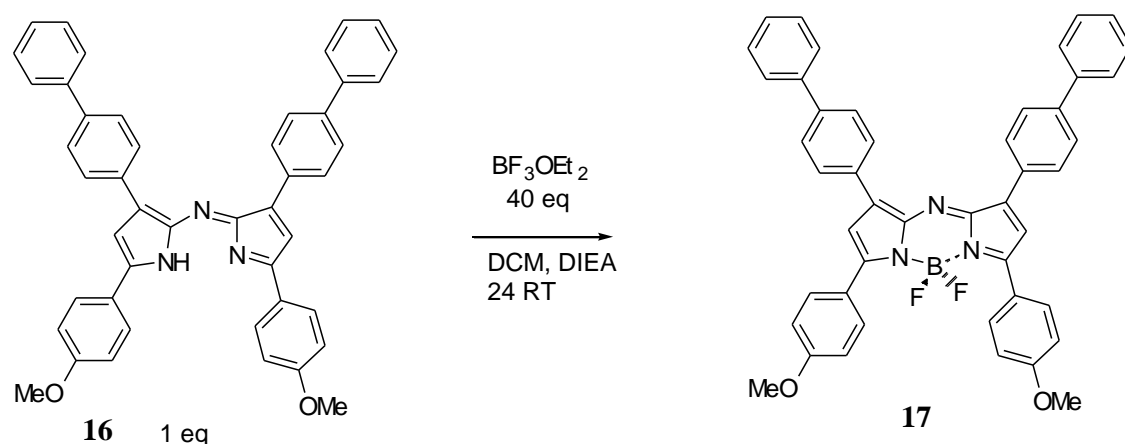
Scheme 11. *Reaction conditions for attempted chelation with boron*

This step proved difficult with no conversion of the starting material into product. A ^{19}F nmr spectrum was taken of the BF_3OEt showing a singlet peak at -153 ppm which is the expected

chemical shift of the equivalent fluorine atoms. There were no other peaks in this spectrum so decomposition of the reagent was ruled out as a possibility for unsuccessful synthesis.

2.3.4 Synthesis of Intermediate for 18

Using the same methods as the previous aldol condensation three intermediates were attempted to give a chalcone that contained a pyridine group (Scheme 12). This would lead to a sensitiser that contained a pyridine group to try to introduce receptors.
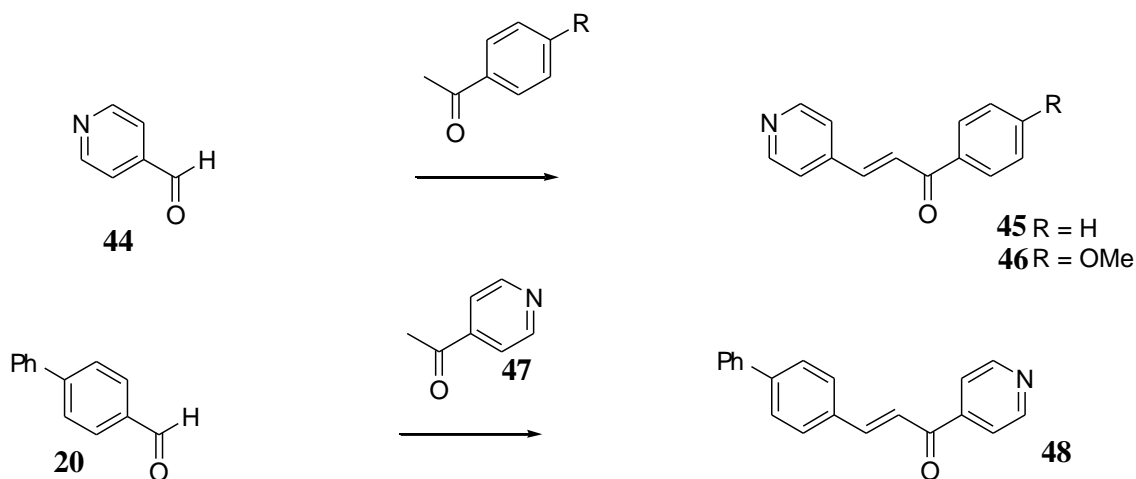
Scheme 12. *Aldol condensation step with various substrates.*

No consumption of starting materials was observed when trying to synthesise the chalcone **45** from 4-pyridine carboxaldehyde **44**. The reaction was attempted using 4-methoxyacetophenone to see if the introduction of an activating group on the aromatic ring of the ketone improved the reactivity. The methoxy chalcone **46** was not observed. Finally the reaction was attempted using a ketone with a pyridine group to give the chalcone **48**. There was no consumption of starting materials again for this reaction so it was decided to vary the reaction conditions (see Appendix 1).

After attempting several different methods,[51,52,53] the chalcone **45** was synthesised and purified by column chromatography. There was a very low yield from the reaction so the optimum reaction conditions have not been found. See section (2.4.3) for spectra.

2.3.5 Synthesis of Intermediate for 19

In addition to the synthesis of initially aza-DIPY compounds that are conjugated enough to absorb above 600 nm. The inclusion of receptors was desired to create potentially more useful compounds.

One possible receptor for ions such as Na$^+$ or Ca^{2+} is a crown ether. The crown ether should quench the phosphorescence in the target molecule by PET when the concentration of these ions is low.
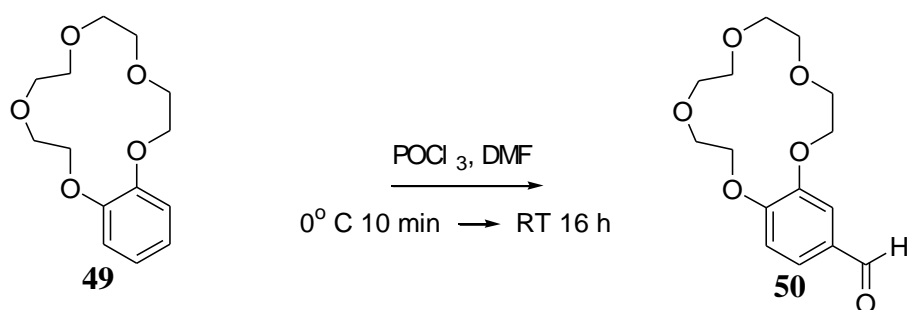
Scheme 13. *Vilsmeier reaction*

Due to the expense of buying an aldehyde already containing a crown-ether, the Vilsmeier reaction was attempted on the benzo 15-crown-5 ether. After several attempts to synthesise[30] the 4'-formylbenzo-15-crown-5, with no formylation of the starting material observed by nmr, the aldehyde was then bought from Sigma-Aldrich.
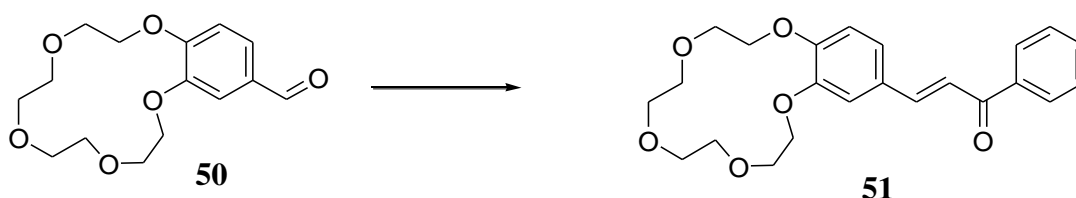
Scheme 14. *Step 1, synthesis of* **51**

The aldol condensation of the 4'-formylbenzo-15-crown-5 with acetophenone was attempted using the reaction conditions used previously with NaOH at RT for 24 h. The synthesis did not give a high yield of crude product. (see 2.4.4.)

37

2.4 Characterisation of Compounds

2.4.1 Characterisation of Compounds Involved in Synthesis of 15

The structure of compound **15** was determined using nmr experiments; ^{1}H nmr, ^{13}C nmr, COSY, HSQC.

The chalcone product of the first reaction consists of an alkene, meaning that there are two isomers possible- the (*E*)-isomer and the (*Z*)-isomer. The (*E*)-isomer is the expected isomer since the reaction is occurring under thermodynamic conditions i.e. the more stable product is expected. Since the (*E*)-isomer is desired for our synthesis we need to prove that the correct isomer has been synthesised. This can be done by comparing the coupling constants of the between the two protons.

22
(*E*)-isomer

52
(*Z*)-isomer
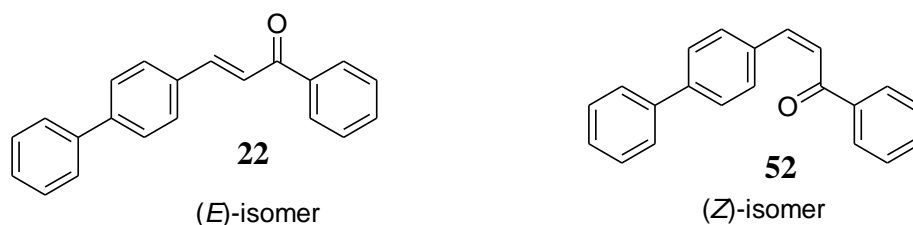
If an (*E*)-isomer **22** has been formed a *trans* coupling constant of $J = 14\text{-}18$ Hz would be found in the ^{1}H nmr spectrum and if a (*Z*)-isomer **52** had been formed a coupling constant of $J = \sim 8$ Hz would be expected. From the COSY spectrum (Figure 7) two peaks were found in the aromatic region with doublet multiplicity coupling with each other, **i** and **j**. (Compound **22** redrawn in Figure 8 with specific hydrogens and carbon atoms labeled for ease of view). When the coupling constants of these two peaks were measured in the ^{1}H nmr spectrum (Figure 10) they had identical coupling constants of $J = 15.7$ Hz indicating the E isomer had been successfully synthesised. From the COSY spectrum (Figure 7) other peaks such as the coupling between the

38

ortho proton **m**; and the meta **n** and para **o** protons can be observed. Using the COSY spectrum along with the HSQC spectrum the peaks in the ^{1}H nmr (Figure 10) and the ^{13}C nmr (Figure 9 and Table 1) were assigned for **22**.
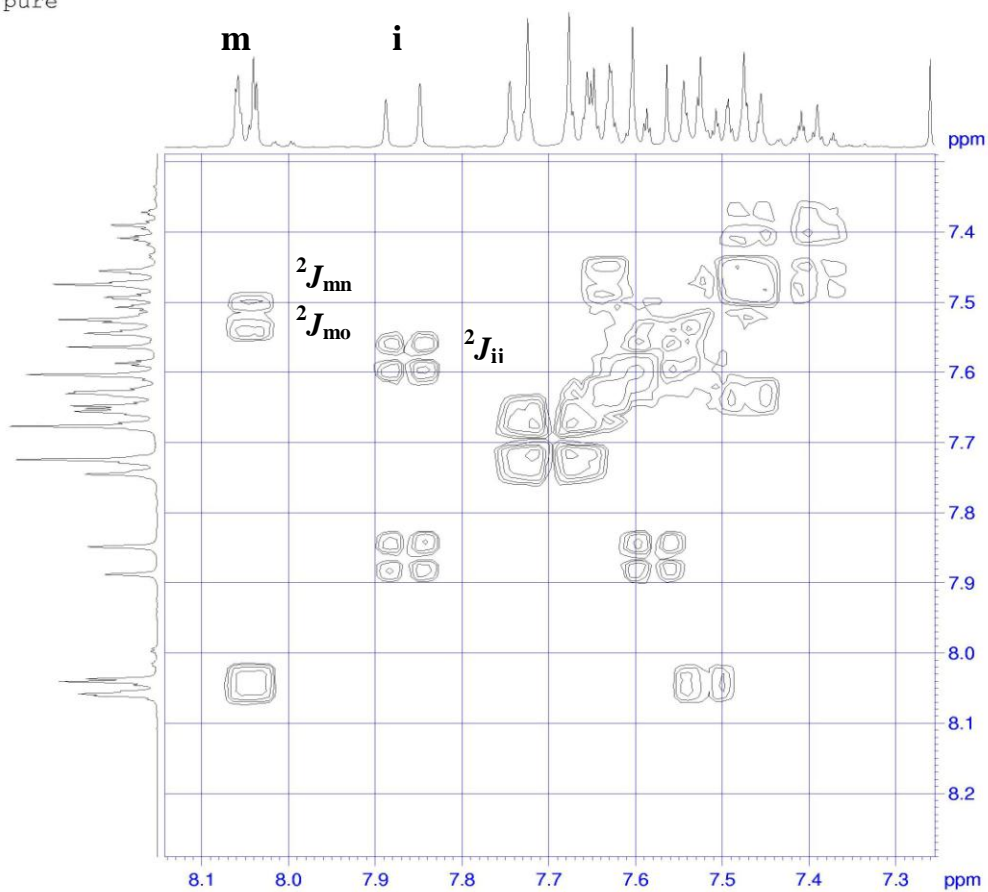
Figure 7. *COSY spectrum of* ***22***
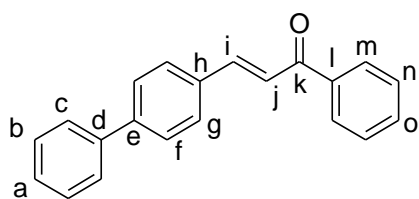
Figure 8. *Compound* ***22*** *with specific hydrogens labeled* ***a-o*** *for clarity.*
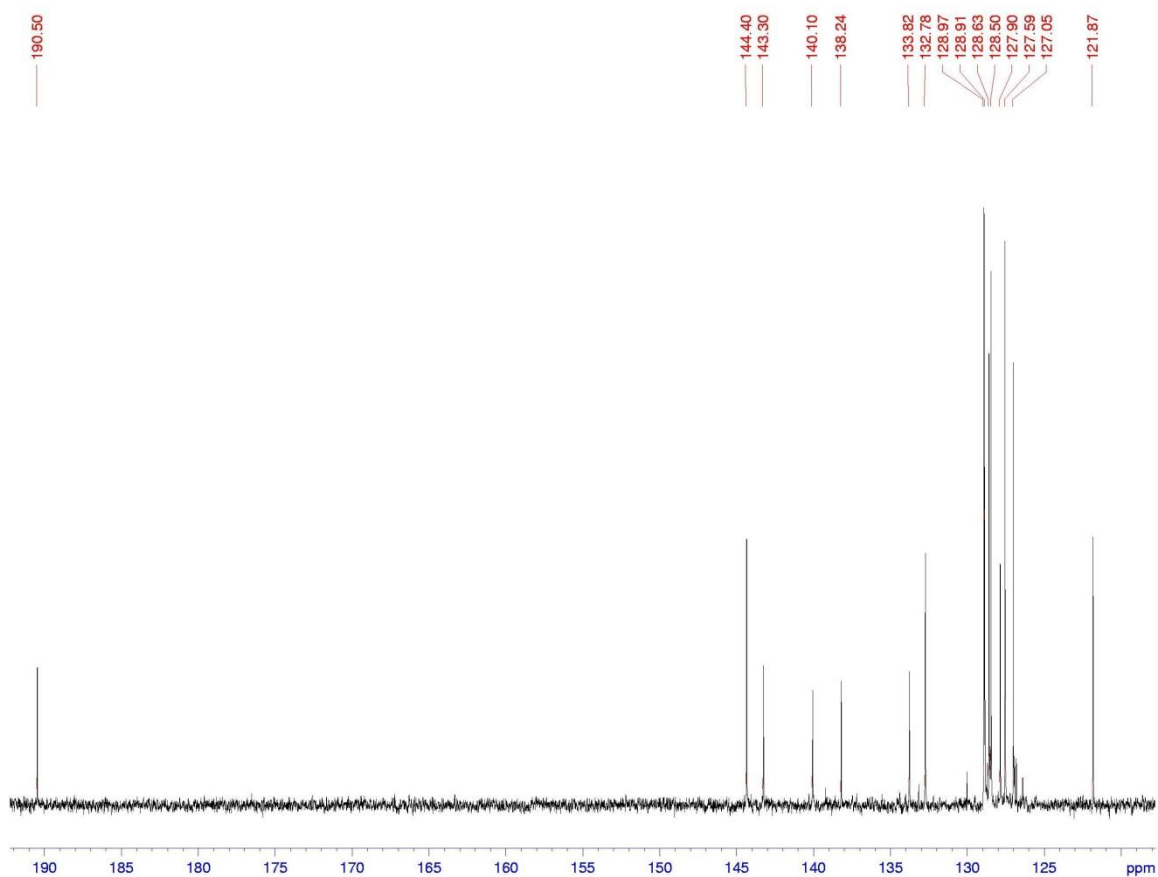
Figure 9. *^{13}C nmr spectrum of* **22**.

Table1. *Chemical shifts of the corresponding peaks shown in Figure 9*

Chemical Shift (ppm)	Carbon atom	Chemical Shift (ppm)	Carbon atom
190.5	k	129.0	a
144.4	i	128.9	f
143.3	l	128.6	n
140.1	d	128.5	m
138.2	e	127.9	b
133.8	h	127.6	g
132.8	o	127.1	c
		121.9	j
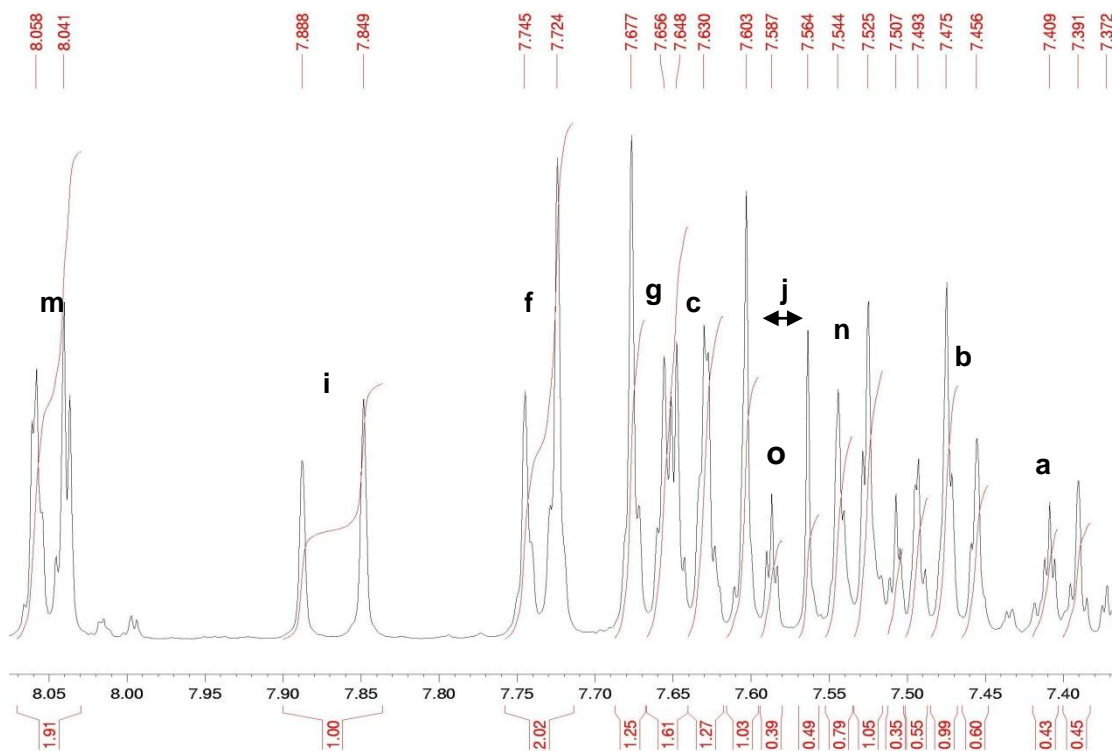
Figure 10. *¹H nmr spectrum of **22** showing the protons in the aromatic region*

The second intermediate of the reaction scheme was generated by the addition of nitromethane to the alkene group, Figure 11.
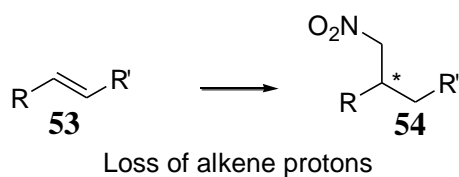
*chiral centre

Figure 11. *Nitromethane intermediate resulting in the loss of unsaturated bond*

This means that the characteristic peaks from the trans coupling of the previous intermediate **22** will disappear in the aromatic region of the ^{1}H nmr spectrum of **23**. In addition there shall be 5 new peaks in the aliphatic region of the spectrum due to non-equivalent protons created by the presence of a chiral centre. If there was no chiral centre we would expect to see only 3 peaks with a simplified multiplicity e.g. a doublet with an integration of 2H for the C$\underline{H}_2$NO$_2$ peak.

     As expected the two peaks corresponding to alkene protons were not observed in the aromatic region of the ^{1}H nmr spectrum of **23** (nmr spectrum displayed in Figure 13 with Compound **23** redrawn in Figure 12 with specific hydrogens labeled for ease of view). The integration of the protons in the aromatic region revealed 14 protons, as expected for the product **23**. In the aliphatic region of the spectrum (Figure 14) there were five peaks. The first two peaks at **p** and **p'** corresponded to the C$\underline{H}_2$NO$_2$ as would be expected due to the strong electronegative nitro group that would de-shield the protons on this carbon atom the most. The chiral proton at **i** has a complex multiplicity due to the interaction of 4 neighbouring protons. The last two, doublet of doublet peaks **j** and **j',** correspond to C$\underline{H}_2$CO.

43
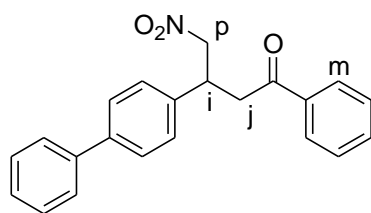
Figure 12. Compound *23* with specific hydrogens labeled *i*, *j*, *p* and *m* for clarity.
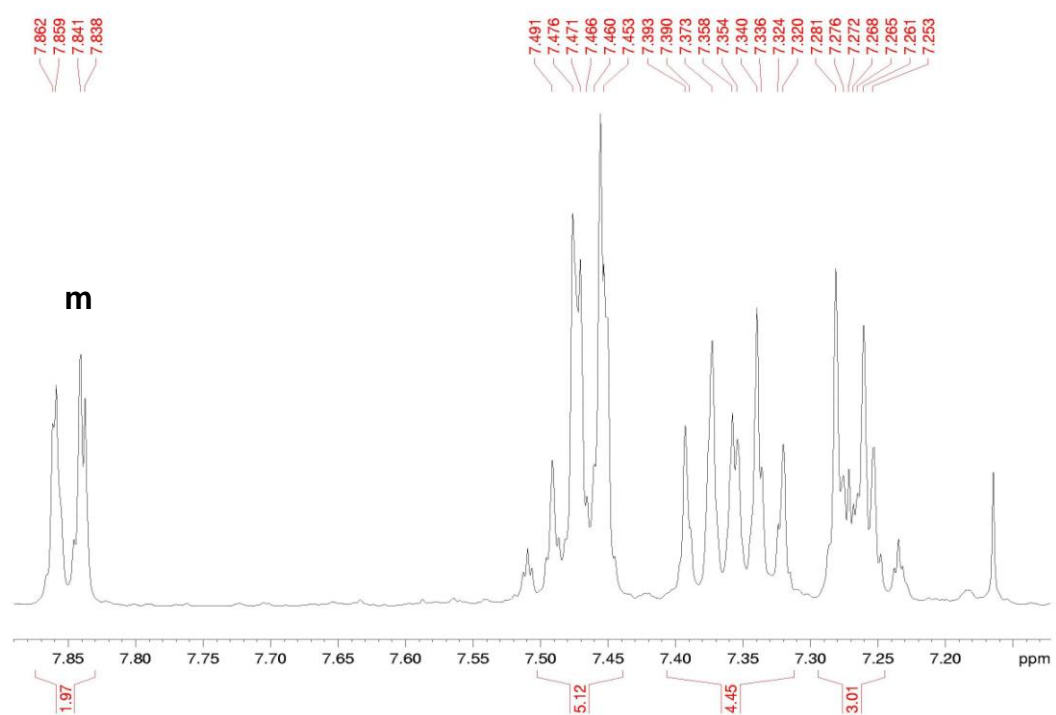
Figure 13. ^1H nmr spectrum of *23*, showing the aromatic region
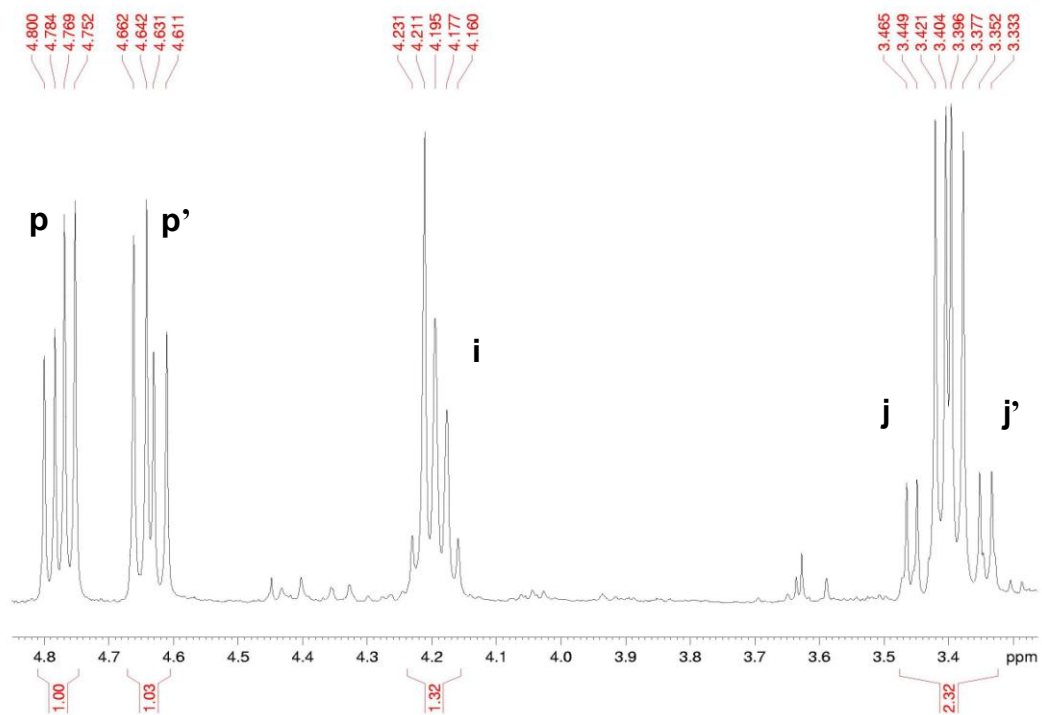
Figure 14. *¹H nmr spectrum of **23**, showing the aliphatic region*
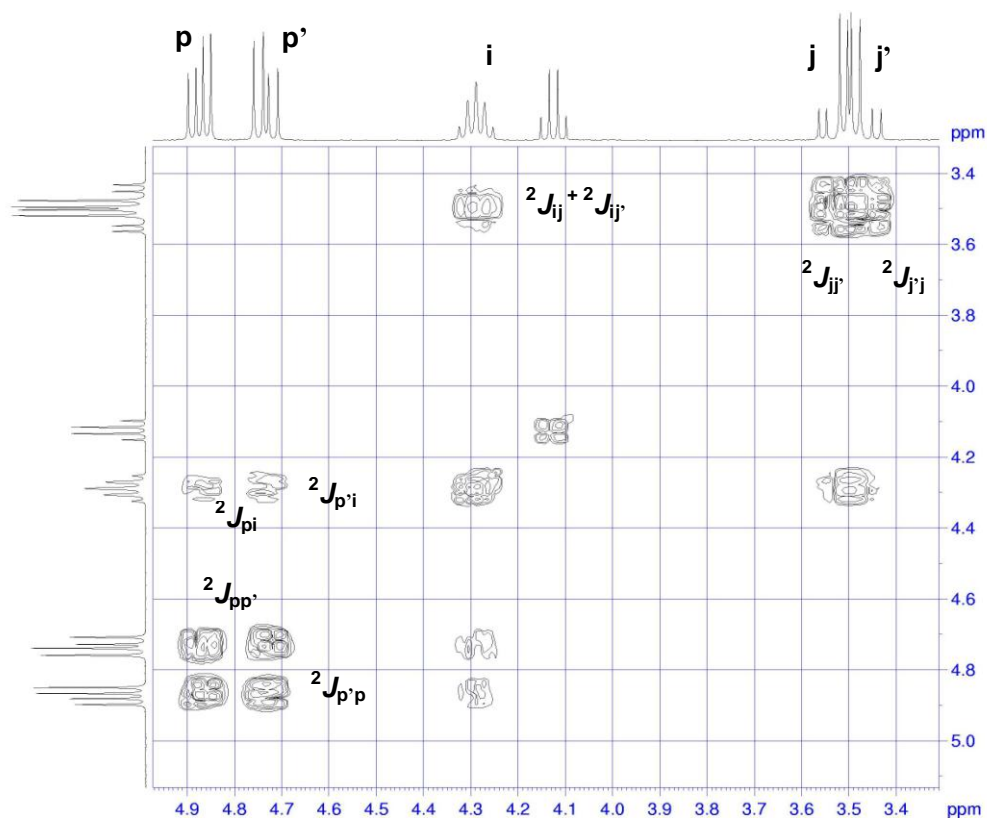
Figure 15. COSY spectrum of **23** showing the aliphatic region of the ^{1}H nmr

The ^{1}H nmr for **15** (Figure 16) showed only 6 multiplet peaks in the aromatic region, as we would expect since the compound is completely conjugated. This also indicates that there is no substrate **23** and that the peaks that are observed are from a different compound that has been synthesised. As **15** is highly conjugated it is very insoluble, but interpretation of the spectrum can still be made. The product is symmetrical so we would also expect that the protons at the plane of symmetry on the bridging nitrogen would be equivalent, therefore the number of protons that we are expecting to see are 15. From the integration of the spectrum, we have 15 protons, although assignment cannot be made due to the signals appearing as multiplets.
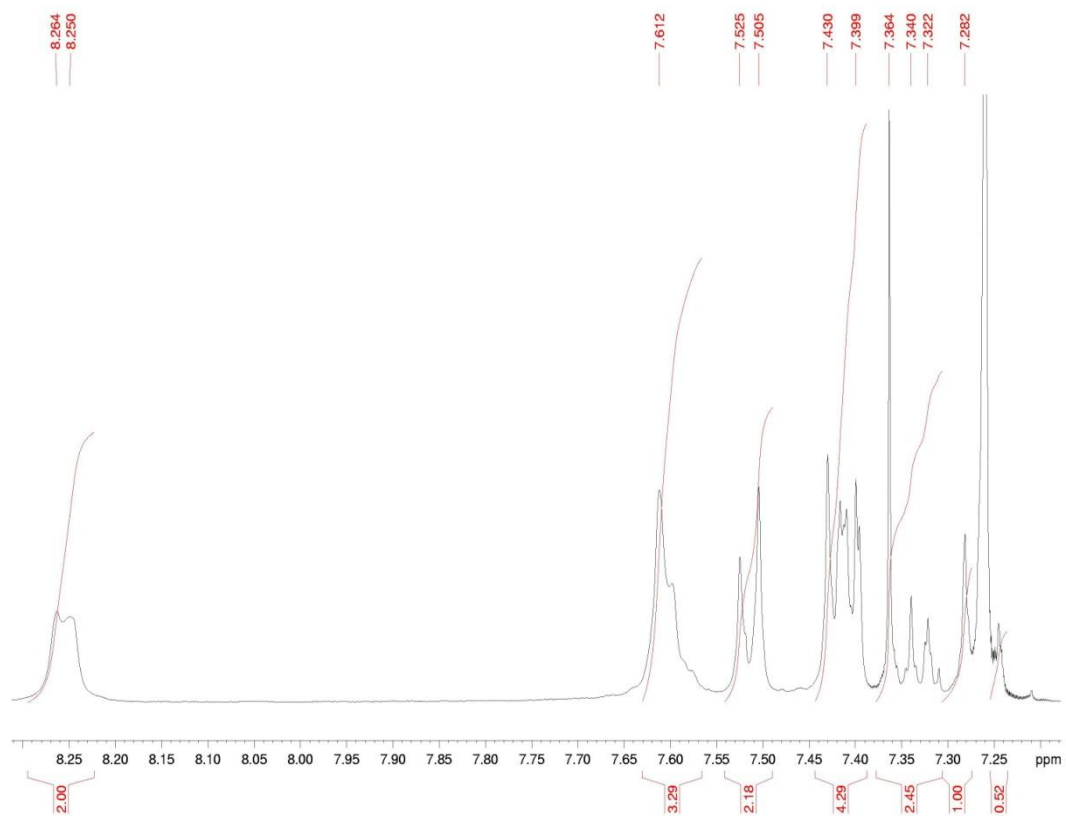
Figure 16. *^{1}H nmr spectrum of* ***15***

A mass spectrum was also obtained (Figure 17) where the molecular weight of **15** (601.3 Da) was observed.
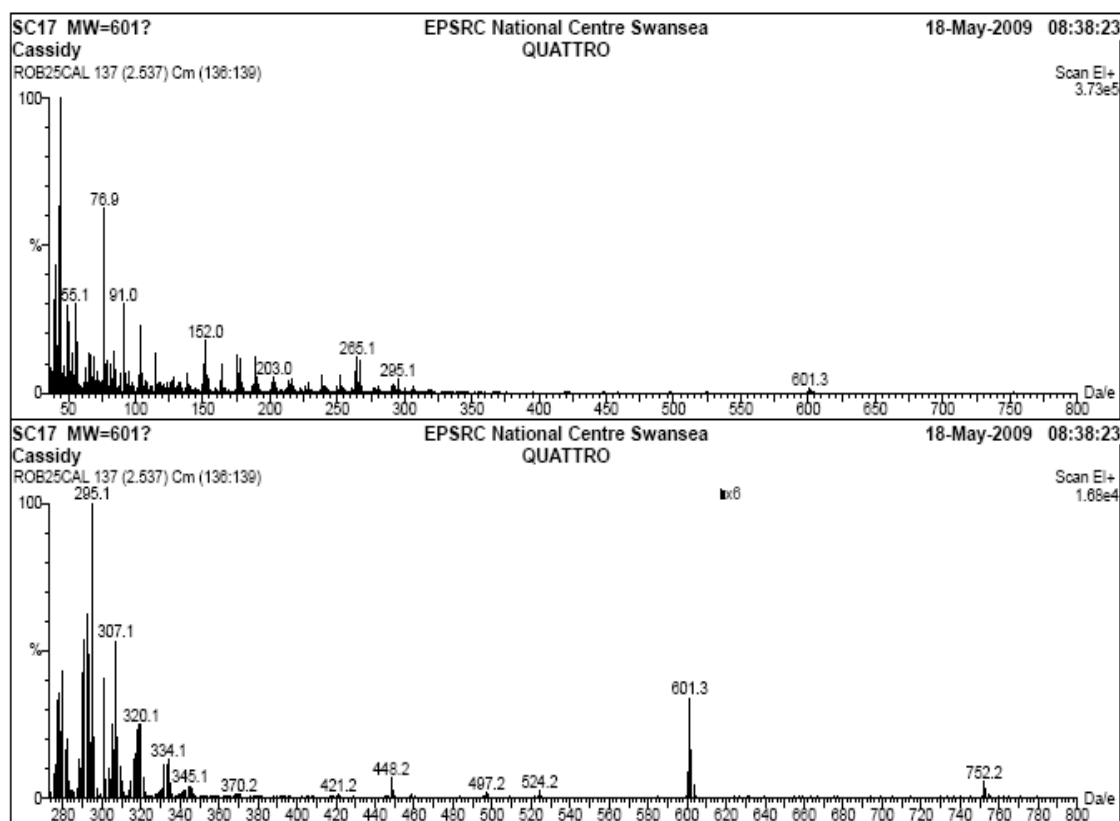
Figure 17. *Mass spectrum showing a peak for the molecular weight of **15** at 601.3 Da*

2.4.2 Characterisation of Compounds Involved in Synthesis of 16

As discussed for **22** (2.4.1) the characteristic peak for the product of the first reaction was the trans coupling observed in the aromatic region of the ^{1}H nmr spectrum. This was also observed for the olefinic group in the spectrum of **32** (Figure 19 with Figure 18 showing Compound **32** with specific hydrogens labeled) in addition to the C$\underline{H}_3$ singlet peak, **p,** more downfield in the spectrum due to the electronegetivity of the oxygen atom. The full characterisation of **32** was determined using nmr experiments in the same way as for **22** and the ^{1}H nmr spectrum (Figure 19) is fully labeled.
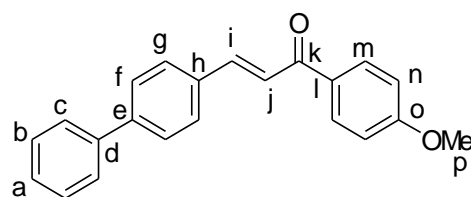
Figure 18. Compound 32 with each non-equivalent hydrogen atoms labeled for characterisation.
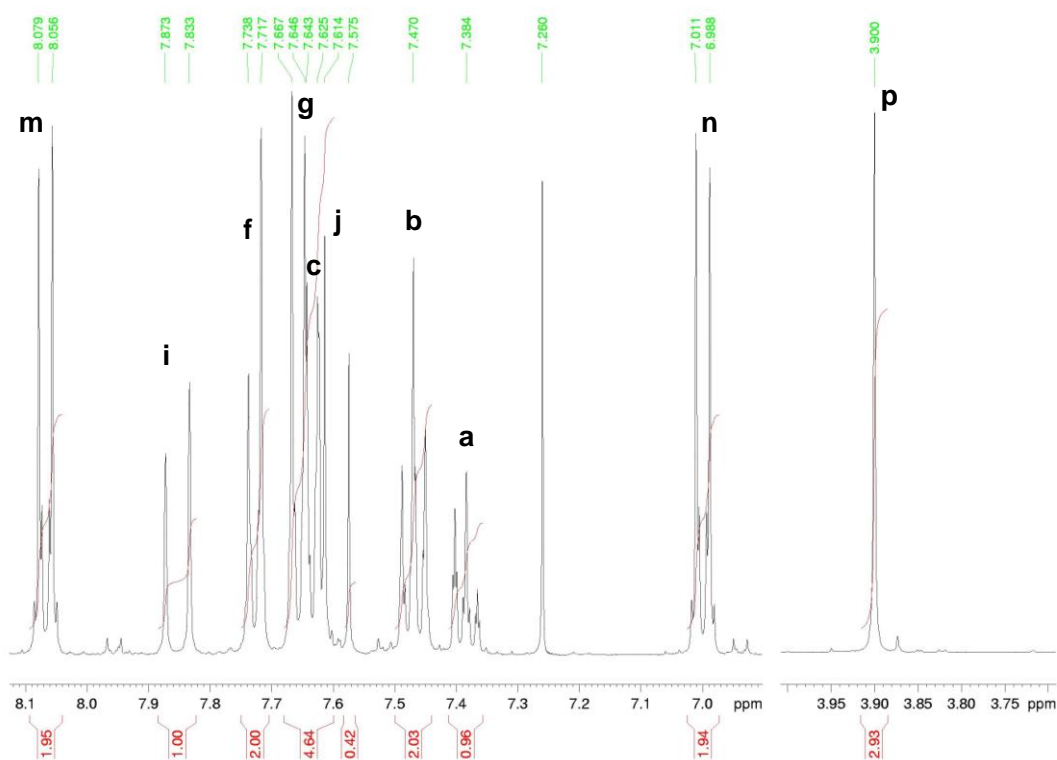
Figure 19. ¹H nmr spectrum of 32, each proton peak has been assigned and labeled according to Figure 18.

The aromatic region of the nmr spectrum of compound **33** (Figure 21), displays the loss of the *trans* protons and the distinctive *ortho* coupling, **m**, still remaining. The integration of the signals gives 13 aromatic protons as expected for **33**, with Figure 20 displaying the labeling used in compound **33**.

49
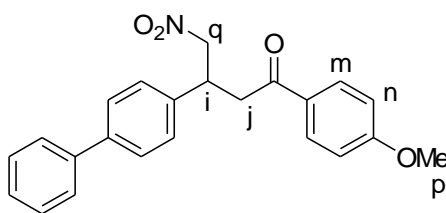
Figure 20. *Compound **33** with specific hydrogen atoms labeled for identification*
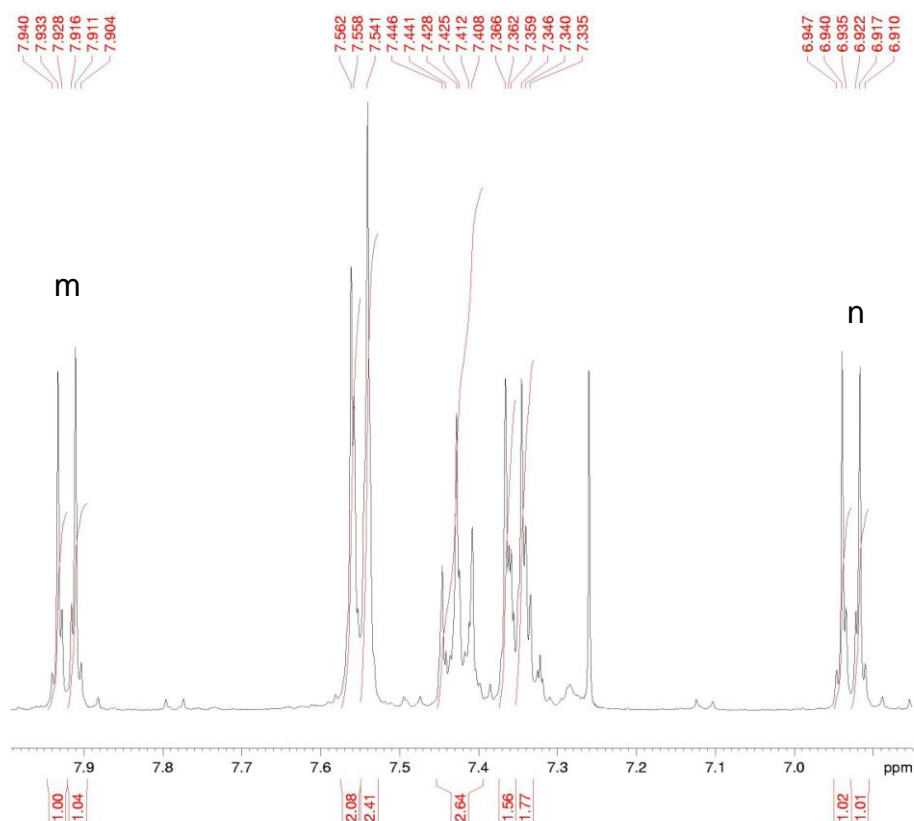
Figure 21. *^{1}H nmr spectrum of **33** highlighting the aromatic region of the spectrum*

Figure 22 displays the aliphatic region of the proton nmr for compound **33**. As expected, there are an increased number of peaks in this region when compared to **32**. The reduction of the C-C bond at **i** and **j** caused by the Michael addition has resulted in the signals for these protons increasing in number and shifting upfield, in addition there has been a new C-C bond created resulting in a further CH$_2$ group, the hydrogen atoms of which have been assigned the label **q**.
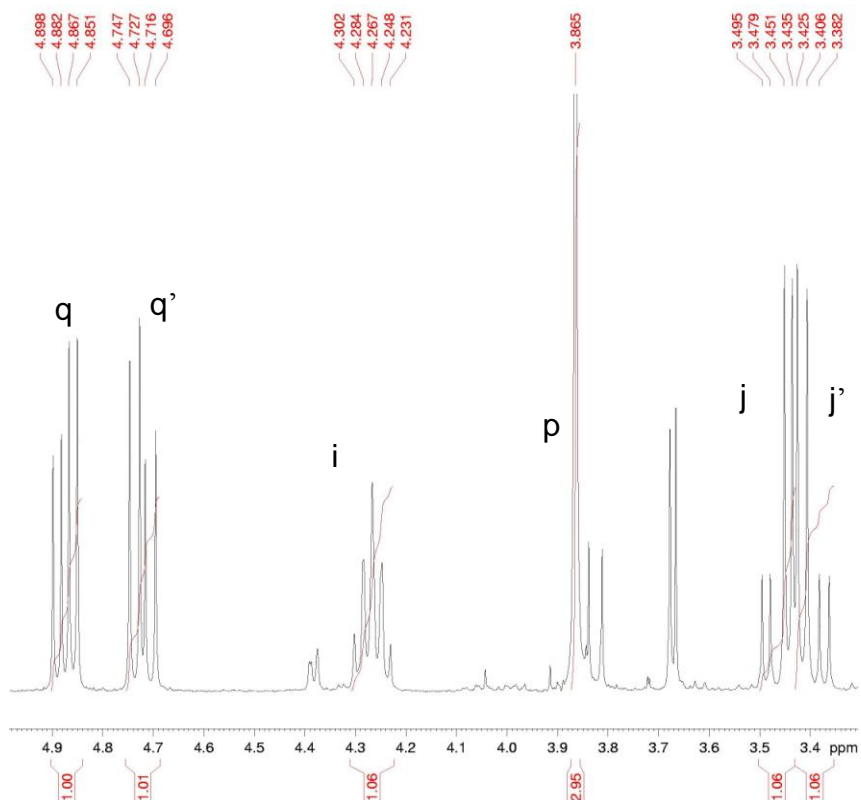
Figure 22. *¹H nmr spectrum of **33** highlighting the aliphatic region*

In the ¹H nmr of **16** (Figure 23) there are 6 multiplet peaks in the aromatic region again as expected and observed in the ¹H nmr of **15** (Figure 16). The singlet peak at 3.93 ppm corresponds to the methoxy protons of **16**, having an integration equivalent to 3 protons. The integration of the aromatic peaks in Figure 23 shows 14 aromatic protons for **16** this corresponds to the 14 equivalent protons expected.
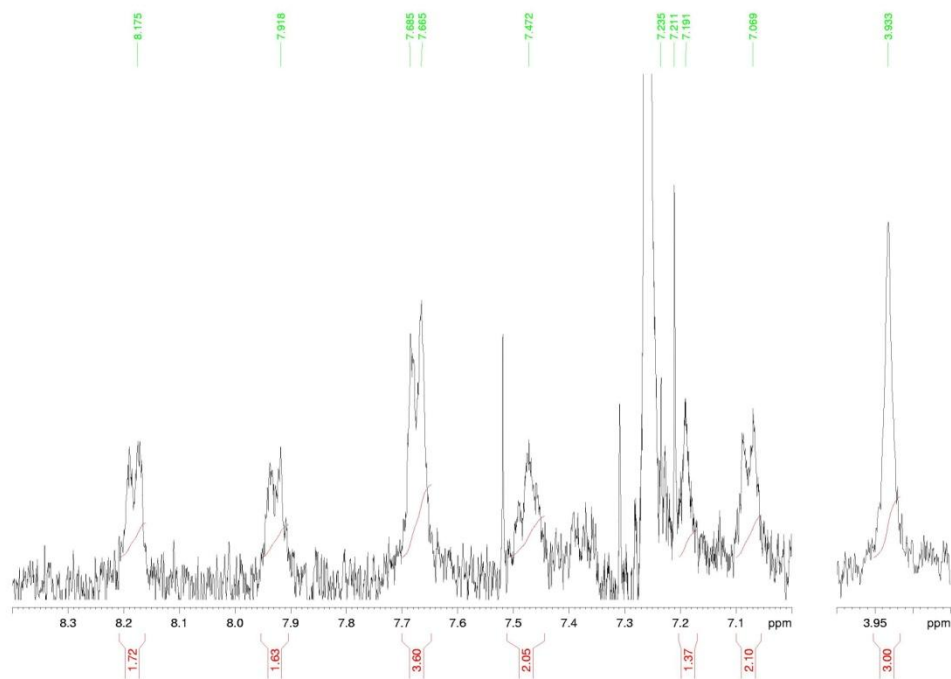
Figure 23. *¹H nmr spectrum of **16***

2.4.3 Characterisation of 45

The ¹H nmr of **45** was evaluated and the compound determined to be pure. Figure 24 displays

the structure of compound **45** with the characteristic hydrogen atoms labeled. Figure 25 displays

the aromatic region of the proton nmr with peaks assigned to the labeled hydrogen's **h, j** and **b**.
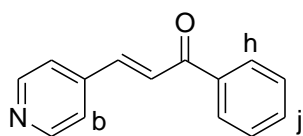
Figure 24. *Structure of **45** with labeling of specific hydrogen atoms*
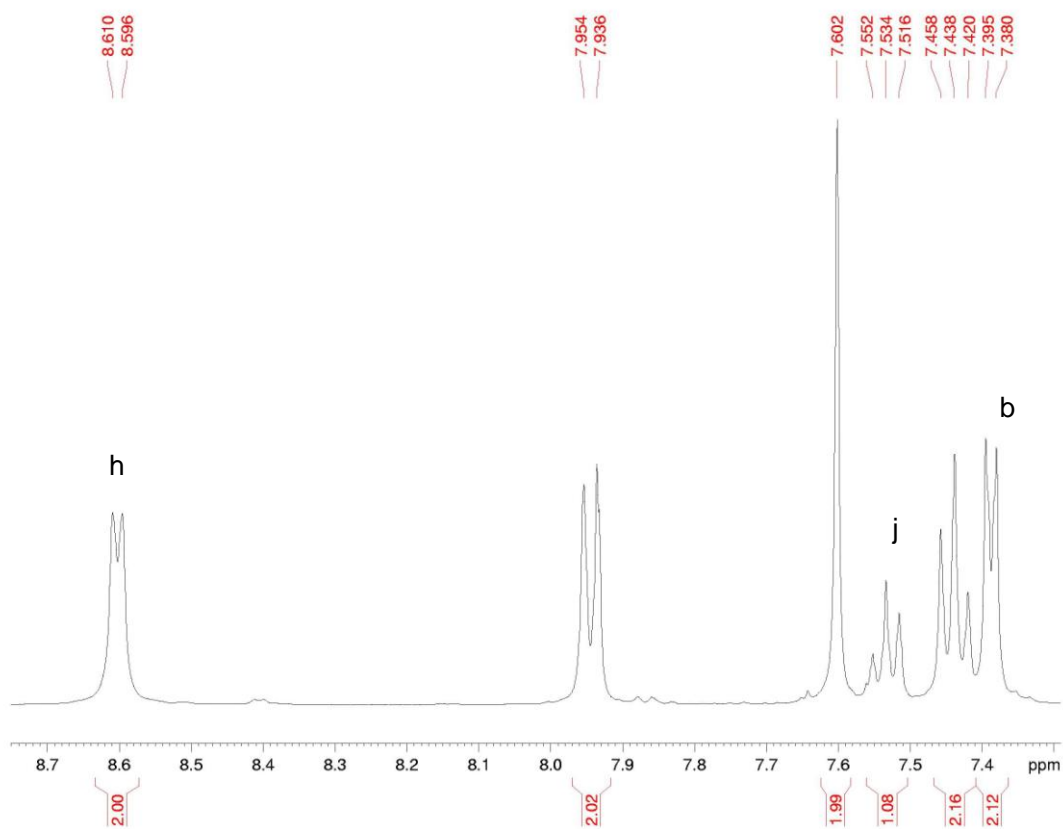
Figure 25. *¹H nmr spectrum of **45***

The molecular weight of compound **45** was determined and as mass spectrum in Figure 26 displays, the parent m/z peak of 210.2 Da shows the most abundant peak as that of the molecular weight of **45** plus one.
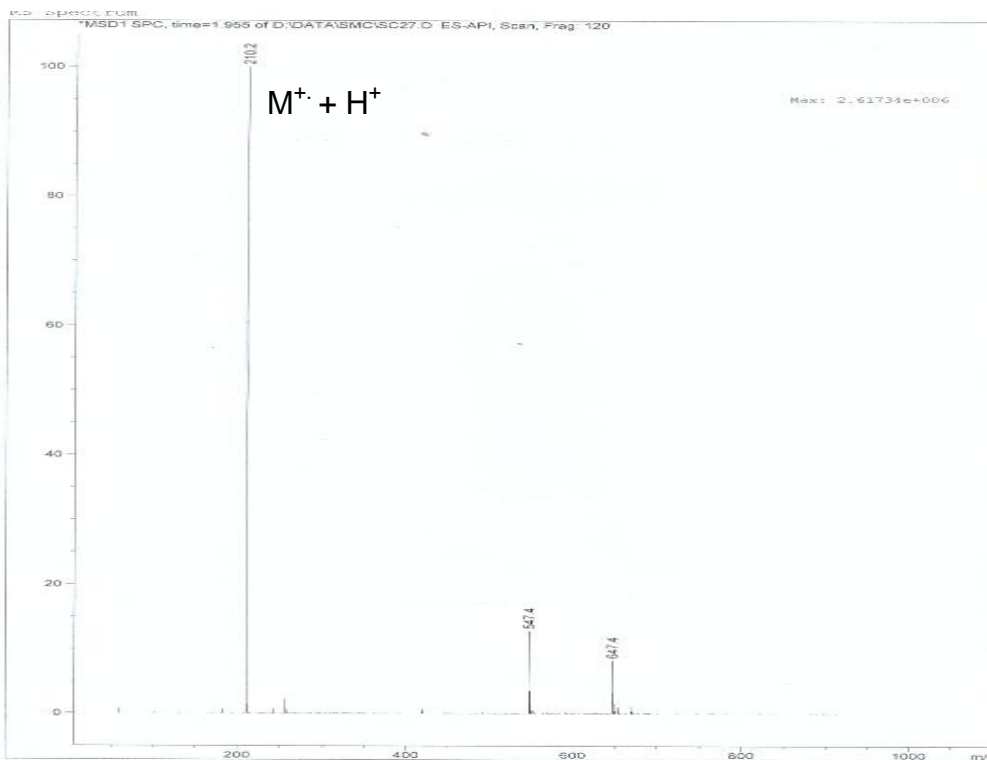
Figure 26. *Mass spectrum of* **45**

2.4.4 Characterisation of Compound 51

The ^{1}H nmr of **51**, Figure 27, indicates that the aldehyde proton from the starting material is no longer present in the spectrum of **51**. This suggests that one of the starting materials has been consumed in the reaction. However, the spectrum is not detailed enough to confirm the structure of the product as **51**. When the mass of the compound was determined, Figure 28, the mass spectrum shows the major peak as the molecular weight of **51** plus a proton (m/z 399 Da), indicating that **51** has been synthesized but will need to be purified before further synthesis can done.
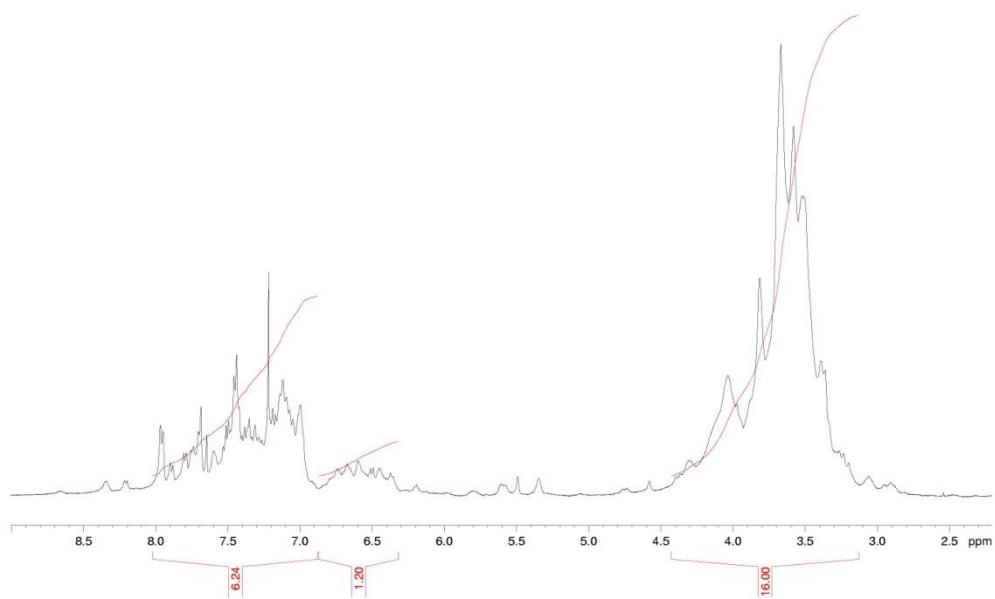
Figure 27. *¹H nmr of* **51**

M⁺· + H⁺
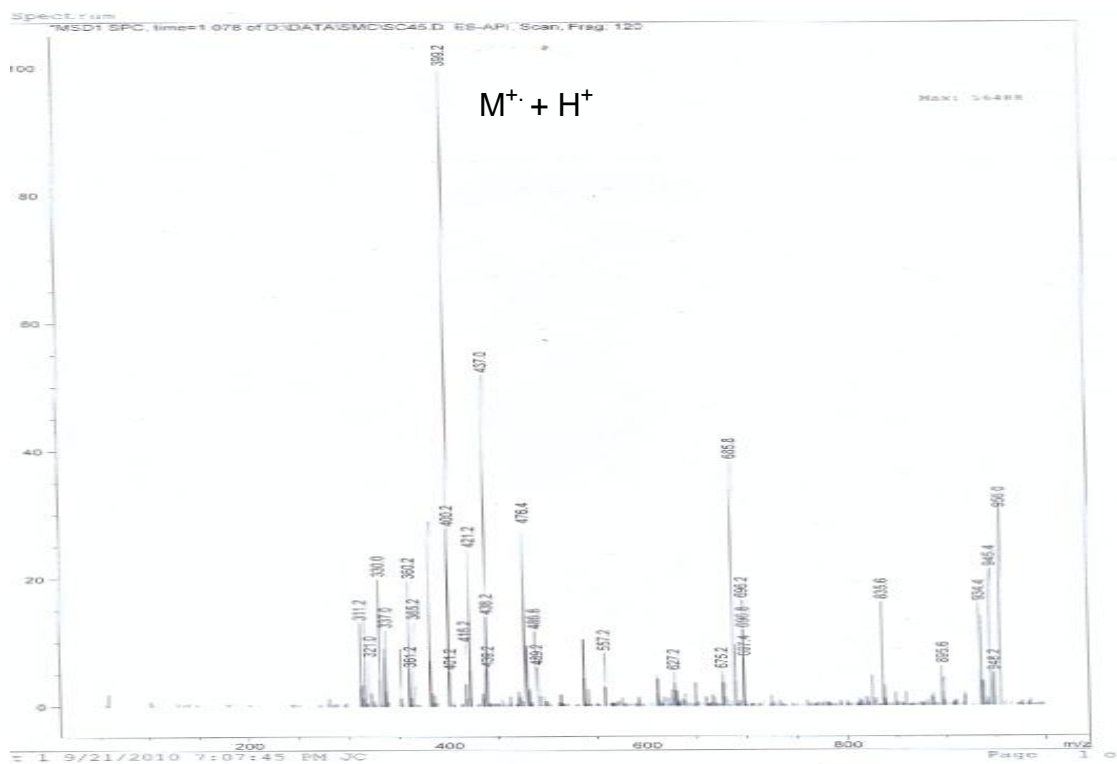
Figure 28. *Mass spectrum of* **51**

Chapter 3

Photophysical Evaluation

3. 1 Introduction to Photophysical Evaluation

The driving force behind the synthesis of compounds **15 – 19** was the generation of novel, more efficient and potentially selective photodynamic agents for use in PDT. Currently in the UK alone there are over 260 new photosensitisers in clinical trials for potential application in PDT.[9] It is of great importance therefore, to have some degree of selection process whereby only the very strong candidates will progress to clinical trials. This can be achieved through the photophysical evaluation of test compounds. From chapter 2, it was concluded that only compounds **15** and **16** were pure and efficiently uncomplicated in their synthesis to allow for further investigation. By the collection of the absorbance and emission spectra of the two compounds the appropriate wavelength of light required for the PDT process can be determined, as well as gaining some information regarding the relaxation process of the excited fluorophore. Finally, the compounds will be investigated as potential singlet oxygen generators. It is imperative that the new PDT agents have the ability to generate sufficient phosphorescence in order to transform the surrounding molecular oxygen into the cytotoxic reactive species that has the ability to destroy the damaged tissue as this underpins the PDT mechanism.

3.2 Absorbance Measurements for Compounds 15 and 16

The absorbance spectra for each of the two novel photosensitisers were recorded in isopropyl alcohol (IPA) and the maximum wavelength determined. The spectrum for **15** is displayed in Figure 29 and **16** in Figure 30. The absorbance spectrum is as expected with little difference between the two compounds. Each compound has a rather broad absorbance spectrum; this would be as expected from the rather large conjugated area with the absorbance being red shifted to a maxima value greater than 600 nm. Both Figures 29 and 30 display an absorbance from the compounds at a wavelength as far shifted as 700 nm. This wavelength would be suitable for deeper tissue penetration than ordinarily used from PDT.

57
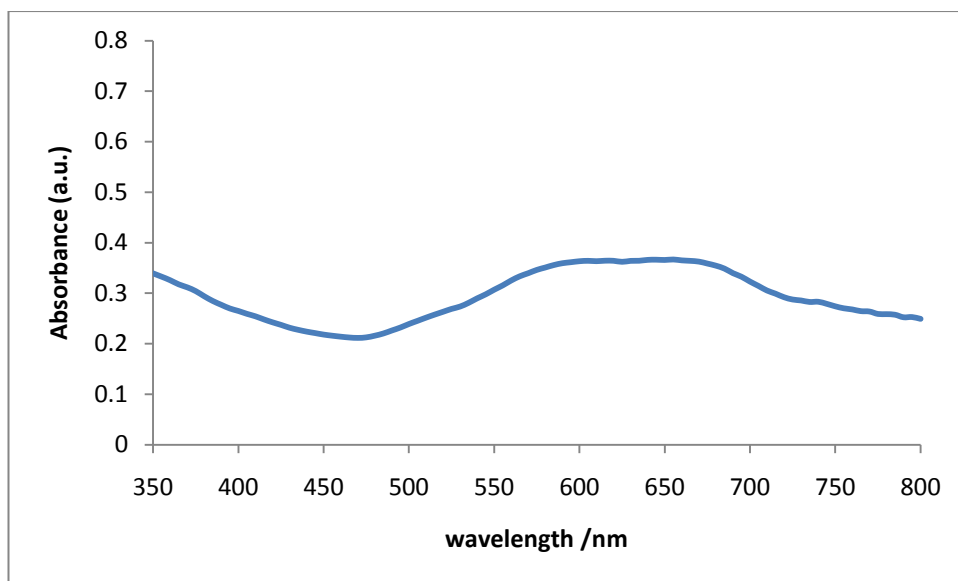
Figure 29. *Absorbance spectrum of **15** in IPA, absorbance maxima 660 nm.*
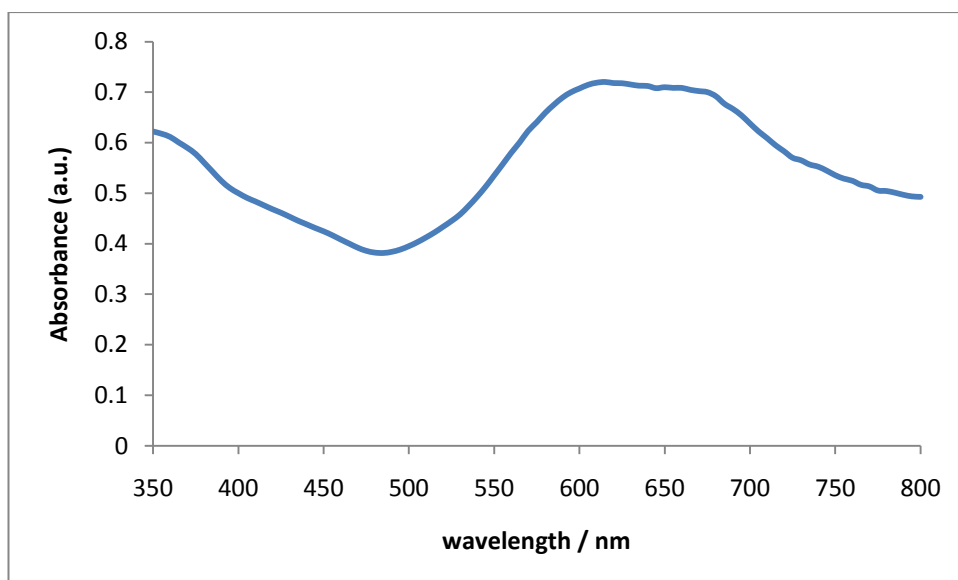
Figure 30. *Absorbance spectrum of **16** in IPA, absorbance maxima 625 nm.*

3.3 Emission Measurements for Compounds 15 and 16

Compounds **15** and **16**, as previously mentioned, contain an extended area of conjugation. This is typical for compounds capable of behaving as chromophores as it allows for effortless transitions between the electronic orbitals (n - π^* and $\pi - \pi^*$ transitions) as they contain relatively close packed band gaps. The emission spectrum attributed to the photosensitiser compounds will therefore be of interest in the determination of PDT agent efficacy.

In section 1.2 the mechanism of action for the transformation of molecular oxygen to the reactive oxygen species, singlet oxygen, is discussed. The requirements for the photosensitiser compound to undergo intersystem crossing and have an electron in the excited triplet state is paramount in the production of the cytotoxic agent. Evidence that the compound reaches the T_1 state would be if the compound emitted phosphorescence. Phosphorescence is much more difficult to measure than fluorescence due to the differences in lifetimes of the two radiative pathways. The lifetime of fluorescence emission is generally between $0.5 - 20$ nanoseconds where as the lifetime of a compounds phosphorescence can be anywhere ranging from milliseconds up to several hours. The fluorescence emission spectrum achieved will give an indication of the compounds ability to fluoresce and indirectly its ability to phosphoresce. Figure 31 displays the emission spectrum for a solution of **15** in IPA excited at a wavelength of 650 nm with Figure 32 displaying the emission spectrum of compound **16.** It can be concluded from the two spectra that neither compound effectively fluoresces.
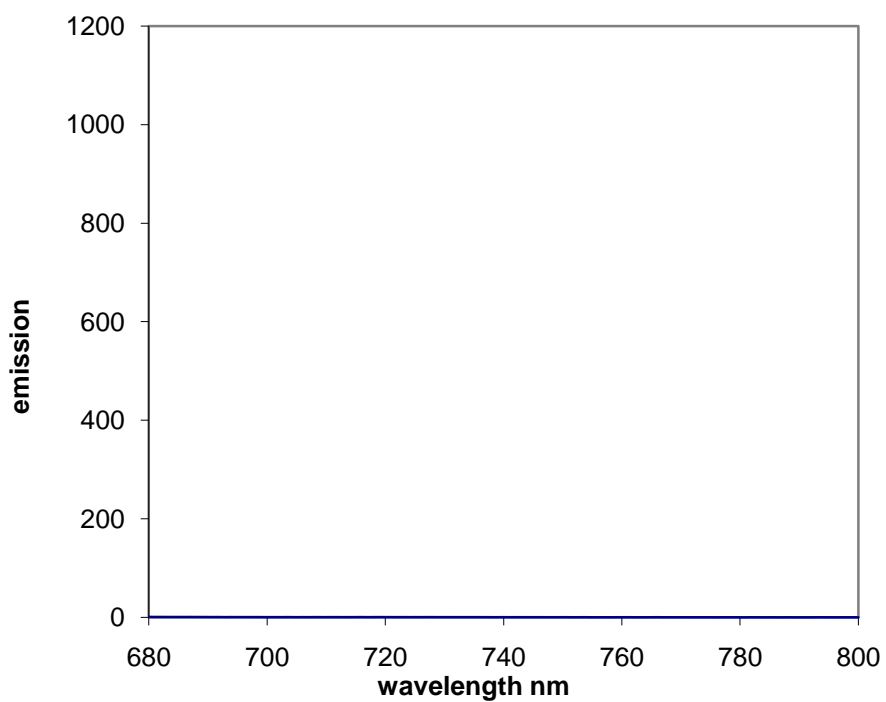
Figure 31. Emission spectra of 15 excited by fluorescence at 650 nm in IPA
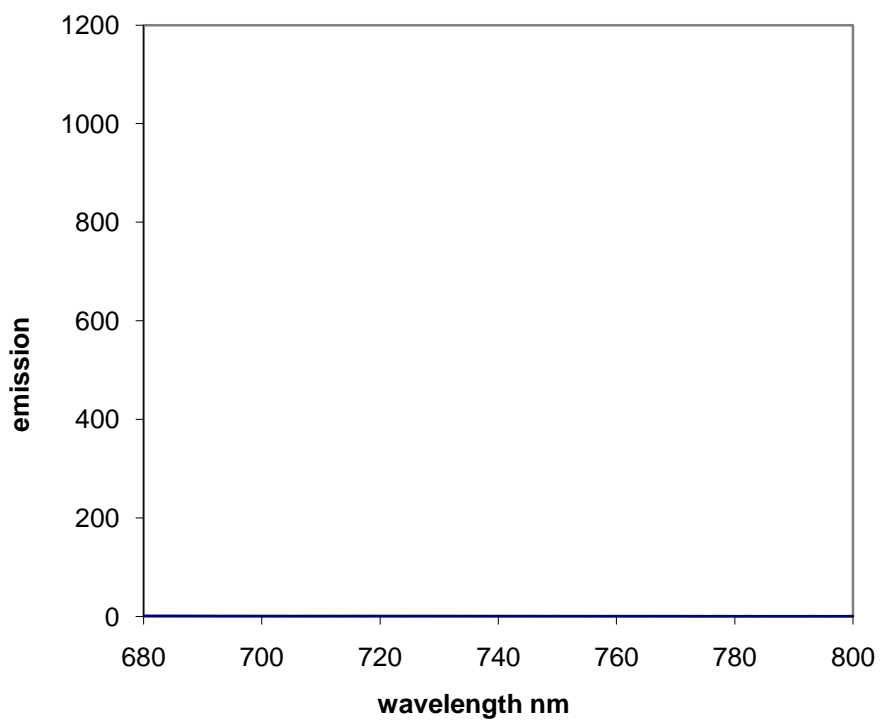
Figure 32. Emission spectra of 16 excited by fluorescence at 650 nm in IPA

60

3.4 Singlet Oxygen Generation

The efficiency of the photosensitisers **15** and **16** as potential PDT agents can be determined by their ability to generate singlet oxygen. There are a number of ways to quantitatively measure the production of singlet oxygen. Singlet oxygen has an emission wavelength of 1280 nm[54] and therefore can be directly detected with the appropriate spectrometer and filters. However, chemical trapping is the most common and sensitive technique used in the quantitative determination of this excited species.[55] These chemical traps are varied in structure and form a new species when in direct contact with singlet oxygen in an equimolar ratio. The detecting parameter is generally light, for example, fluorescence, as in the case for 2,7 dichlorodihydrofluorescein diacetate (DCFH-DA) , which has no fluorescence until it becomes oxidised by singlet oxygen to the fluorescent 2,7 dichlorofluorescein (DCF), Scheme 15.[56] The increase in emission is monitored at 525 nm.
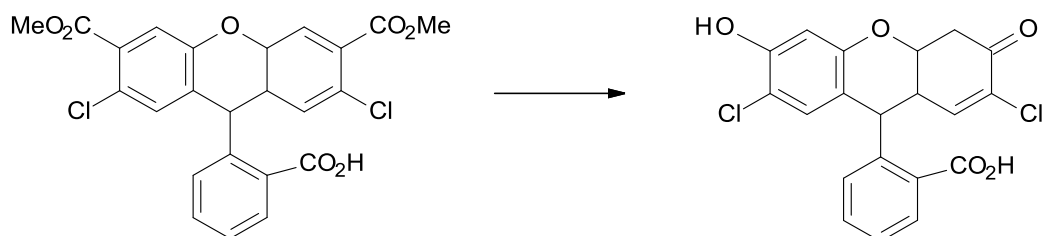
Scheme 15. *Deacetylation and oxidation of DCFH-DA (non fluorescent) resulting in the fluorescent DCF following reaction with singlet oxygen.*

The second common light-based parameter for the detection of singlet oxygen is absorbance, as discussed in section 1.2.2 DBDF **3** has a maximum excitation wavelength of 410 nm, this is illustrated in the absorbance spectra of **3** displayed in Figure 33.
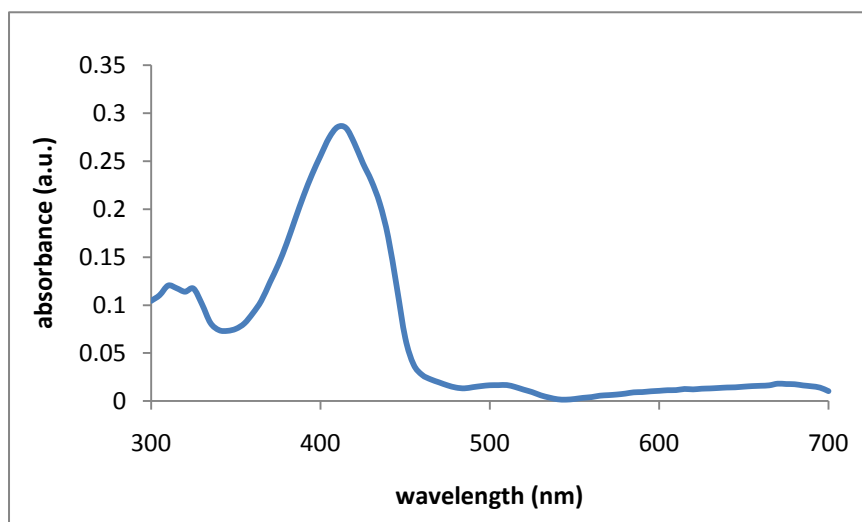
Figure 33. Absorbance spectra of compound 3, displaying the absorbance maxima at 410 nm. Spectra recorded in Isopropyl alcohol.

In the presence of singlet oxygen, the DBDF reacts via a 1,4 Diels-Alder reaction, leading to the furan ring system becoming destroyed and a significant degree of conjugation being lost within the compound resulting in a newly formed di-ketone molecule (Scheme 16). The distinctly different structure has blue shifted absorbance maxima. The depletion of the 410 nm band is directly proportional to the amount of singlet oxygen present in the solution. By monitoring the absorbance of **3** at 410 nm in the presence of the photosensitiser and an appropriate light source the amount of singlet oxygen generated can be determined.
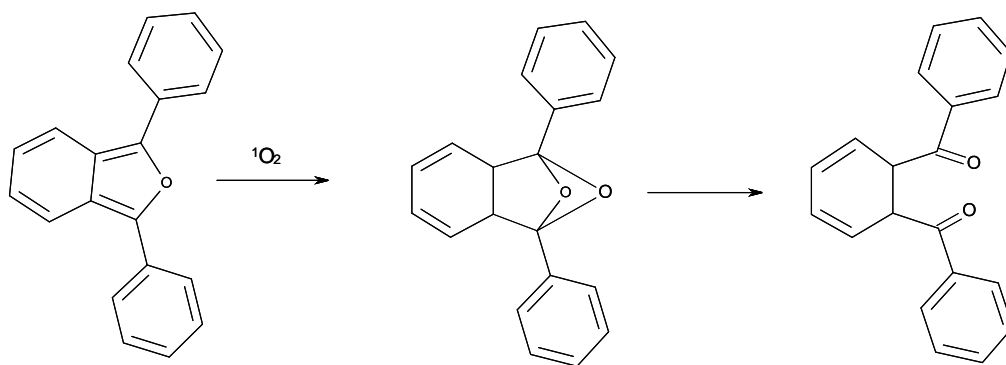
Scheme 16 . *Reaction of 3 with singlet oxygen, oxidised via a 1,4 Diel- Alder addition reaction resulting in a di-keto product with no absorbance at 410 nm.*

The singlet oxygen generation of photosensitisers **15** and **16** was determined using the quantitative singlet oxygen dependence absorbance of **3**.

3.4.1 Singlet Oxygen Quantum Yield

The quantum yield for singlet oxygen generation, Φ_Δ, is a measure of how efficient a photosensitiser generates singlet oxygen.[57] If every photon absorbed by a photosensitiser leads to a molecule of singlet oxygen being created by energy transfer, then $\Phi_\Delta = 1$. If no absorbed photon leads to a the creation of a molecule of singlet oxygen then $\Phi_\Delta = 0$.[12] The values of Φ_Δ vary between different photosensitisers, solvents and are affected by pH.[57]

53
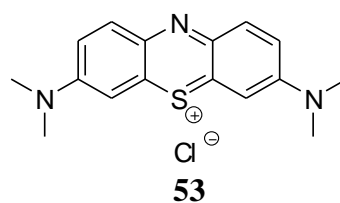
A known photosensitiser, methylene blue **53** was chosen as a reference compound for singlet oxygen generation. Methylene blue has a rather long excitation wavelength and a recorded singlet oxygen quantum yield of 0.52 in D_2O.[58]

3.4.2 Light Sources for Excitation

A number of different light sources were investigated for the quantitative determination of singlet oxygen. The light source requires an emitting wavelength in the region of 600 nm, while also ensuring that it causes minimal depletion to the furan signal at 410 nm in the absence of any photosensitiser. Prior to any light source being investigated using compound **3**, the amount of depletion of the furan had to be established in dark conditions, the results of which are displayed in Figure 34. It was concluded from this experiment carried out in complete darkness that there is no significant depletion of the furan over the time period tested under dark conditions.
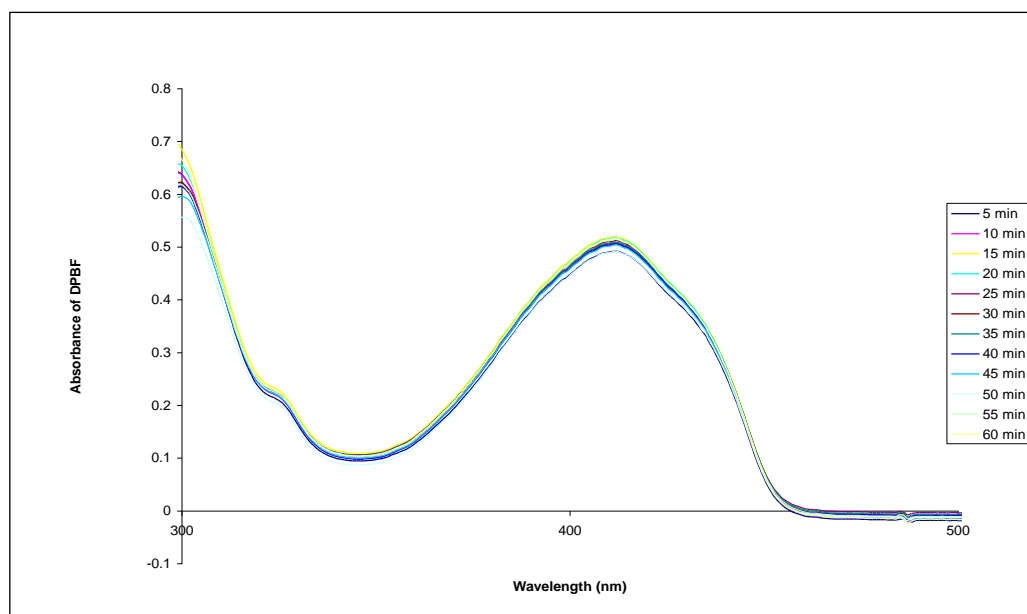
Figure 34. *Absorbance spectra of **3** (5×10^{-5} M) in isopropyl alcohol in dark conditions with samples taken every 5 min for 1 hr.*

The first light source to be considered was regular unfiltered white light, the wavelength range is generally in the region of 400 -700 nm. It can be seen from Figure 34 that there is a significant depletion in the amount of absorbed light at 410 nm for compound **3** in the absence of any photosensitiser.

64
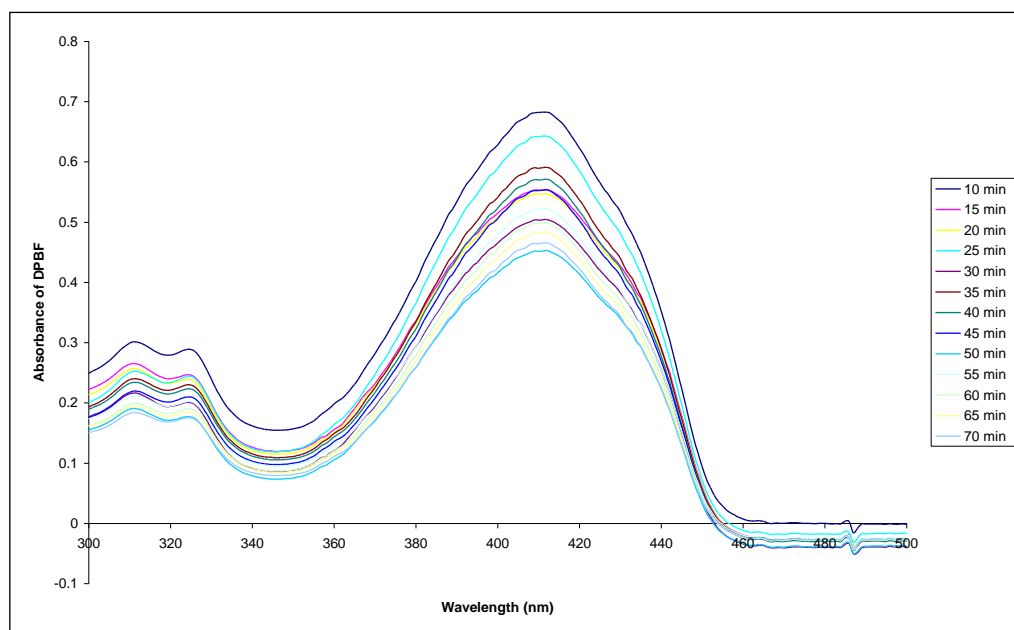
Figure 35. *Absorbance spectra of **3** ($5x10^{-5}$ M) in isopropyl alcohol (50 mL) in white light with samples taken every 5 min for 1 hr*

This is not wholly unexpected as the wavelength range of white light is so broad that compound **3** is most likely decomposing photochemically as some of the white light is being absorbed by the compound. It can be concluded from Figure 35 that any investigation into the generation of singlet oxygen using compound **3** as a chemical trap must be carried out in dark conditions with the sample being subjected to light of a particular wavelength.

After a number of different light sources were investigated, including red light bulbs and red Light emitting Diodes (LEDs) (see Appendix 2), it was decided that the most appropriate light source was that from a Carey Fluorescent Spectrometer with an additional fibre optic cable attached to allow for the fine tuning of excitation wavelength. This ensured that the most appropriate wavelength, as determined from Figures 29 and 30, was used for the excitation of compounds **15** and **16**.

3.4.3 Control Experiments for Singlet Oxygen

Further to the investigation into different light sources and experimental conditions, the initial requirement for the investigation into singlet oxygen generation from compounds **15** and **16**, synthesised in this thesis, was to establish a control experiment. This experiment allows for the verification of the technique of measurement as well as generating a reference compound which has an already established singlet oxygen quantum yield, allowing for a direct comparison to be made with compounds **15** and **16**.

As discussed in some detail in chapter one, there is a large number of different types of compounds available to use as photosensitisers. Currently the most widely approved photosensitiser specific for use in photodynamic therapy is Photofrin, a purified derivative of the monomer hematophorphyrin **2**. Hematoporphyrin was tested as a control substance, however, it proved to be difficult to work with as the absorbance had some degree of overlapping with the absorbance of the singlet oxygen chemical trap, compound **3** (see Appendix 3) as well as displaying poor repeatability. This is most likely due to the ease of hydrolysis of this compound as well as the lack of dimers and oligomers in the purchased compound.

A more successful control compound was methylene blue. Methylene blue (**52**) has many diverse uses; it has been used as redox indicators, chemical dyes and as an antimalarial drug [59] as well a photosensitiser compound for use in PDT[60].

As mentioned previously the singlet oxygen quantum yield (Φ_Δ) of an individual compound is likely to be dependent on solvent systems, reaction conditions as well as techniques used in the measurement. With this in mind it was imperative that the generation of singlet oxygen was determined using our measurement technique for a known photosensitiser, such as methylene blue. For the purpose of this thesis the Φ_Δ of methylene blue was taken as 0.52. The absorbance

66

spectrum of methylene blue is displayed in Figure 36. It can be seen from the spectra that there is little absorbance in the region of the singlet oxygen trapping compound **3** (410 nm) with the maximum absorbance occurring at the red region of the spectrum around 670 nm.
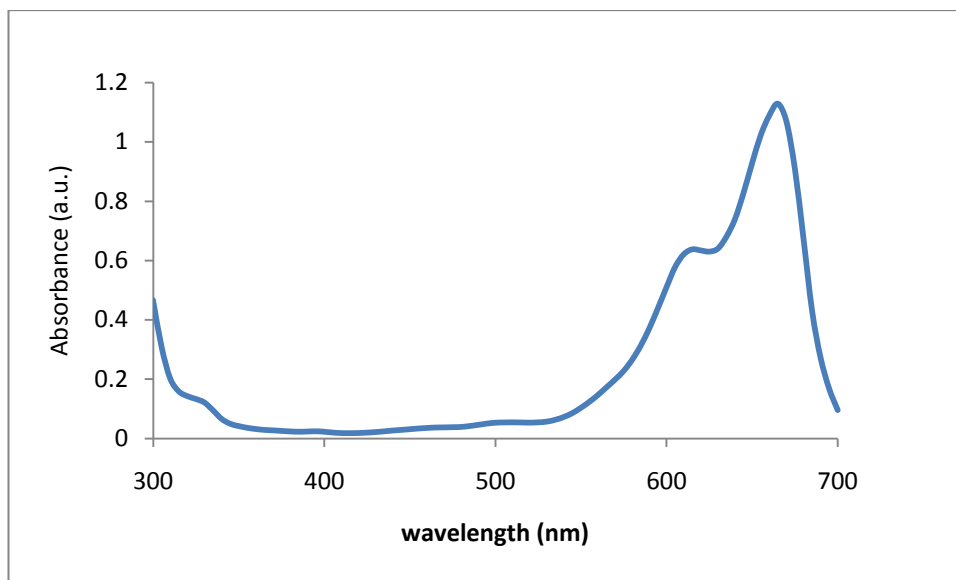
Figure 36. *Absorbance Spectrum of methylene blue showing the absorbance maxima at ~ 670 nm with minimal absorbance at 410 nm.*

A control experiment using methylene blue and **3** in a 10:1 molar ratio with the absence of excitation wavelength was executed. As expected there is little derivation of the absorbance of the furan at 410 nm, this is displayed in Figure 37.
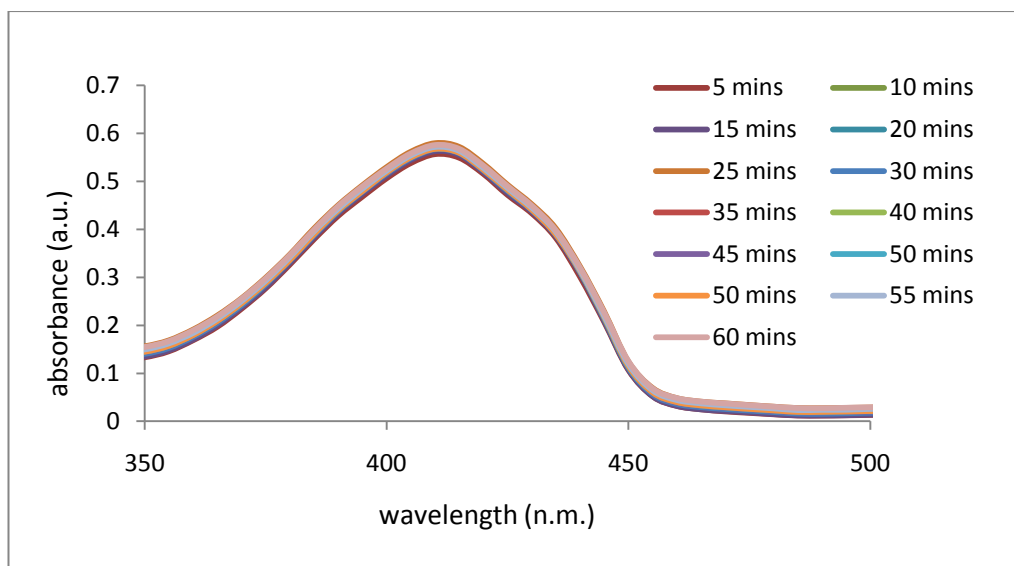
Figure 37. *Control experiment using methylene blue and Compound 3, 10 :1 molar ratio in EtOH:water 1:1 (vol:vol), experiment carried out in darkness.*

However, when the same experiment was carried out under similar conditions but in the presence of the fibre optic light source set at an excitation wavelength of 660 nm, the depletion of the absorbance at 410 nm is much more pronounced. This is attributed to the formation of singlet oxygen produced by the methylene blue and the furan (**3**) being depleted following the mechanism shown in Scheme 3.2.
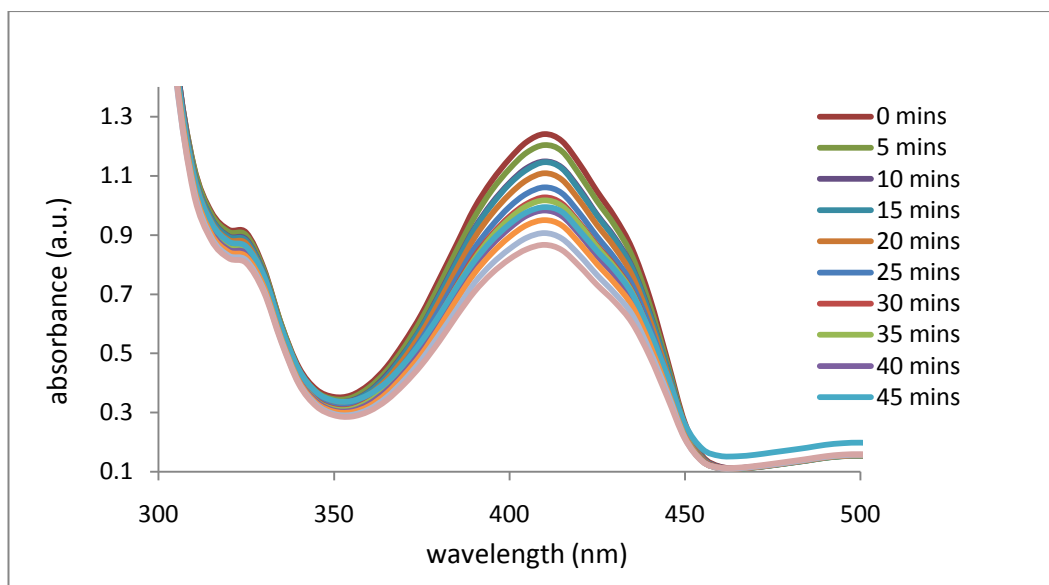
Figure 38. *Depetion of absorbance of compound 3 due to the formation of singlet oxygen.*
Methylene blue and Compound 3, 10 :1 molar ratio in EtOH:water 1:1 (vol:vol), experiment
carried out with an excitation wavelength of 660 nm.

For ease of view the information from Figure 38 is displayed in Figure 39 showing the
absorbance at 410 against time. This absorbance depletion at 410 nm can then be directly
transferred into the quantum yield of singlet oxygen for comparison with compounds **15** and **16**.
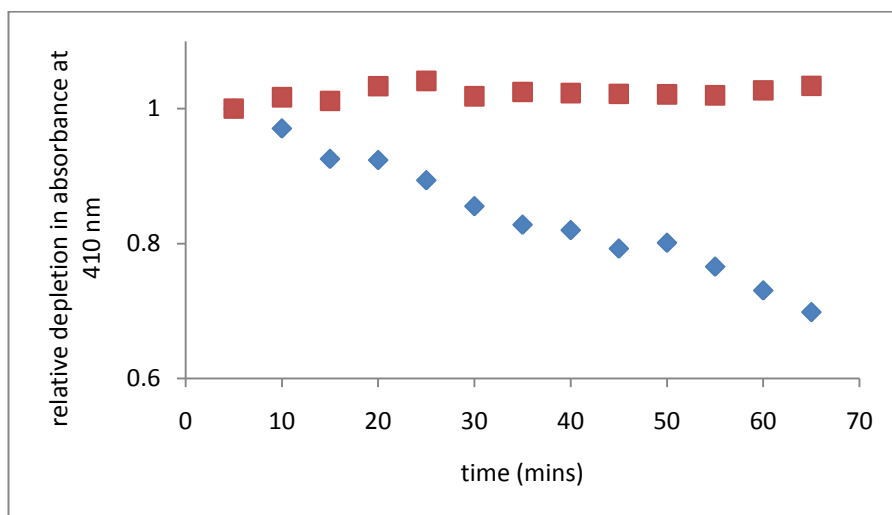
Figure 39. *Relative depletion in absorbance comparing Methylene Blue and 3 without light (top*
line) excitation wavelength 650 nm (Bottom line)

69

3.4.4 Singlet Oxygen Generation for Compounds 15 and 16

Following similar procedures to that followed for the control experiment using methylene blue, compounds **15** and **16** were investigated for potential singlet oxygen generation using compound **3** as the chemical trap. One of the main differences between the novel photosensitisers prepared in this thesis and methylene blue is the differences in solubility. Methylene blue contains a positive charge and as such is readily water soluble, compound **15** and **16** are neutral compounds and therefore have to be solubilised in Isopropyl alcohol for the study.

The depletion of **3** in Isopropyl alcohol with **15** (Figure 40) and the depletion of **3** with **16** (Figure 41) is shown. It is clear from these two graphs that the depletion observed for **3** with **15** and **16** is minor when compared to the depletion observed when methylene blue was used (Figure 38).
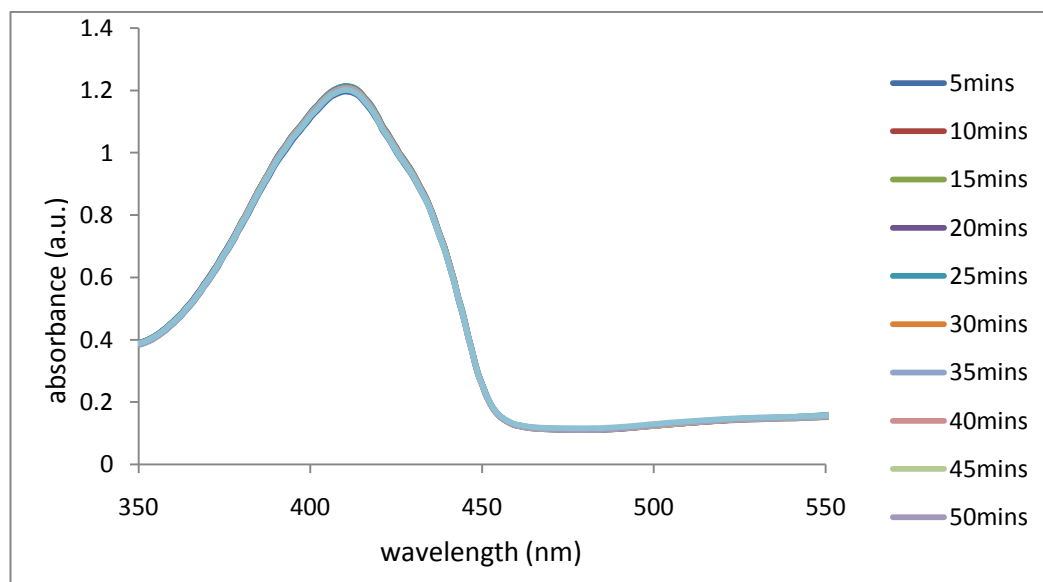
Figure 40. *Absorbance of compound **3** with **15**, 10 :1 molar ratio in Isopropyl, experiment carried out with an excitation wavelength of 650 nm.*
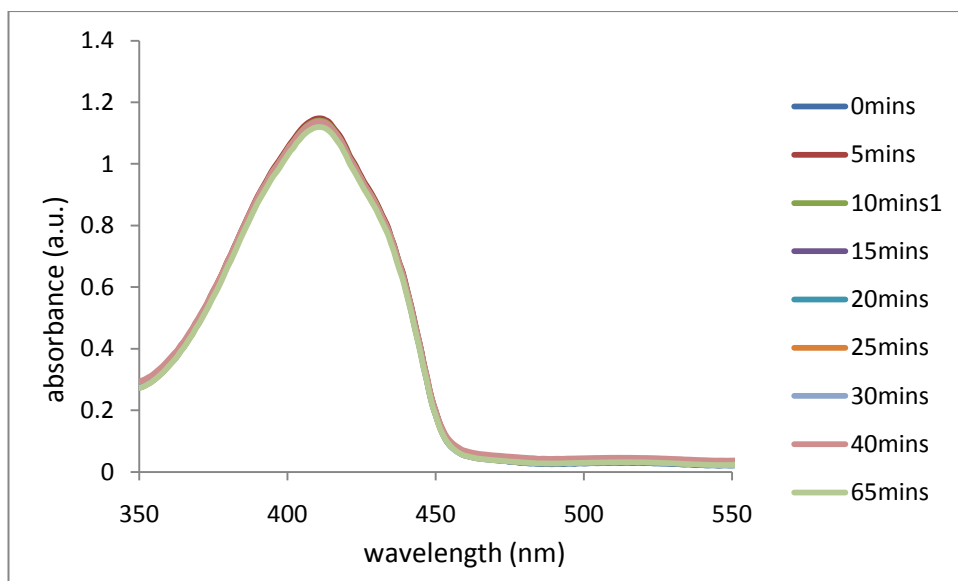
Figure 41. *Absorbance of compound **3** with **16**, 10 :1 molar ratio in Isopropyl, experiment carried out with an excitation wavelength of 650 nm.*

The relative absorbance at 410 nm for **15** and **16** compared against the absorbance at 410 nm without any photosensitiser is shown in Figure 42 and Figure 43 for **15** and **16** respectively. Both show a slight depletion in absorbance at 410 nm when compared to the control, with the depletion of absorbance using **16** slightly more pronounced than **15**. This could be due to **16** being more solouble than **15** and indicate more phosphorescence being generated.
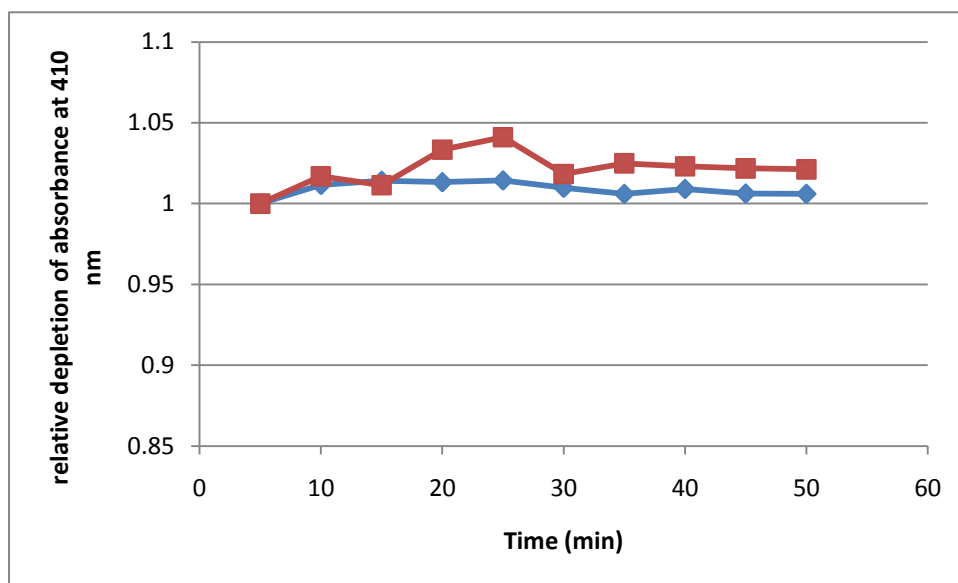
Figure 42. *Relative depletion in absorbance comparing **3** without **15** (top line) and with **15** (bottom line) excitation wavelength of 650 nm*
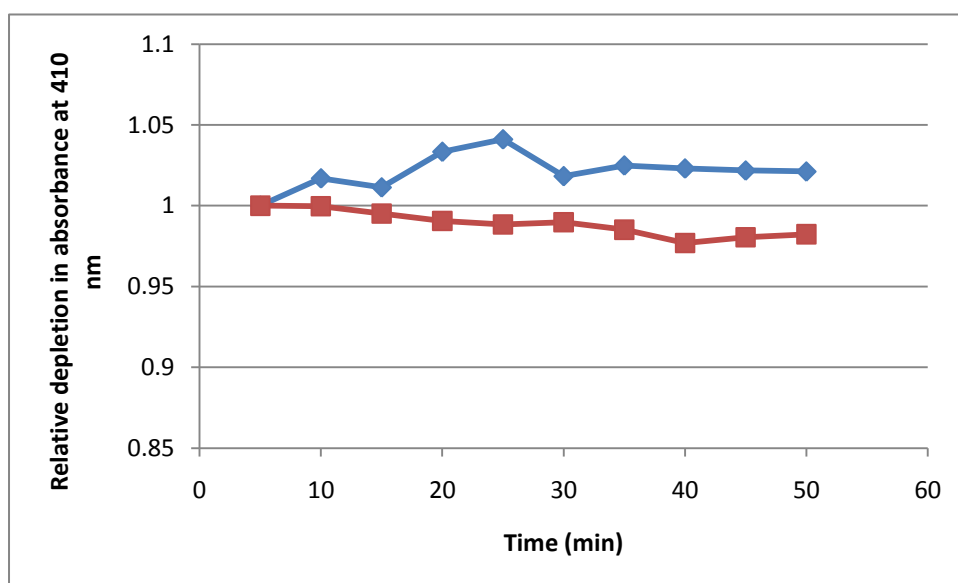
Figure 43. *Relative depletion in absorbance comparing **3** without **16** (top line) and with **16** (bottom line) excitation wavelength of 650 nm*

Methylene blue depletes the absorbance of **3** at 410 nm by 30.2% (Figure 38). If we take this depletion to indicate a quantum yield (Φ_Δ) of 0.52 then the quantum yield of **15** and **16** can be determined by comparison of their depletion. Using the values of 0.7% and 2.1% from the

depletion of **3** in Figures 40 and 41 the quantum yields (Φ_Δ) for **15** and **16** in isopropyl alcohol are 0.01 and 0.04, respectively.

Chapter 4

Conclusion

In this thesis, the successful synthesis of target compounds **15** and **16** for investigation as photosensiters is reported. The synthesis of these compounds is discussed and presented allowing for full structural elucidation of the intermediates **22**, **23** (see 2.3.1) and **32**, **33** (see 2.3.2) for the complete synthesis of **15** and **16** respectively. The absorbance maxima for both these compounds was found to be within the desired range 600 – 900 nm as would be expected for compounds with such a high degree of conjugation. Neither **15** nor **16** showed any fluorescence emission (see section 3.3) and tests for singlet oxygen generation were carried out using the singlet oxygen scavenger **3** to assess whether the compounds were able to excite molecular oxygen by energy transfer. The values of quantum yield (Φ_Δ) of singlet oxygen generation were obtained and found to be 0.01 and 0.04 for **15** and **16** respectively. These values were extrapolated from comparison of the depletion at 410 nm of **3** using methylene blue, known to have a quantum yield of 0.52. It is evident from these values that when compared to the known photosensitiser the values for **15** and **16** are small. One possible explanation for this could be due to the poor solubility of these compounds, since the compound which has the best solubility, **16**, is the one that has the higher quantum yield. If there are fewer molecules in solution due to this lower solubility a more powerful light source such as a filtered lamp may give improved results that show an increased difference between **15** and **16**.

Another possibility is that there was not a sufficient concentration of molecular oxygen dissolved within the solvent for **15** and **16** to generate singlet oxygen. The synthesis of more water-soluble compounds would enable the used of solvents that contain a higher level of dissolved oxygen and mimic more accurately physiological conditions.

The chelation of **16** with boron was attempted in the hope that the product **17** would be structurally more stable and more efficient at reaching the T_1 state due to minimizing loss of energy by collisions of molecules in solution.

75

Due to time constraints target compounds **18** and **19**, designed to include parameter specific receptors, were unable to be synthesised. To create a photosensitiser with a pyridine group as a receptor (as in compound **18**) the synthesis of three different chalcones were attempted - **45**, **46** & **48**. After attempting various reaction conditions, the synthesis of **45** was successful with the characterisation of this compound discussed in section 2.3.4. However, due to the mimimal yield of **45**, a scale-up of this intermediate compound would be required in future work to provide enough substrate for the next two steps in the complete synthesis of **18** before any photophysical evaluation could be carried out.

The first step in the synthesis of **18** proved difficult to drive to completion, indicating that different reaction conditions would be needed to give enough of intermediate **51** that could be purified and still leave a realistic amount to for further synthesis. The disadvantage of this synthesis was the expense of the starting material, limiting the number of potential reaction pathways that could be investigated.

The next logical step in the development of this research would be to incorporate a halogen, such as bromine (Figure 44), to **15** and **16** to investigate if there is an increased phosphorescence emission that could be caused in theory by the "heavy-atom effect", of which the mechanism is still not understood.
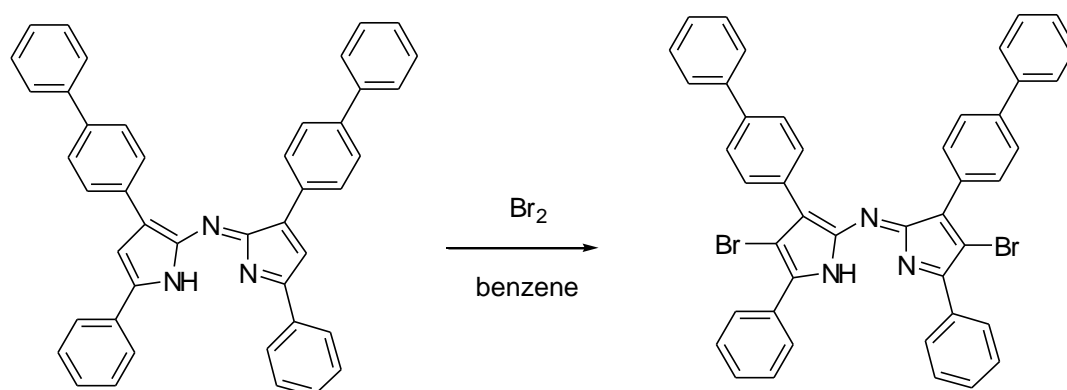
Figure 44. *Bromination of **15** in benzene*

It can be concluded from the investigation carried out in this thesis that the photosensitisers deigned and synthesised in this thesis did indeed increase the potential wavelength of PDT application. However, the quantum yield of singlet oxygen is too low to merit further investigation on these compounds without further modification, such as those discussed above.

Chapter 5

Experimental Techniques

5.1 Experimental techniques

NMR

^{1}H NMR spectra were obtained on a Brucker (400 MHz) NMR spectrophotometer. Samples were dissolved ~15 mg in 2 mL of $CDCl_3$ unless otherwise stated. All samples were run at room temperatire with the samples being spun at 20 rpm.

Mass spectrometry

An Aligent Technologies 6100 Single Quadrupole LC/MS was used to obtain positive and negative electrospray spectra. Samples were dissolved in a concentration not exceeding 1 mg/ 1 mL in MeOH and direct infusion onto the instrument.

Chromatography

Thin layer chromatography was carried out on Macherey-Nagel 60 UV_{254} plates. Compounds absorbed in the visible region with additional visualisation, were required, carried out by using short-wavelength UV light.

Flash chromatography was carried out in columns packed with silica gel (silica 60, Alfa Aesar), 70-230 mesh with the mobile phase being varied accordingly.

5.2 Synthetic Procedure for Individual Compounds

22 (*E*)-3-(biphenyl-4-yl)-1-phenylprop-2-en-1-one

To biphenyl-4-carboxaldehyde (2.5 g, 13.0 mmol) stirring in ethanol (7.4 mL) acetophenone (1.4 mL, 11.0 mmol) was added followed by NaOH (0.67 g) in H_2O (3.7 mL) and left stirring at RT for 24h. Addition of 1M HCl revealed a precipitate which was filtered and dried in oven under vacuum at 50 °C. Crude yield 95.5 % Purification by column chromatography on silica eluting with EtOAc/Hexane (15:85) gave the chalcone yield 80% ^{1}H NMR (CDCl$_3$) δ: 8.06-8.04 (m, 2H, Ar-H), 7.87 (d, *J* = 15.7 Hz, 1H, *Trans*-H), 7.89-7.85 (m, 2H, Ar-H), 7.68-7.59 (m, 5H, Ar-H), 7.59 (d, *J* = 15.8 Hz, 1H, Trans-H), 7.54-7.46 (m, 4H, Ar-H), 7.41-7.37 (m, 1H, Ar-H) ^{13}C NMR (CDCl$_3$) δ: 190.5, 144.4, 143.3, 140.1, 138.3, 133.9, 132.8, 129.0, 128.9, 128.7, 128.5, 127.9, 127.6, 127.1, 121.9, m/z calculated, 285.12 found 285.1

23 3-(biphenyl-4-yl)-4-nitro-1-phenylbutan-1-one

A 50 mL round-bottomed flask was charged with **22** (2.0 g, 7.04 mmol) in methanol (1 mL) and diethylamine (1.8 mL, 35 mmol) then stirred at RT while nitromethane (2.4 mL, 36 mmol) was added and the reaction brought to reflux at 90 °C for 24 h. 1M HCl added and the precipitate was filtered and dried over night in a vacuum oven at 50 °C. This afforded a brown solid, yield 86 % ^{1}H NMR (CDCl$_3$) δ: 7.86-7.84 (m, 2H, Ar-H), 7.49-7.45 (m, 5H, Ar-H), 7.39-7.32 (m, 4H, Ar-H), 7.28-7.25 (m, 3H, Ar-H), 4.80 (dd, *J* = 6.6 Hz, 12.5 Hz, 1H, C*H*NO$_2$), 4.66 (dd, *J* = 8.0 Hz, 12.5 Hz, 1H, C*H*NO$_2$), 4.23-4.16 (m, 1H, C*H*CH$_2$NO$_2$), 3.46 (dd, *J* = 6.4 Hz, 17.7 Hz, 1H, C*H*CO), 3.40 (dd, *J* = 7.4 Hz, 17.7 Hz, 1H, C*H*CO) ^{13}C NMR (CDCl$_3$) δ: 195.8 (C=O), 139.7 (C$_{IV}$), 139.4 (C$_{IV}$), 137.1 (C$_{IV}$), 135.3 (C$_{IV}$), 132.6 (CH), 127.8 (CH), 127.7 (CH), 127.0 (CH), 126.9 (CH), 126.7 (CH), 126.4 (CH), 126.0 (CH), 78.5 (CH$_2$), 40.5 (CH$_2$), 37.9 (CH), m/z calculated 345.39, found 345.2

15 (*Z*)-3-(biphenyl-4-yl)-*N*-(3-(biphenyl-4-yl)-5-phenyl-2*H*-pyrrol-2-ylidene)-5-phenyl-1*H*-pyrrol-2-amine

A 50 mL round-bottomed flask was charged with **23** (166 mg, 481 mmol) dissolved in Butan-1-ol (20 mL), ammonium acetate (1.30 g, 17 mmol) in butan-1-ol (5 mL) added and refluxed at 117 °C for 48 h, concentrated on rotary evaporator and filtered. Washed with ethanol and dried in oven overnight at 50 °C under vacuum. ^{1}H NMR (CDCl$_3$) δ: 8.26-8.24 (m, 4H, aryl-H), 7.60-7.59 (m, 7H, Ar-H), 7.52-7.50 (m, 4H), 7.42-7.39 (m, 8H), 7.36-7.31 (m, 6H), 7.27-7.24 (m, 2H), m/z calculated 602.25, found 602.20

32 (E)-3-(biphenyl-4-yl)-1-(4-methoxyphenyl)prop-2-en-1-one

A 50 mL round-bottomed flask was charged with biphenylcarboxaldehyde (1.22 g, 6.7 mmol), 4-methoxyacetophenone (1.0 g, 6.7 mmol) added to ethanol: water (11.4 mL: 2 mL). Then KOH (0.01 g, 0.2 mmol) added and left stirring at RT. After 24 h a white precipitate formed which was filtered off and dried in oven under vacuum overnight. ^{1}H NMR (CDCl$_3$) 8.07 (d, *J* = 8.9 Hz, 2H, Ar-H), 7.85 (d, *J* = 15.6 Hz, 1H, *Trans*-H), 7.73 (d, *J* = 8.3 Hz, 2H, Ar-H), 7.66 (d, *J* = 8.3 Hz, 2H, Ar-H), 7.64-7.63 (m, 2H), 7.60 (d, *J* = 15.6 Hz, 1H, *Trans*-H), 7.49-7.46 (m, 2H, Ar-H), 7.40-7.37 (m, 1H, Ar-H), 7.01-6.99 (m, 2H, Ar-H), 3.90 (s, 3H, C*H*$_3$O) ^{13}C NMR (CDCl$_3$) δ: 163.8, 143.9, 143.4, 140.5, 134.4, 131.5, 131.2, 129.2, 128.2, 127.9, 127.4, 122.0, 114.2.

33 3-(biphenyl-4-yl)-1-(4-methoxyphenyl)-4-nitrobutan-1-one

32 (500 mg, 1.6 mmol) was dissolved in methanol (4.8 mL) and diethylamine (0.4 mL, 8 mmol) then nitromethane (0.55 mL, 8 mmol) was added while stirring at RT. The reaction was brought to relfux at 90 °C and left stirring for 24 h. Upon cooling a brown solid precipitated, 1M HCl was added and the solid was filtered. The dried precipitate weight was 458 mg. ^{1}H NMR (CDCl$_3$) δ: 7.94-7.90 (m, 2H, Ar-H), 7.56-7.54 (m, 4H, Ar-H), 7.55 (d, J = 8.3 Hz, 2H, Ar-H), 7.45-7.41 (m, 3H, Ar-H), 7.37-7.34 (m, 2H, Ar-H), 6.95-6.91 (m, 2H, Ar-H), 4.87 (dd, J = 12.5, 6.5 Hz, 1H, C$\underline{H}_2$NO$_2$), 4.72 (dd, J = 12.5, 8.2 Hz, 1H, C$\underline{H}_2$NO$_2$), 4.27 (m, 1H, C$\underline{H}$CH$_2$NO$_2$), 3.87 (s, 3H, C$\underline{H}_3$O), 3.47 (dd, J = 17.5, 6.4 Hz, 1H, C$\underline{H}_2$CO), 3.39 (dd, J = 17.5, 6.4 Hz, 1H, C$\underline{H}_2$CO)

16 (*Z*)-3-(biphenyl-4-yl)-*N*-(3-(biphenyl-4-yl)-5-(4-methoxyphenyl)-2*H*-pyrrol-2-ylidene)-5-(4-methoxyphenyl)-1*H*-pyrrol-2-amine

A 50 mL round-bottomed flask was charged with **33** (0.2 g, 0.53 mmol), ammonium acetate (1.46 g, 19 mmol) and butan-1-ol (2 mL) and stirred under reflux at 117 °C. After 48 h the reaction mixture was allowed to cool, the deep purple precipitate was filtered and washed in ethanol. ^{1}H NMR (CDCl$_3$) δ: 8.18 (d, 2H, Ar-H), 7.92 (d, 2H, Ar-H), 7.69-7.67 (m, 4H, Ar-H), 7.48 (m, 4H, Ar-H), 7.21-7.19 (m, 2H, Ar-H), 7.07 (m, 2H, Ar-H), 3.93 (s, 3H, OC$\underline{H}_3$)

17 1,9-di(biphenyl-4-yl)-5,5-difluoro-3,7-bis(4-methoxyphenyl)-5*H*-dipyrrolo[1,2-c:1',2'-*f*]triazaborinin-4-ium-5-uide

To a 50 mL round-bottomed flask **16** (14 mg, 0.02 mmol) was dissolved in dry DCM (4 mL) under N$_2$. BF$_3$OEt$_2$ (0.1 mL, 0.8 mmol) in dry DCM (1 mL) was prepared, then 0.2 mL of this dilution was added to **16** while stirring under N$_2$. Then diisopropylethylamine (0.01 mL, 0.06 mmol) added and the reaction left under N$_2$ for 24 h at RT. The reaction was washed with 2 ×

82

50 mL of H$_2$O, then the organic layer separated and dried over Na$_2$SO$_4$ before dried in oven under vacuum overnight. Weight of solid, 13 mg.

45 (*E*)-1-phenyl-3-(pyridine-4-yl)prop-2-en-1-one

Method 1:

A 100 mL round-bottomed flask was charged with 4-pyridine carboxaldehyde (1.0 mL, 10.6 mmol) and acetophenone (1.3 mL, 10.6 mmol) in H$_2$O (30 mL) and stirred at RT. Then 10% Na$_2$CO$_3$ (4mL) was added and the reaction was monitored by TLC. Disappearance of acetophenone was faint, reaction was left overnight after which there was no precipitate. TLC with (DCM/ MeOH 1%) showed that there was still starting material unreacted. Ethanol (5 mL) was added and monitored by TLC, after 3 h a precipitate had formed. The precipitate was purified by preparative TLC using EtOAC as the eluent.

Method 2:

A 100 mL round-bottomed flask was charged with 4-pyridine carboxaldehyde (2.3 mL, 18.7 mmol) and acetophenone (2.3 mL, 18.7 mmol) were added to a mixture of ethanol: water (9 mL: 53 mL) at RT, then 10% K$_2$CO$_3$ (2 mL) was added. After 3 h no precipitate had formed and the reaction was left overnight. A preparative TLC using Hexane:DCM 50:50 gave a crude product in a small yield.

Method 3:

To a 100 mL round-bottomed flask charged charged with NaOH (80 mg, 2 mmol) in H$_2$O (13.3 mL) and ethanol (2.3 mL), 4-pyridine carboxaldehyde (500 mg, 4.67 mmol) was added at RT. Then acetophenone (560 mg, 4.67 mmol) was added and after 8 h a precipitate had formed. This was then purified on a column with SiO$_2$ using toluene: EtOAc 50:50 as the eluent. ^{1}H NMR

(CDCl$_3$) δ: 8.61-8.60 (m, 2H, ortho Ar-H), 7.95 (d, J = 7.3 Hz, 2H, ortho Ar-H), 7.60-7.59 (m, 2H), 7.53 (t, J = 7.4 Hz, 1H, para Ar-H), 7.46-7.38 (m, 4H), m/z calculated 210.08, found 210.0

Method 4:

Into a solution of 10 % KOH (30 mL) at O°C 4-pyridine carboxaldehyde (1.22 mL, 10 mmol) in EtOH (10 mL) was added and allowed to stir for 15 min. Then acetophenone (1.24 mL, 10 mmol) added dropwise over a period of 10 min. The reaction mixture was left in the ice bath for 5 h then the mother liquor poured through a Buchner funnel, the resulting yellow precipitate was isolated: 1 g.

46 (*E*)-1-(4-methoxyphenyl)-3-(pyridin-4-yl)prop-2-en-1-one

A 50 mL round-bottomed flask was charged with 4-pyridine carboxaldehyde (0.5 mL, 5.3 mmol) in a stirred solution of Na$_2$CO$_3$·H$_2$O (303 mg, 1.1 mmol) in H$_2$O (10.6 mL). Then 4-methoxyacetophenone (796 mg, 5.3 mmol) was added and the reaction was stirred at RT for 24h.

52 (*E*)-3-(2,3,5,6,8,9,11,12-octahydrobenzo[*b*][1,4,7,10,13]pentaoxacyclopentadecin-15-yl)-1-phenylprop-2-en-1-one

Method 1:

A solution of 4'-formylbenzo-15-crown-5 (0.2 g, 0.68 mmol) in ethanol (1 mL) was added gradually to an aqueous solution of 10% KOH (3 mL) at 0°C for 15 min. Acetophenone (0.084 mL, 0.68 mmol) added slowly dropwise and the mixture was then allowed to attain room temperature (25°C) and stirred for 24 h, then the flask placed in the fridge overnight. 1M HCl

added, extracted using DCM and the organic layer dried using Mg_2SO_4 and concentrated on the rotary evaporator. Crude weight 0.169 g

Method 2:

Acetophenone (81 mg, 0.7 mmol) added to KOH 10% (3 mL) at O°C and stirred for 15 min. Then 4'-formylbenzo-15-crown-5 (200 mg, 0.68 mmol) added and the reaction was stirred for 15 min, then allowed to reach RT and stirring continued for 4 h. The flask was placed in a fridge overnight, 1M HCl was added and the precipitate was filtered.

50 2,3,5,6,8,9,11,12-octahydrobenzo[*b*][1,4,7,10,13]pentaoxacyclopentadecine-15-carbaldehyde

Benzyl-15-crown-5 (200 mg, 0.75 mmol) and DMF (0.35 mL) added to flask purged with nitrogen- flask in ice bath for 10 mins. $POCl_3$ added dropwise (0.13 mL) slowly. Flask left for 1 min then allowed to reach RT and reaction stirred for 16 h. Then heated to 60 °C for 1 h and allowed to cool. The reaction mixture was added to 1.2 g of ice, flask rinsed with 0.2 mL water. The combined solution brought to pH 7 with saturated K_2CO_3. Extracted in chloroform (2x1.2 mL) dried with $MgSO_4$ and allowed to stand for 1 h, then pipetted into flask and concentrated by rotary evaporator. Crystals formed, showed starting material.

Chapter 6

References

1. Cancer Research UK. *Cancer incidence-UK Statistics.* [homepage on the Internet]. London: Cancer Research UK; **2010** [updated 2010 Mar 17; cited 2010 Nov 18]. Available from: http://info.cancerresearchuk.org/cancerstats/incidence/

2. Moan, J.; Peng, Q.; An outline of the history of PDT. In: T. Patrice, Editor, Photodynamic Therapy. Comprehensive Series of Photochemical and Photobiological Sciences, RSC Publ., London (**2003**), pp. 3–37.

3. Dolphin, D.; Photomedicine and Photodynamic therapy. *Canadian Journal of Chemistry*, **1994**, 72, 1005-10132.

4. Sharman, M.W.; Allen, C.M.; van Lier, J.E.; Photodynamic therapeutics: basic principles and clinical applications. *Drug Discovery Today*, **1999**, 4, 507-517.

5. Pandey, R.K.; Smith, K.M.; Dougherty, T.J.; Porphyrin Dimers as Photosensitizers in Photodynamic Therapy. *Journal of Medicinal Chemistry*, **1990**, 33, 2032-2038.

6. Detty, M.R.; Gibson, S.L.; Wagner, S.J.; Current Clinical and Preclinical Photosensitisers for Use in Photodynamic Therapy. *Journal of Medicinal Chemistry*, **2004**, 47, 3897-3915.

7. Kolarova, H.; Ditrichova, D.; Wagner, J.; Penetration of the Laser Light Into the Skin In Vitro. *Lasers in Surgery and Medicine*, **1999**, 24, 231-235.

8. Bonnett, R.; Photosensitizers of the Porphyrin and Phathalocyanine Series for Photodynamic Therapy. *Chemical Society Reviews*, 1995, 24, 19-33.

9.Clinical Trials.gov. Available from: http://clinicaltrials.gov/ct2/results?term=photodynamic+therapy

10. Konan, Y.N.; Gurny, R.; Allemann, E. State of the art in the delivery of photosensitizers for photodynamic therapy, *Journal of Photochemistry and Photobiology B: Biology*, **2002**, 66, 89-106.

11. Donnelly, R.F.; McCarron, P.A.; Woolfson, D.; Drug Delivery Systems for Photodynamic Therapy. *Recent Patents on Drug Delivery & Formulation*, **2009**, 3, 1-7.

12. Atkins, P.; de Paula, J.; Elements of Physical Chemistry. 2006, 4th ed. Oxford University Press.

13. Sibata, C.H.; Colussi, V.C.; Oleinick, N.L.; Kinsella, T.J. Photodynamic therapy in oncology, *Expert Opinion on Pharmacotherapy*, **2001**, 2(6), 917-927.

14. Atkins, P.; de Paula, J.; Physical Chemistry. 2002, 7th ed. Oxford University Press.

15. Schweitzer, C.; Schmidt, R.; Physical Mechanisms of Generation and Deactivation of Singlet Oxygen. *Chemical Reviews*, **2003**, 103, 1685-1757.

16. Weishaupt, K.R.; Gomer, C.J.; Dougherty, T.J.; Identification of Singlet Oxygen as the Cytotoxic Agent in Photo-inactivation of a Murine Tumor. *Cancer Research*, **1976**, 36, 2326-2329.

17. Obata, M.; Hirohara, S.; Tanaka, R.; Kinoshita, I.; Ohkubo, K.; Fukuzumi, S.; Tanihara, M.; Yano, S.; In Vitro Heavy-Atom Effect of Palladium(II) and Platinum(II) Complexes of Pyrrolidine-Fused Chorin in Photodynamic Therapy. *Journal of Medicinal Chemistry*, **2009**, 52, 2747-2753.

18. Brancaleon, L.; Moseley, H. Laser and Non-laser Light Sources for Photodynamic Therapy, *Lasers in Medical Science*, **2002**, 17, 173-186

19. Peng, Q.; Moan, J.; Ma, L.W.; Nesland, J.M.; Uptake, Localization, and Photodynamic Effect of meso-Tetra(hydroxyphenyl)porphine and Its Corresponding Chlorin in Normal and Tumor Tissues of Mice Bearing Mammary Carcinoma. *Cancer Research*, **1995**, 55, 2620-2626.

20. Mitra, S.; Foster, T.H.; Photophysical Parameters, Photosensitiser Retention and Tissue Optical Properties Completely account for the Higher Photodynamic Efficacy of meso-Tetra-Hydroxyphenyl-Chlorin vs Photofrin. *Photochemistry and Photobiology*, **2005**, 81, 849-859.

21. Kübler, A. C.; Haase, T.; Staff, C.; Kahle, B.; Rheinwald, M.; Mühling, J.; Photodynamic Therapy of Primary Nonmelanomatous Skin Tumours of the Head and Neck. *Lasers in Surgery and Medicine*, **1999**, 25, 60-68.

22. Peng, Q.; Berg, K.; Moan, J.; Kongshaug, M.; Nesland, J.M.; 5-Aminolevulinic Acid-Based Photodynamic Therapy: Principles and Experimental Research. *Journal of Photochemistry and Photobiology*, **1997**, 65, 235-251.

23. Gaullier, J.M.; Berg, K.; Peng, Q.; Anholt, H.; Selbo, P.K.; Ma, L.W.; Moan, J.; Use of 5-Aminolevulinic Acid Esters to Improve Photodynamic Therapy on Cells in Culture. *Cancer Research*, **1997**, 57, 1481-1486.

24. Morrow, D.I.J.; McCarron, P.A.; Woolfson, A.D.; Juzenas, P.; Juzeniene, A.; Iani, V.; Moan, J.; Donnelly, R.F.; Novel patch-based systems for the localised delivery of ALA-esters. *Journal of Photochemistry and Photobiology B: Biology*, **2010**, 101, 59-69.

25. Star, W.M.; van't Veen, A.J.; Robinson, D.J.; Munte, K.; de Haas, E.R.M.; Sterenborg, H.J.C.M.; topical 5-Aminolaevulinic Acid Mediated Photodynamic Therapy of Superficial Basal Cell Carcinoma Using Two Light Fractions with a Two-hour Interval: Long-term Follow-up. *Acta Dermato Venereologica*, **2006**, 86, 412-417.

26. Piacquadio, D.J.; Chen, D.M.; Farber, H.R.; Fowler, J.F.Jr.; Glazer, S.D.; Goodman, J.J.; Hruza, L.L.; Jeffes, E.W.B.; Ling, M.R.; Phillips, T.J.; Rallis, T.M.; Scher, R.K.; Taylor, C.R.; Weinstein, G.D.; Photodynamic Therapy with Aminolevulinic Acid Topical Solution And visible Blue Light in the Treatment of Multiple Actinic Keratoses of the Face and Scalp. *Archives of Dermatology*, **2004**, 140, 41-46.

27. Jeffes, E.W.; McCullough, J.L.; Weinstein, G.D.; Kaplan, R.; Glazer, S.D.; Taylor, J.R.; Photodynamic therapy of actinic keratoses with topical aminolevulinic acid hydrochloride and fluorescent blue light. *Journal of the American Academy of Dermatology*, **2001**, 45, 96-104.

28. de Silva, A.P.; Gunaratne, N.H.Q.; Gunnlaugsson, T.; Huxley, A.J.M.; McCoy, C.P.; Rademacher, J.T.; Rice, T.E.; Signalling Recognition Events with Fluorescent Sensors and Switches. *Chemical Reviews*, **1997**, 97, 5, 1515-1566.

29. Bissell, R.A.; de Silva, A.P.; Phosphorescent PET (Photoinduced Electron Transfer) Sensors: Prototypical Examples for Proton Monitoring and a 'Message in a Bottle' Enhancement Strategy with Cyclodextrins. Journal of the Chemical Society, *Chemical Communications*, **1991**, 1148-1150.

30. Huari, He.; Mortellaro, M.A.; Leiner, M.J.P.; Young, S.T.; Fraatz, R.J. Tusa. J.K.A.; Fluorescent Chemosensor for Sodium Based on Photoinduced Electron Transfer. *Analytical Chemistry*, **2003**, 75, 549-555.

31. Killoran, J.; Allen, L.; Gallagher, J.F.; Gallagher, W.M.; O'Shea, D.F.; Synthesis of BF$_2$ Chelates of tetraarylazadipyrromethenes and evidence for their photodynamic therapeutic behaviour. *Chemical Communications*, **2002**, 1862-1863.

32. Yogo, T.; Urano, Y.; Ishitsuka, Y.; Maniwa, F.; Nagano, T.; Highly Efficient and Phtostable Photosensitizer Baed on BODIPY Chormophore. *Journal of the American Chemical Society*, **2005**, 127, 12162-12163.

33. Gorman, A.; Killoran, J.; O'Shea, C.; Kenna, T.; Gallagher, W.M.; O'Shea, D.F.; In Vitro Demonstration of the Heavy-Atom Effect for Photodynamic Therapy. *Journal of the American Chemical Society*, **2004**, 126, 10619-10631.

34. Loudet, A.; Burgess, K.; BODIPY Dyes and Their Derivatives: Syntheses and Spectroscopic Properties. *Chemical Reviews*, **2007**, 107, 4891-4932.

35. Loudet, A.; Bandichhor, R.; Wu, L.; Burgess, K.; Functionalized BF$_2$ chelated azadipyrromethene dyes. *Tetrahedron*, **2008**, 64, 3642-3654.

36. McDonnell, S.O.; Hall, M.J.; Allen, L.T.; Byrne, A.; Gallagher, W.M.; O'Shea, D.F.; Supramolecular Photonic Therapeutic Agents. *Journal of the American Chemical Society*, **2005**, 127, 16360-16361.

37. Ozlem, S.; Akkaya, E.U.; Thinking Outside the Silicon Box: Molecular AND Logic As an Additional Layer of Selectivity in Singlet Oxygen Generation for Photodynamic Therapy. *Journal of the American Chemical Society*, **2009**, 131, 48-49.

38. Sharman, W.M.; van Lier, J.E.; Allen, C.M.; Targeted photodynamic therapy via receptor mediated delivery systems. *Advanced Drug Delivery Reviews*, **2004**, 56, 53-76.

39. Maziere, J. C.; Morliere, P.; Santus, R.; New Trends in Photobiology The role of the low density lipoprotein receptor pathway in the delivery of lipophilic photosensitizers in the photodynamic therapy of tumours. *Journal of Photochemistry and Photobiology B: Biology*, **1991**, 8, 351-360.

40. Versluis, A.J.; Rensen, P.C.N.; Kuipers, M.E.; Love, W.G.; Taylor, P.W.; Interaction between zinc(II)-phthalocyanine-containing liposomes and human lowdensity lipoprotein. *Journal of Photochemistry and Photobiology B: Biology*, **1994**, 23, 141-148.

41. Derycke, A.S.L.; de Witte, P.A.M.; Liposomes for photodynamic therapy. *Advanced Drug Delivery Reviews*, **2004**, 56, 17-30.

42. Jiang, F.; Lilge, L.; Grenier, J.; Li, Y.; Wilson, M.D.; Chopp, M.; Photodynamic therapy of U87 human glioma in Nude Rat Using Liposome-Delivered Photofrin. *Lasers in Surgery and Medicine*, **1998**, 22, 74-80.

43. Nawalany, K.; Rusin, A.; Kepczynski, M.; Mikhailov, A.; Kramer-Marek, G.; Snietura, M.; Poltowicz, J.; Krawczyk, Z.; Nowakowska, M.; Comparison of photodynamic efficacy of tetraarylporphyrin pegylated or encapsulated inliposomes: In vitro studies. *Journal of Photochemistry and Photobiology B: Biology*, **2009**, 97, 8-17.

44. Gerweck, L. E.; Seetharaman, K.; Cellular pH Gradient in Tumor verus Normal Tissue: Potential Exploitation for the Treatment of Cancer. *Cancer Research*, **1996**, 56, 1194-1198.

45. Ricchelli, F.; Photophysical properties of porphyrins in biological membranes. *Journal of Photochemistry and Photobiology B: Biology*, **1995**, 29, 109-118.

46. Hans, M.L.; Lowman, A.M.; Biodegradable nanoparticles for drug delivery and targeting. *Current Opinion in Solid State and Material Science*, **2002**, 6, 319-327.

47. Bechet, D.; Couleaud. P.; Frochot, C.; Viriot, M.L.; Guillemin, F.; Barberi-Heyob, M.; Nanoparticles as vehicles for delivery of photodynamic therapy agents. *Trends in Biotechnology*, **2008**, 26, 612-621.

48. Barth, R.R.; Coderre, J.A.; Vicente, M.G.H.; Blue, T.E.; Boron neutron capture therapy of cancer: current status and future prospects. *Clinical Cancer Research*, **2005**, 11, 3987-4002.

49. Kahl, S.B.; Li, J.; Synthesis and characterization of a Boronated Metallophthalocyanine for Boron Neutron Capture Therapy. *Inorganic Chemistry*, **1996**, 35, 3878-3880.

50. Jori, g.; Soncin, M.; Friso, E.; Vecente, M.G.H.; Hao, E.; Miotto, G.; Colautti, P.; Moro, D.; Esposito, J.; Rosi, G.; Nava, E.; Sotti, G.; Fabris, C.; A novel boronated-porphyrin as a radio-sensitizing agent for boron neutron capture therapy of tumours: In vitro and in vivo studies. *Applied Radiation and Isotopes*, **2009**, 67, s321-s324.

51. Wakimoto, I.; Tomioka, Y.; Kawanami, Y.; Catalytic enantioselective conjugate addition of diethylzinc to chalcones using chiral amino alcohol–nickel complexes. *Tetrahedron*, **2001**, 57, 8185-8188.

52. Marvel, C.S.; Coleman, L.E.; Scott, G.P.; Pyridine Analogs of Chalcone and their Polymerization Reactions. *Journal of Organic Chemistry*, **1955**, 20, 1785-1792.

53. Vatsadze, S.Z.; Nuriev, V.N.; Leshcheva, I.F.; Zyk, N.V.; New aspects of the aldol condensation of acetylpyridines with aromatic aldehydes. *Russian Chemical Bulletin, International Edition*. **2004**, 53, 4, 911-915.

54. Bromberg. A.; Foote, C.S.; Solvent Shift of Singlet Oxygen Emission wavelength. *Journal of Physical chemistry*, **1989**, 93, 3968-3969.

55. Soh, N.; Recent advances in fluorescent probes for the detection of reactive oxygen species. *Analytical & Analytical Biochemistry*. **2006**, 386: 532-543.

56. Ratogi, P.R.; Singh, S. P.; Hader, D.;Sinha, R.; Dection of reactive oxygen species (ROS) by the oxidant-sensing probe 2',7'-dichlorodihydrofluorescein diacetate in the cyanobacterium Anabaena variabilis PCC 7937. *Biochemical and Biophysical Research Communications*, **2010**, 397, 603-607.

57. Tanielian, C.; Wolff, C.; Esch, M.; Singlet Oxygen Production in Water: Aggregation and Charge-Transfer Effects. *Journal of Physical chemistry*. **1996**, 100, 6555-6560.

58. Chin, K.K; Trevithick-Sutton, C.C.; McCallum, J.; Jockusch, S.; Turro, N.J.; Scaiano, J.C.; Foote, C.S.; Garcia-Garibay, M.A.; Quantitative Determination of Singlet Oxygen Generated by Excited State Aromatic Amino Acids, Proteins, and Immunoglobulins. *Journal of American Chemical Society*, **2008**, 130, 6912-6913.

59. Schirmer H, Coulibaly B, Stich A, *et al*. Methylene blue as an antimalarial agent—past and future. *Redox Report*, **2003**, 8(5): 272–276.

60. Donnelly, R.F.; Cassidy, C.M.; Loughlin, R.G.; Brown, A.; Tunney, M.M.; Jenkins, M.G.; McCarron, P.A.; Delivery of Methylene Blue and meso-tetra (N-methyl-4-pyridyl) porphine tetra tosylate from cross-linked poly(vinyl alcohol) hydrogels: A potential means of photodynamic therapy of infected wounds. *Journal of Photochemistry and Photobiology B: Biology*, **2009**, 96, 223-231.

Appendix 1-

Methods for Synthesis of

Compound 45

Method 1 (solvent used- H_2O):

The synthesis was carried out using the method reported in the paper, using water as the only solvent [53]. Monitoring the reaction by TLC (DCM/ 1%MeOH) there was only faint disappearance of the acetophenone spot, even after 24 h when the paper reported that the disappearance should occur within a few hours. When a TLC of an aliquot of the reaction mixture was taken the organic and aqueous layers were separated. The organic layer gave a strong spot for acetophenone and 3 other bands close together, the aqueous layer also contained a spot for acetophenone and 3 very faint spots relating to the spots in the organic layer.

Ethanol was then added to improve the solubility of the reactants and monitored by TLC. After 1 h the TLC still contained starting material but after a further 3 h a bulky yellow precipitate and a fluffy white precipitate had appeared. These two precipitates were filtered and compared by TLC using EtOAc. There were matching bands with varying degrees of intensity, showing that there was mix of the same products in both precipitates. The yellow precipitate was further dried in a vacuum oven and turned into an oil. This was dissolved in DCM and a preparative TLC was ran in EtOAc. There were three bands; the first corresponded to acetophenone, the second contained a mixture of acetophenone and 4-pyridine carboxaldehdye, the third contained a mix of compounds with peaks in the aromatic region differing from the starting materials.

Method 2 (solvent used- H_2O + ethanol):

When the reaction was repeated the conditions were changed to have a 1:6 ethanol:H_2O ratio. Again though within 3 h no precipitate had formed, so the reaction was left to occur over night. A small sample of 2 mL was taken of the mother liquor, which was acidified (1M HCl) and the aqueous layer was extracted, then NaOH 1M was added and the organic layer was extracted in DCM. The TLC of the organic layer showed faint starting material plus a third band. This

97

procedure was adapted for the whole reaction mixture. The organic layer was dried and a column was performed using DCM as the eluent, however this was far too polar and separation of the products was not achieved. The collected crude product was instead purified using preparative TLC with Hexane:DCM 1:1, to reveal a band which gave off fluorescence under the long range UV. It was hoped this band would correspond to the product of the reaction which would be expected to absorb UV of this wavelength. The ^{1}H nmr of this band did not show any starting material and the intergration, multiplicity and shift of the peaks were in accordance with what would be expected from the spectrum of the product.

Method 3 (NaOH used as base instead of K_2CO_3):

The majority of the reaction mixture did contain starting material so the usefulness of the above method for synthesising an intermediate was limited. In an effort to increase the conversion of the reactants to the chalcone, NaOH was used in place of K_2CO_3 (10%) or Na_2CO_3 (10%). Since the hydroxide is a stronger base than the carbonate it was hoped that there would be more enolate formed to push the reaction forward. When NaOH was used a precipitate did form when using a similar ratio of ethanol to water that was already attempted with the previous base.

**Appendix 2-
Red LED Light Source
Spectra**

A red LED light was used as the light source for compounds **15** and **16** to exclude light of wavelength out with the 600-900 nm range. Figure 45 and Figure 46 show that there is no significant depletion of **3** with either compound. This could be attributed to the wavelength of light not having sufficient intensity to excite the sensitiser, inducing phosphorescence that would generate singlet oxygen .
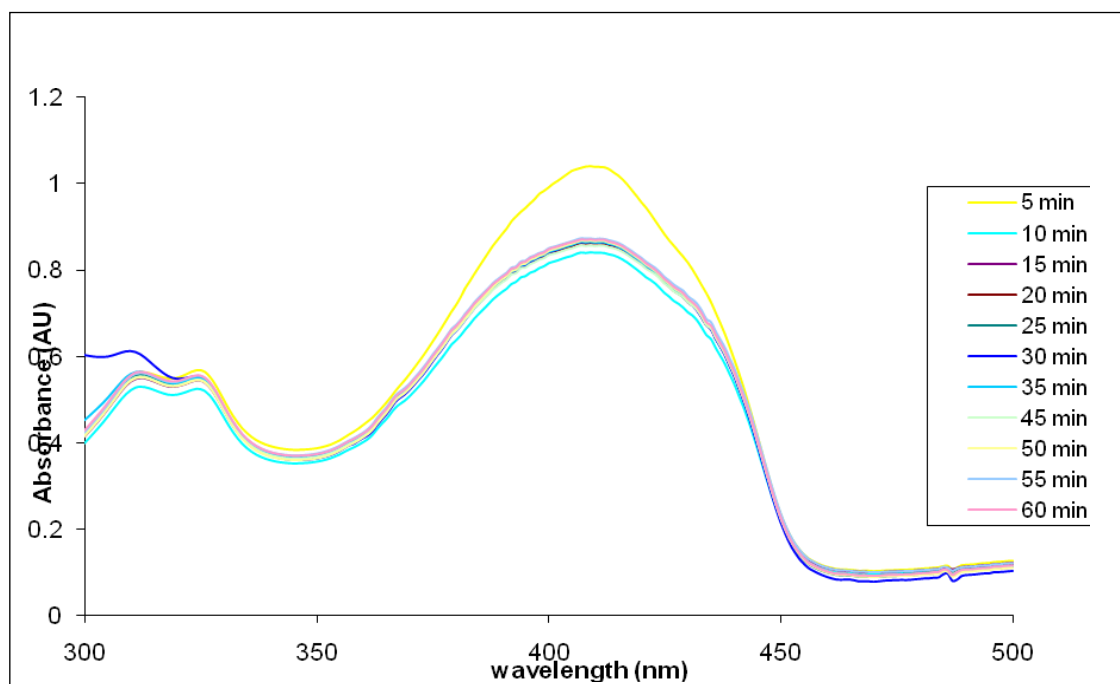
Figure 45*. Absorbance spectrum of **3** (5x10^{-5}M) in Isopropyl alcohol with **15** (5x10^{-6}M), experiment carried out using red LED light source.*
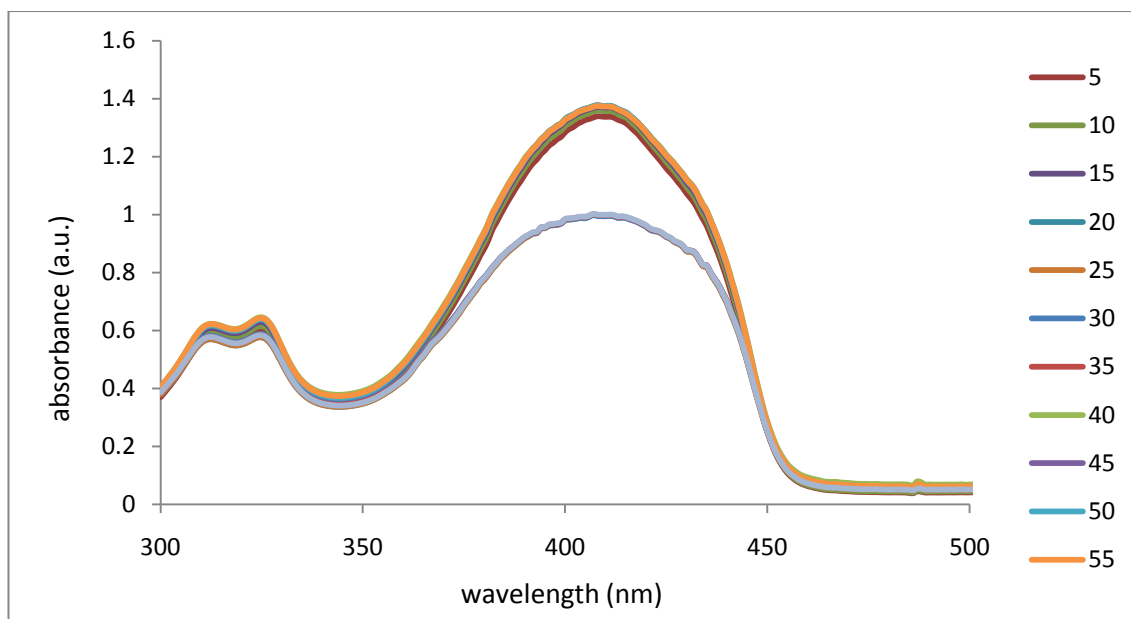
Figure 46. *Absorbance spectrum of **3** (5x10⁻⁵M) in Isopropyl alcohol with **16** (5x10⁻⁶M), experiment carried out using red LED light source.*

101

Appendix 3-

Hematoporphyrin as

Control Photosensitiser Spectra
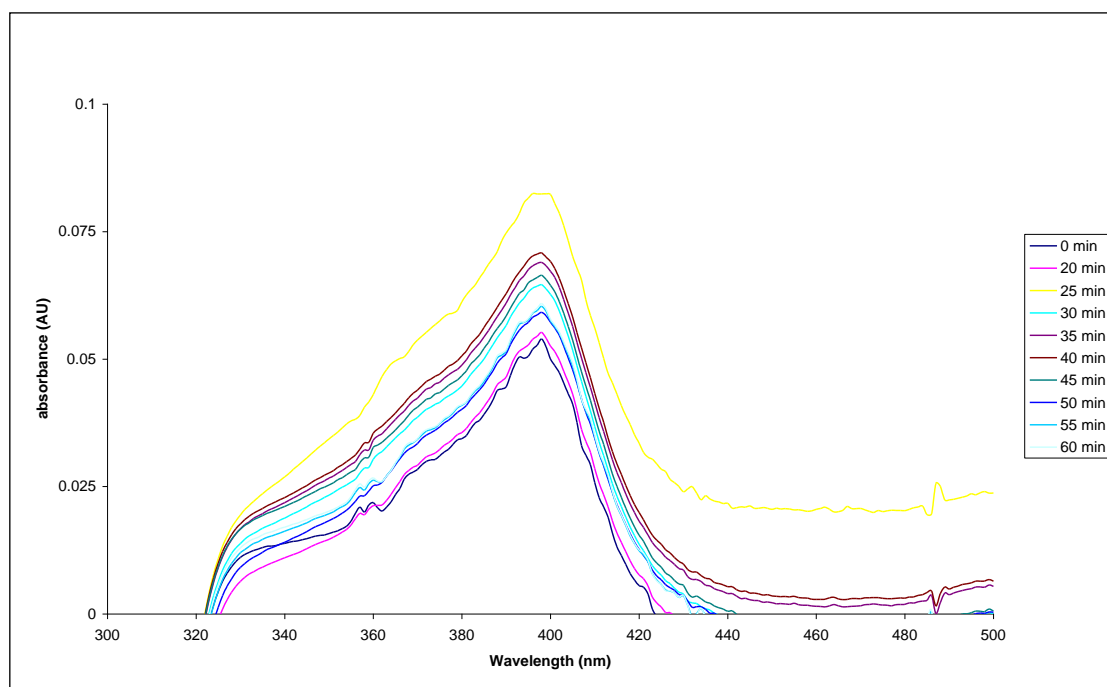
Figure 47. *Absorbance of* **3** *with hematoporphyrin, in Isopropyl alcohol, 10 :1 molar ratio excited with white light.*
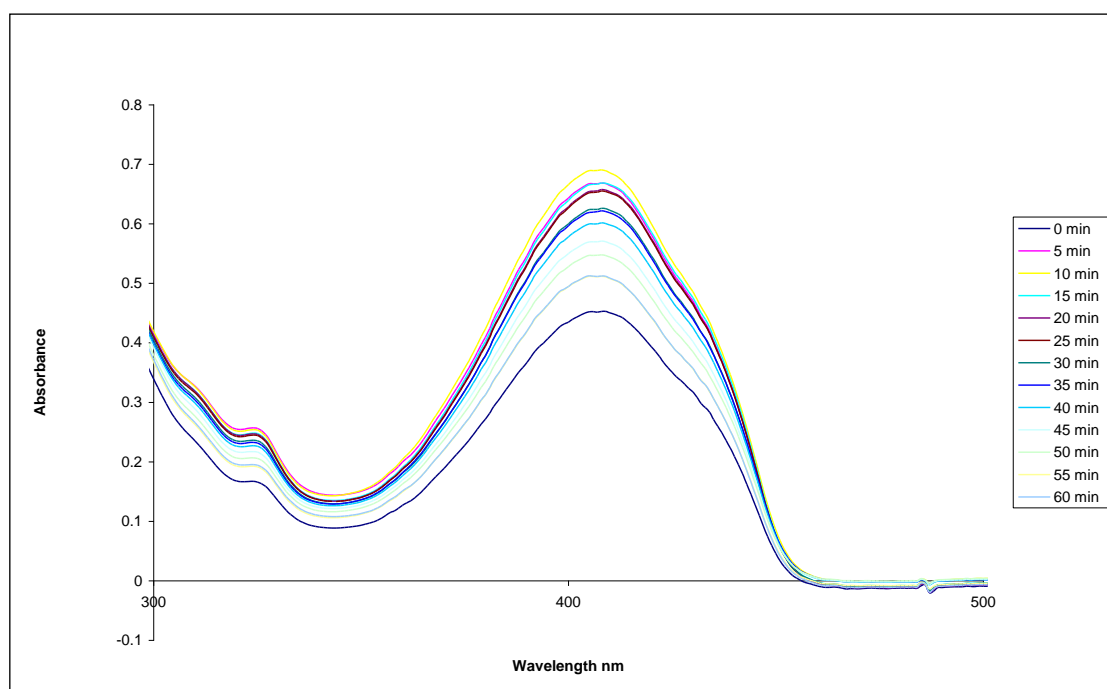
Figure 48. *Absorbance of* **3** *with hematoporphyrin, in Isopropyl alcohol, 100 :1 molar ratio excited with white light.*